ISTANBUL TECHNICAL UNIVERSITY ★ GRADUATE SCHOOL

BIDIRECTIONAL BUCK BOOST CONVERTER DESIGN

M.Sc. THESIS

İlyas SARIGÜL

Department of Electronics and Communication Engineering

Electronics Engineering Programme

AUGUST 2024

ISTANBUL TECHNICAL UNIVERSITY ★ GRADUATE SCHOOL

BIDIRECTIONAL BUCK BOOST CONVERTER DESIGN

M.Sc. THESIS

İlyas SARIGÜL
(504211211)

Department of Electronics and Communication Engineering

Electronics Engineering Programme

Thesis Advisor: Assoc. Prof. Dr. Yüksel ÇAKIR

AUGUST 2024

ISTANBUL TEKNİK ÜNİVERSİTESİ ★ LİSANSÜSTÜ EĞİTİM ENSTİTÜSÜ

ÇİFT YÖNLÜ ÇALIŞABİLEN DÜŞÜRÜCÜ YÜKSELTİCİ DÖNÜŞTÜCÜ TASARIMI

YÜKSEK LİSANS TEZİ

İlyas SARIGÜL
(504211211)

Elektonik ve Haberleşme Mühendisliği Anabilim Dalı

Elektronik Mühendisliği Programı

Tez Danışmanı: Doç. Dr. Yüksel ÇAKIR

AĞUSTOS 2024

İlyas SARIGÜL, a M.Sc. student of ITU Graduate School student ID 504211211, successfully defended the thesis entitled "BIDIRECTIONAL BUCK BOOST CONVERTER DESIGN", which he prepared after fulfilling the requirements specified in the associated legislations, before the jury whose signatures are below.

Thesis Advisor :	**Assoc. Prof. Dr. Yüksel ÇAKIR** İstanbul Technical University	....
Jury Members :	**Prof. Dr. Müştak Erhan YALÇIN** Istanbul Technical University	....
	Assoc. Prof. Dr. Nihan KAHRAMAN Yildiz Technical University	....

Date of Submission : 28 May 2024
Date of Defense : 09 August 2024

To my loved ones

FOREWORD

I would like to thank my supervisor Asst. Prof. Dr. Yüksel ÇAKIR for all of his support and guidance during my M. Sc. Thesis.

I would like to thank my company, Turkish Aerospace Industries, and its employees for providing me with the necessary flexibility and providing all kinds of support for my graduate education. I would like to thank my chief, TAI Avionics Design Directorate Analog Design Chief Engineer Serkan Murat KARABACAK, who is also the consultant of my work within the company, for his ideas and technical support.

Finally, I would like to thank my family and my best friends.

AUGUST 2024

İlyas SARIGÜL
(Electrical - Electronics Engineer)

TABLE OF CONTENTS

Page

ABBREVIATIONS

A : Ampere
AC/DC : Alternative Current to Direct Current
ADC : Analog Digital Converter
BIDABC : Bi-directional Isolated Dual Active Bridge Converter
BIFBC : Bi-directional Isolated Flyback Converter
BIHC : Bi-directional Isolated Hybrid Converter
BIMC : Bi-directional Isolated Modular Converter
BIRC : Bi-directional Isolated Resonant Converter
BIRSC : Bi-directional Isolated Reduced Switch Converter
BIZSC : Bi-directional Isolated Z-Source Converter
BMS : Battery Management System
BNIC : Bi-directional Non-Isolated Converter
BNICC : Bi-directional Non-Isolated Cascaded Converter
BNICIC : Bi-directional Non-Isolated Coupled Inductor Converter
BNIIC : Bi-directional Non-Isolated Interleaved Converter
BNIMSC : Bi-directional Non-Isolated Multiple Switched Converter
BNIRC : Bi-directional Non-Isolated Resonant Converter
BNISCC : Bi-directional Non-Isolated Switched-Cap Converter
BNISSC : Bi-directional Non-Isolated Soft-Switched Converter
CAN : Controller Area Network
DC : Direct Current
DC to DC : Direct Current to Direct Current
ESR : Equivalent Series Resistance
GND : Ground
GPIO : General Purpose Input Output
Hz : Hertz
I/O : Input/Output
I2C : Inter-Integrated Circuit
IC : Integrated Circuit
KB : Kilobyte
kHz : Kilohertz
LDO : Low Dropout Regulator
LED : Light Emitting Diode
mA : miliampere
MHz : Megahertz
MOSFET : Metal Oxide Semiconductor Field Effect Transistor
NMOS : N-Type Channel Metal Oxide Semiconductor
NVIC : Nested Vectored Interrupt Controller
PLC : Power Line Communication
PMOS : P-Type Channel Metal Oxide Semiconductor
PWM : Pulse Width Modulation
RAM : Random Access Memory
RTC : Real Time Clock
SOA : Safe Operation Area
SSI : Synchronous Serial Interface
UART : Universal Asynchronous Receiver-Transmitter
UPS : Uninterruptible Power Systems
USB : Universal Serial Bus

V : Voltage
VDC : Voltage Direct Current
W : Watt
ZVS : Zero Voltage Switching

SYMBOLS

°C	: Degree Celsius
C	: Capacitance
Cboot	: Bootstrap capacitance
Cgate	: MOSFET gate capacitance
CIN	: Input capacitance
COUT	: Output capacitance
D	: Duty cycle
Fsw	: Switching frequency
IF	: Forward current
IL(PP)	: Inductor peak to peak current
IOUT	: Output current
IOUT(MAX)	: Maximum output current
ISW(MAX)	: Maximum switching current
L	: Inductance
PD	: Power dissipation
POUT	: Output power
Rdson	: MOSFET conduction resistance
SW	: Switch
Tsw	: Switching time
V	: Voltage
VF	: Forward voltage
VIN	: Input voltage
VINMAX	: Maximum input operating voltage
VINMIN	: Minimum input operating voltage
VOUT	: Output voltage
ΔIL	: Inductor ripple current
ΔVOUT	: Output voltage ripple
ΔVOUT(ESR)	: Output voltage ripple with ESR
η	: Efficiency

LIST OF TABLES

Page

LIST OF FIGURES

Page

BIDIRECTIONAL BUCK BOOST CONVERTER DESIGN

SUMMARY

The importance of DC to DC converters increases with developing technology. Many of the electronic devices that we use contain AC/DC or DC to DC converters. One of the areas where DC to DC converters are most used is electric vehicles. DC to DC converters are used to charge the battery and energize the electric motors with the charged battery. There are many different types of DC to DC converters. Some of these have an isolated structure, while some have a non-isolated structure. The isolation status of the converter is determined according to the design needs.

Converters operating as standard make a one-way conversion from the input direction to the output direction. However, due to the change and increase in today's needs, one-way DC to DC converters have become ineffective. Where bi-directional operation is required, two DC to DC converters had to be designed. This made the design both larger and less efficient. Therefore, using standard DC to DC converters bidirectionally by making some additions and arrangements is one of the most effective ways. Bi-directional operation is possible in both isolated and non-isolated DC to DC converter structures. Bi-directional buck boost converter can produce a regulated voltage both from input to output and from output to input. In this study, the details of the non-isolated structure that can operate bi-directionally are included.

The non-isolated bi-directional converter is in buck boost converter topology. It contains four switching components in this structure. It is possible to operate this structure bidirectionally with the 4 MOSFETs used. While it operates in buck mode, buck boost mode and boost mode in the forward direction, it can operate in buck mode, buck boost mode and boost mode in the reverse direction. The way to achieve these modes is to determine the forward and reverse operating characteristics. The conditions under which the structure operates in forward or reverse direction depend on the input and output voltages.

If appropriate source voltage is applied to the input of DC to DC, the structure works in the forward direction and produces output voltage. If the input and output voltage are not within an appropriate range, DC to DC converter goes into protection mode and produces no output. If the appropriate source voltage is applied to the DC to DC converter’s output, the output side acts as an input and the input side acts as the output. It is possible to get voltage from the input side with the voltage applied from the output side.

The bi-directional buck boost converter structure basically includes the following circuits: bi-directional current measurement circuits, voltage divider circuit MOSFET driver circuits, MOSFETs, switching inductor, microcontroller, auxiliary circuits and temperature measurement circuits. Management of operations within the converter is provided by the microprocessor. The microprocessor performs the operations of measuring input/output voltages, measuring bi-directional input/output currents,

measuring temperature from the temperature sensor, and driving MOSFETs according to a certain algorithm. The operating mode of the converter is determined by the voltage and current measurement circuits in the structure. For forward operation, if the input voltage is greater than the output voltage, the converter operates in buck mode, if the input voltage is close to the output voltage, it operates in buck boost mode, and if the input voltage is lower than the output voltage, it operates in boost mode. In reverse operation, if the output voltage is greater than the input voltage, the converter operates in buck mode, if the output voltage is close to the input voltage, it operates in buck boost mode, and if the output voltage is lower than the input voltage, it operates in boost mode.

Signals of certain pulse widths are applied to MOSFETs to produce input or output voltages. The width of these signals is determined by the voltage values the microcontroller measure from the input and output. This measurement takes place continuously. To obtain a constant output voltage in a structure where the input voltage varies, the pulse width must be constantly adjusted. The same is necessary for obtaining constant input voltage.

As the current measurement circuits included in the converter design, both bi-directional current reading and limiting can be provided. The current can be read from both the input and output sides. If more current is drawn from the input or output of the DC to DC converter than the specified current limit, the current is limited. This limiting process is possible by adjusting the pulse width of the signal applied to the MOSFETs, just like adjusting the voltage.

ÇİFT YÖNLÜ ÇALIŞABİLEN DÜŞÜRÜCÜ YÜKSELTİCİ DÖNÜŞTÜRÜCÜ TASARIMI

ÖZET

DC to DC dönüştürücülerin kullanımı hem düşük güçlerde hem yüksek güçlü devre yapılarında her geçen yıl artmaktadır. Bunun en temel nedenlerinden birisi ise gelişen teknolojinin hayatımızda eskisinden daha fazla yerini almasından kaynaklanmaktadır. DC to DC dönüştürücülerin önemi otomotiv, beyaz eşya, savunma ve havacılık sektörleri için büyük önem arz etmektedir. Özellikle elektrikli araçların yaygınlaşması ile yüksek güçlü elektrik sistem tasarımın en kritik kısımlarını DC to DC dönüştürücüler oluşturmaktadır. Birçok farklı tipte topolojiler bulunmaktadır.

Elektronik devrelerin beslemeleri ise çoğunlukla doğru akımdır. Uygun değerde doğru akımı sağlamanın yolu da DC to DC dönüştürücülerden geçmektedir. Çünkü elektronik devrenin beslemesi için ihtiyaç duyduğu gerilim değeri standart olarak üretilen gerilim değerlerine göre yüksek veya düşük kalabilmektedir. En temel ifadeyle DC to DC dönüştürücüler gelen giriş gerilimini farklı anahtarlama teknikleri kullanarak çıkışında, girişten daha büyük, girişten daha küçük veya girişe eşit gerilime dönüştürürler. Giriş gerilimi çıkış geriliminden büyükse yükseltici dönüştürücü, giriş gerilimi çıkış geriliminden küçükse düşürücü dönüştürücü ve giriş gerilimi çıkış gerilimine neredeyse eşitse düşürücü yükseltici dönüştürücü olarak adlandırılmaktadır. DC to DC dönüştürücüler izolasyon durumuna göre iki tipte bulunmaktadır. Bunlardan ilki izoleli yapıdır. İzole DC to DC dönüştürücüde giriş ile çıkış arasında doğrudan bir elektriksel bağlantı bulunamamaktadır. İzolasyon için transformatörler kullanılır. Giriş ve çıkış aynı GND hatlarına sahip olmazlar. Bu yapılar hem düşük güçlü DC to DC dönüştürücülerde hem de yüksek güçlü dönüştürücülerde kullanılmaktadır. İzoleli DC to DC dönüştürücüler gerilimin hem yükseltilmesinde hem de düşürülmesinde kullanılır. Giriş ve çıkış gerilim aralıkları oldukça geniştir. Giriş ve çıkışta yüksek gerilim farkları olsa bile anahtarlamanın yanında transformatörün sarım sayısı ile bu güçlük kolayca aşılır. Bu yapının en önemli avantajlarından birisi dönüştürücünün girişinde veya çıkışında yaşanan olumsuz durumdan diğer tarafından etkilenmemesidir. Özellikle elektromanyetik uyumluluk kapsamında değerlendirildiğinde büyük avantajları ortaya çıkmaktadır. Girişten gelen gürültü transformatör kullanılmasından dolayı direkt olarak çıkışa etki edemez. Çıkışa yansıyan gürültü giriştekine göre çok daha düşük seviye olur. İzoleli DC to DC dönüştürücülerin verimlilikleri de oldukça yüksektir. Bu da yüksek güçlü uygulamalar için büyük avantaj oluşturmaktadır. DC to DC dönüştürücü içerisinde yer alan transformatör oldukça fazla yer kaplamaktadır. Bu da DC to DC dönüştürücünün boyutunda ve ağırlığında artışa neden olmaktadır.

İzolesiz DC to DC dönüştürücülerde transformatör yer almaz. Transformatör yerine genellikle bobin kullanılır. Bu sayede DC to DC dönüştürücünü boyutu daha küçük ve ağırlığı daha azdır. İzolesiz DC to DC dönüştürücülerde giriş ve çıkış birbirinden izole değildir. Yani giriş ile çıkış arasında elektriksel bir bağlantı bulunur. İzolesiz DC to DC dönüştürücüler özellikle düşük ve orta güçlü güç ihtiyacı olan uygulamalar için vazgeçilmezdir. Yapıda çok büyük komponentler olmamasında dolayı az yer kaplar. Hemen hemen her elektronik devre için bir veya birden fazla DC to DC dönüştürücü kullanılır. DC to DC dönüştürücüler genellikle tek yönlü olarak çalışmaktadır. DC to DC dönüştürücünün girişine uygun gerilim uygulanması durumunda çıkışta ayarlanan gerilim oluşmaktadır. Bu durumda dönüştürücü giriş yönünden çıkış yönüne tek yönde çalışma gerçekleştirir. Çift yönlü DC to DC dönüştürücü ise hem giriş tarafından çıkış tarafına hem de çıkış tarafından giriş tarafına doğru çalışma gerçekleştirmektedir. Çift yönlü çalışmanın ihtiyaç olduğu yerlerde iki adet tek yönlü çalışan DC to DC dönüştürücü de kullanmak mümkündür. Fakat iki adet tek yönlü çalışan DC to DC dönüştürücü maliyet, ağrılık ve boyut açısından olumsuz etkiler oluşturmaktadır.

Çift yönlü çalışan birçok tipte DC to DC dönüştürücü topolojisi bulunmaktadır. Tez çalışmam kapsamında topoloji olarak çift yönlü çalışan DC to DC düşürücü yükseltici dönüştürücü tasarlanmaktadır. Çift yönlü DC to DC dönüştürücü ileri ve ters olmak üzere iki yönde çalışmaktadır. Çift yönlü çalışan DC to DC dönüştürücü temel olarak; 4 adet N kanallı MOSFET, MOSFET sürücü devreleri, akım ölçüm devreleri, gerilim ölçüm devreleri, anahtarlama bobini, hassas akım ölçüm dirençleri, mikrodenetleyici, sıcaklık sensörü, gösterge ledleri pasif direnç, kapasitör ve bobin elemanlarını içermektedir.

Tüm çalışmanın merkezinde TM4C123GH6PM mikroişlemcisi yer almaktadır. Mikroişlemci dönüştürücü içerisindeki çevresel birimlerden ölçümler almaktadır. Bu ölçümlere göre MOSFET sürücü devresini ve gösterge ledlerini kontrol eder. Mikroişlemci C programlama ile dili ile kodlanmıştır. Algoritma yapısı ile hem ileri yönlü hem de ters yönlü çalışmayı çalışmaya imkân sağlamaktadır. DC to DC dönüştürücü tasarımında gerilim ve akım sürekli olarak okunmaktadır. Yapı çift yönlü çalışıyor olmasından dolayı akım hem ileri yönde hem de ters yönde okunabilmektedir. Gerilim ise giriş ve çıkıştan okunmaktadır. Akım ve gerilim ölçüm işlemleri için harici bir analog dijital dönüştürücü kullanılmamaktadır. Mikroişlemcinin kendi analog dijital dönüştürücüsü kullanılmaktadır. Toplamda 5 adet analog sinyal bulunmaktadır. Bunlar giriş gerilimi, çıkış gerilimi, giriş akımı, çıkış akımı ve sıcaklık sensörü verileridir. 4 adet anahtarlama elemanı giriş ve çıkış gerilimlerinin değerlerine göre 3 farklı modda çalışırlar. Bu modlar düşürücü mod, düşürücü yükseltici mod ve yükseltici moddur. Bu 3 mod hem ileri yönde hem de geri yönde çalışmaktadır.

Dönüştürücün anahtarlama işlemi o hangi modda olmasıyla alakalıdır. İşlemci çıkışında dört adet sinyal genişlik modülasyonu (PWM) yer almaktadır. Bunlardan iki tanesi direkt olarak MOSFET anahtarlamasını giriş sağlarken, diğer ikisi MOSFET'lerin %100 PWM'de sürülmesi için kullanılmaktadır. MOSFET'ler giriş tarafında yer alan ve çıkış tarafında yer alan olmak üzere iki ayrı grupta değerlendirilmektedir. Giriş tarafından yer alan iki adet anahtarlama elemanı için bir adet PWM sinyal ve çıkış tarafında yer alan iki adet anahtarlama elemanı için bir adet PWM sinyal kullanılmaktadır. Giriş tarafındaki PWM sinyali donanımsal bir devreden geçerek birbirine zıt iki adet PWM sinyale dönüşmektedir ve bu PWM sinyaller MOSFET'lerin ihtiyaç duymuş olduğu gerilim seviyelerindedir. Çıkış tarafındaki PWM sinyali de donanımsal bir devreden geçerek birbirine zıt iki adet PWM sinyale dönüşmektedir ve bu PWM sinyaller MOSFET'lerin ihtiyaç duymuş olduğu gerilim seviyelerindedir. Bu işlemlerin gerçekleştiği yer MOSFET sürücü devresidir. Tasarımda entegre devre kullanmadan ayrık devre yapıları ile MOSFET sürücü devreleri oluşturulmuştur. Bu yapı 50kHz-300kHz frekans aralığı için optimum çalışmayı sergilemektedir.

DC to DC dönüştürücü de akım okuma ve limitleme işlemi girişten ve çıkıştan çift yönlü olarak yapılmaktadır. Bunun için dört farklı değerde parametre belirlenmektedir. Bunlar; ileri yönde giriş akımı, geri yönde giriş akımı, ileri yönde çıkış akımı ve geri yönde çıkış akımıdır. Bu değerler parametrik olarak ihtiyaca göre düzenlenebilmektedir.

Dönüştürücünün çalışma gerilim aralığı 9V-50V aralığıdır. Bu değer aralığının altında bulunması durumunda düşük gerilim koruması, bu değer aralığının üzerinde bir değerde ise yüksek gerilim korumasına girmektedir. Bu çalışma aralığı giriş ve çıkış tarafları için ortaktır. Dönüştürücü devresinde dört adet gösterge ledi bulunmaktadır. Bu gösterge ledleri dönüştürücünü çalışma durumunu belirtir. Bu göster ledlerinden ilki ileri yönde çalışması sırasında yanmaktadır. İkincisi ise geri yönde çalışması sırasında yanmaktadır. Üçüncüsü gerilim koruması oluşması durumunda yanmaktadır. Dördüncü olan ise yazılımsal düzenleme yaparken anahtarlamanın yapıldığı belli etmek üzere, anahtarlamanın olmadığı zamanlarda yanmaktadır. Tüm bunlara ilave olarak dönüştürücü de sıcaklık sensörü yer almaktadır. Bu dönüştürücü üzerindeki en sıcak yüzeyde bulunur. Sıcaklık değeri ayarlanan maksimum sıcaklık değerini aştığında dönüştürücü korumaya girmektedir. Aynı sıcaklık sensörü sayesinde anlık olarak sıcaklık okuması yapılabilmektedir.

1 INTRODUCTION

One of the most significant part of power electronics is DC to DC converters. DC to DC converters are commonly found in many electronic devices. The voltage values required by electronic circuits are provided by using DC to DC converters. There are many types of DC to DC converters. The type of converter is determined according to the parameters required by the circuit. The power value required by the circuit, input voltage range, output voltage, output current, isolation status and efficiency can be listed as the most important parameters of the design. DC to DC converter can work in one direction as well as in two directions. In one-way operation, voltage conversion occurs from the input direction to the output direction. In order to get a constant output voltage, switching frequency and pulse width changes are made. Converters are closed loop systems. The output should be minimally affected by input voltage changes or instantaneous changes in the output current. The way to achieve this is a closed loop with the correct parameters set. Bi-directional DC to DC converters are commonly used in designs, such as hybrid electric vehicle energy systems [1]–[4], uninterrupted power supplies [5], [6], fuel-cell hybrid power systems [7]–[10], photovoltaic hybrid power systems [11], [12], and battery chargers [13]–[15].

A design of a bi-directional buck boost converter is shown in **Figure 1.1** [16].

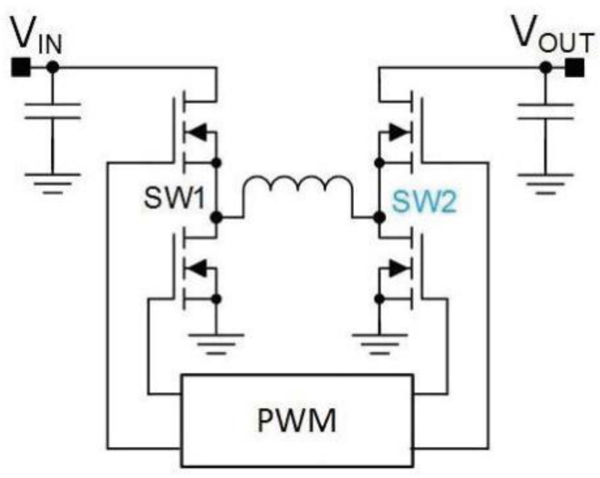

Figure 1.1 : Single inductor buck-boost converter.

The difference between bi-directional systems and unidirectional systems is that they can transform voltage from input to output and from output to input. The bi-directional DC to DC converter has the ability to operate unidirectionally.

Within the scope of this thesis study, bi-directional buck boost converter design is discussed. The converter continually measures the input voltage, output voltage, input current and output current and produces input or output voltage accordingly. Since the structure is bi-directional, all control units can be supplied from both the input and output. There is a microprocessor at the center of the structure that provides all control. The converter works in 3 different modes. It consists of buck, buck boost and boost operating modes. The operation of the DC to DC converter occurs in two different directions: Forward and Reverse operation. Buck, Buck Boost and Boost modes are valid for both Forward and Reverse mode.

1.1 Literature Review

Bi-directional Buck Boost converter topologies are widely used today. **Figure 1.2** [17] shows the visual of Buck Boost converter structures that can operate bi-directionally. Bi-directional buck boost converters are evaluated in two different categories in terms of isolation: isolated and isolated. Selection of the converter type is made according to the isolation required by the design. Types of isolated DC to DC converters are as follows:

- BIRC,
- BIDABC,
- BIMC,
- BIRSC,
- BIZSC,
- BIFBC.

Types of non isolated DC to DC converters are as follows:

- BNIRC,
- BNICIC,
- BNISSC,

- BNIIC,
- BNICC,
- BNISCC,
- BNIMSC.

With today's studies, efforts are being made to convert isolated DC to DC converters into non-isolated structures and non-isolated DC to DC converters into isolated structures [17]. The non-isolated solution can be easily produced for an isolated structure. With this flexibility provided to designs, design activities are gaining momentum. Bi-directional DC to DC converters have many differences compared to each other. The main differences are the switching frequency switching techniques, coil numbers, transformer numbers and types, soft switching techniques, casdade structures, snubber structures and the number of components used in the circuit.

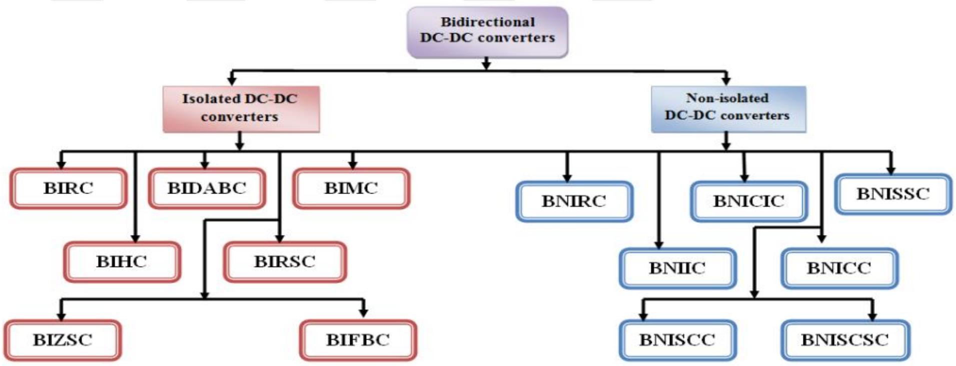

Figure 1.2 : Bi-directional buck boost converter topologies.

Bi-directional buck boost converter structures are widely used for energy storage purposes today. Battery back-up and energy storage solutions are essential in various industrial settings, such as server systems, uninterruptible power supplies (UPSs) and telecom rectifiers, as well as for powering line communication (PLC) systems [18]. **Figure 1.3** shows a typical energy storage system. Battery charger charges the Battery Bank with the voltage it receives from DC BUS. Battery discharger transfers the energy it receives from the battery to DC BUS. This structure is controlled by a controller and BMS. As can be seen from the image, battery charger and battery discharger consist of a single converter. In this way, a second converter is not needed for charging and discharging the battery.

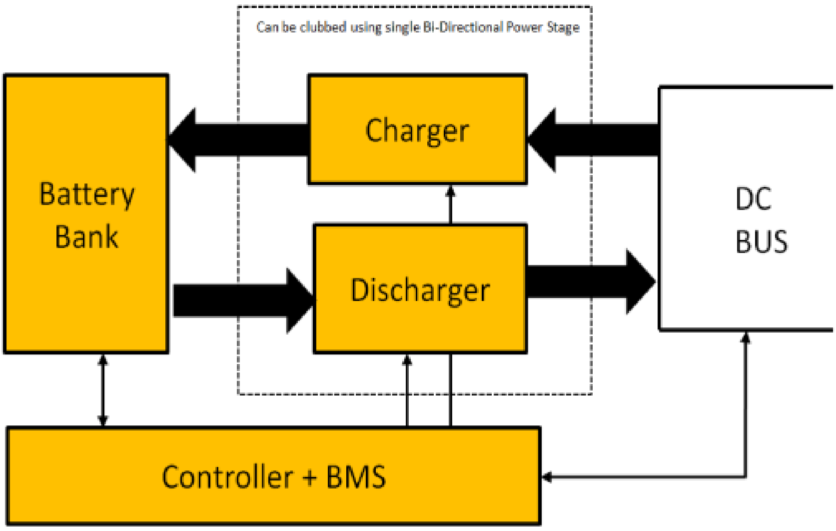

Figure 1.3 : Block diagram of general battery back-up system.

1.2 Motivation

Bi-directional buck boost converter topologies are actively used in electric vehicles, energy storage systems and industry. The importance of electric vehicles is that by using a bi-directional converter, there is no need for two separate converters to charge and discharge the battery in the vehicle. The optimum design solution can be achieved by operating a single converter bidirectionally. Energy storage systems such as UPS have similar logic to electric vehicles. There is a single converter for charging and discharging the battery. The ability to instantly change direction in UPS devices greatly increases the response speed of the system.

With the developing technological needs, studies on this subject are gaining momentum. The structure of the DC to DC converter is both isolated and non-isolated. In this way, it greatly increases the application potential of the bi-directional DC to DC converter. In some systems, the need to establish an isolated structure becomes a necessity. However, in some systems there is no such obligation. For these structures, a bi-directional insulated system contributes greatly to the creation of the most suitable solution. The existence of many academic publications and studies technically reveals the advantages and disadvantages of the subject. The increasing need for this structure day by day and the achievements of academic and industrial studies on it constitute the motivation of my thesis.

2 DC TO DC CONVERTER MODELLING

Power supplies used today require features such as high efficiency, small volume, low price, and constant output voltage [19]. Features vary depending on the topology used in the designed power supplies. In the first stage of the design, converter selection and design are made according to the requirements of the circuit. The converter's output power, efficiency, input voltage range and output voltage range constitute the most basic criteria. The isolation of the DC to DC converter in some designs creates another hysteria. There is no need for isolation for the converter made within the scope of this thesis study. That's why non-isolated converter topology is used. There are three different converter structures based on the bi-directional buck boost converter. Depending on the input and output voltage values, the converter operates in buck mode, buck boost mode or boost mode. It brings together many structures with its converter circuit structure.

2.1 Buck Converter

Buck converter is a type of converter that converts the input voltage to a lower voltage at the output by switching and produces a non-isolated output voltage.

Figure 2.1 [19] shows the circuit structure of the buck converter.

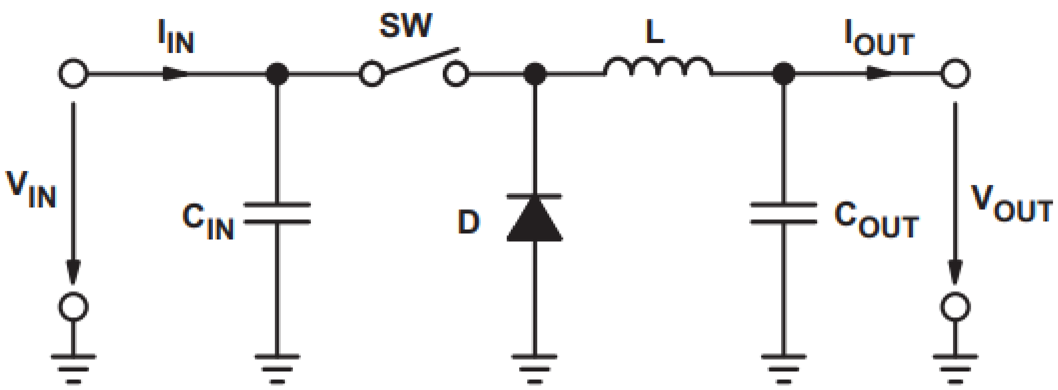

Figure 2.1 : Power stage of buck converter.

The circuit structure basically includes input capacitor (CIN), switching element (SW), switching diode (D), switching inductor (L) and output capacitor (COUT).

Input capacitance (CIN) suppresses sudden changes in input voltage. It serves as a source for the inrush currents drawn by the Buck converter during its start-up. Inrush currents of the buck converter are seen especially during the first start-up and the first load draw from the output. If the input capacitor is not used, the converter will provide the starting current it needs from the source that it is connected to. In addition, it also acts as a filter for electromagnetic noise emitted during the operation of the buck converter.

NMOS is generally used as the switching element. PMOS is also used in some circuit structures. However, PMOS is generally not preferred. The main reason for this is the high rdson value, which is the drain-source resistance of PMOS. High drain-source resistance causes increased conduction losses of the buck converter.

The free-pass diode is the circuit element that ensures the completion of the circuit when the switching element is not in conduction. Nowadays, MOSFET is used instead of this diode. Because conduction losses occur due to the conduction voltage on the diode and the current passing through the diode when the switching element is not in conduction. MOSFET causes less power loss due to its low conduction voltage and plays an important role in increasing efficiency.

The switching inductor is a passive circuit element that stores current. It delivers the current needed for the output as charging and discharging during switching.

The output capacitor prevents transients in the output voltage. As the voltage stored on it, it provides constant voltage for the load connected to the output.

When designing a buck converter, minimum input voltage (VINMIN), maximum input voltage (VINMAX), output voltage (VOUT) and output current (IOUT) values must be known.

When designing a buck converter, the duty cycle value must be calculated. Duty cycle value is calculated with equation 2.1.

$$D = \frac{VOUT}{VIN * \eta} \tag{2.1}$$

The maximum duty cycle value is calculated with equation 2.2.

$$D = \frac{VOUT}{VINMAX * \eta} \tag{2.2}$$

To calculate the maximum switching current, the ripple current occurring on the switching inductor must be calculated. The ripple current occurring in the switching coil is calculated with equation 2.3.

$$\Delta IL = \frac{(VINMAX - VOUT) * D}{Fsw * L} \tag{2.3}$$

The maximum switching current is calculated with equation 2.4.

$$\mathrm{ISW(MAX)} = \frac{\Delta \mathrm{IL}}{2} + IOUT(MAX) \tag{2.4}$$

Lower value inductor has smaller dimensions. The required inductance is calculated using equation 2.5.

$$\mathrm{L} = \mathrm{VOUT} * \frac{\mathrm{VIN} - \mathrm{VOUT}}{\Delta \mathrm{IL} * \mathrm{Fsw} * \mathrm{VIN}} \tag{2.5}$$

Inductor ripple current is calculated by equation 2.6. Since the inductor value is not exactly known, the estimated ripple current varies between 20% and 40% of the output current.

$$\Delta \mathrm{IL} = (0.2 \text{ to } 0.4) * \mathrm{IOUT(MAX)} \tag{2.6}$$

The power consumed on the free-pass diode is provided by equation 2.7.

$$PD = IF * VF \tag{2.7}$$

In buck converter designs, output capacitors with low ESR values are selected. Because the lower ESR value decreases the ripple occurring in the output voltage. The minimum output capacity value is provided by equation 2.8.

$$COUT(MIN) = \frac{\Delta \mathrm{IL}}{8 * Fsw * \Delta \mathrm{VOUT}} \tag{2.8}$$

If the ESR value of the selected capacitor is taken into account, the ripple voltage level that will occur at the output is calculated as in equation 2.9.

$$\Delta \mathrm{VOUT(ESR)} = ESR * \Delta \mathrm{IL} \tag{2.9}$$

2.2 Boost Converter

Boost converter is a type of converter that converts the input voltage to a greater output voltage by switching and produces a non-isolated output voltage.

Figure 2.2 [20] shows the circuit structure of the boost converter.

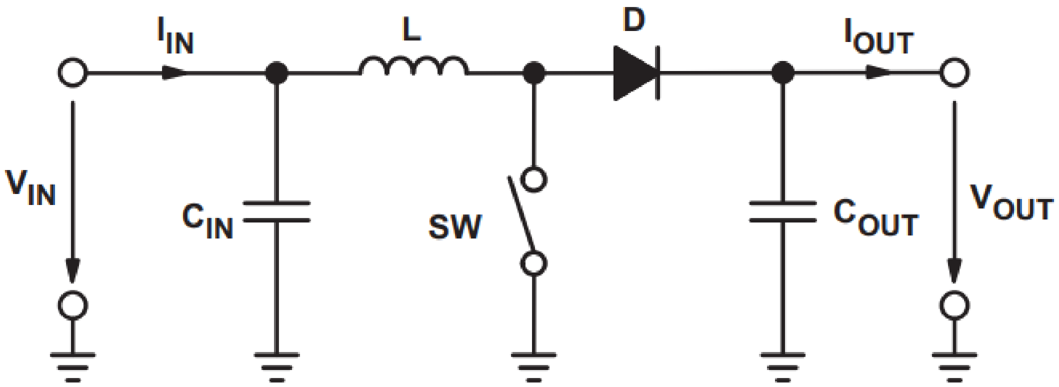

Figure 2.2 : Power stage of boost converter.

The circuit structure basically includes input capacitor (CIN), switching inductor (L), switching element (SW), free switching diode (D), and output capacitor (COUT). In terms of circuit structure, it has almost the same structure as the buck converter.

Input capacitance (CIN) suppresses sudden changes in input voltage. In this way, every transient occurring at the input does not cause sudden changes in the output voltage. The switching inductor is a passive circuit element that stores current. It delivers the current needed for the output as charging and discharging during switching. Switching element (SW) is the circuit element that enables the switching of the inductor. The free-pass diode ensures the completion of the circuit when the switching element is not in conduction. The output capacitor prevents transients in the output voltage.

When designing a boost converter, the duty cycle value must be calculated. Duty cycle value is calculated with equation 2.10.

$$D = 1 - \frac{VIN * \eta}{VOUT} \tag{2.10}$$

The maximum duty cycle value of the boost converter is calculated with equation 2.11.

$$D = 1 - \frac{\text{VINMIN} * \eta}{VOUT} \tag{2.11}$$

To calculate the maximum switching current, the ripple current occurring on the switching inductor must be calculated. The ripple current occurring in the switching inductor is calculated with equation 2.12.

$$\Delta IL = \frac{VINMIN * D}{Fsw * L} \tag{2.12}$$

The maximum switching current is calculated with equation 2.13.

$$\mathrm{ISW(MAX)} = \frac{\Delta\mathrm{IL}}{2} + \frac{IOUT(MAX)}{1-D} \tag{2.13}$$

Lower value inductors have smaller dimensions. As the coil inductance value and inductor current increases, the size of the inductor also increases. The required inductor value is calculated using equation 2.14.

$$\mathrm{L} = \frac{\mathrm{VIN} * (\mathrm{VOUT} - \mathrm{VIN})}{\Delta\mathrm{IL} * \mathrm{Fsw} * \mathrm{VOUT}} \tag{2.14}$$

Inductor ripple current is calculated with equation 2.15. Since the coil value is not exactly known, the estimated ripple current varies between 20% and 40% of the output current.

$$\Delta\mathrm{IL} = (0.2 \text{ to } 0.4) * \mathrm{IOUT(MAX)} * \frac{VOUT}{VIN} \tag{2.15}$$

The power consumed on the free-pass diode is provided by equation 2.16, just like in the buck converter.

$$PD = IF * VF \tag{2.16}$$

In DC to DC converter designs, capacitors with low ESR values are selected. Because the lower ESR value decreases the ripple occurring in the output voltage. The minimum output capacitor value is provided by equation 2.17.

$$COUT(MIN) = \frac{IOUT(MAX) * D}{Fsw * \Delta\mathrm{VOUT}} \tag{2.17}$$

If the ESR value of the selected capacitor is taken into account, the ripple voltage level that will occur at the output is calculated as in equation 2.18.

$$\Delta\mathrm{VOUT(ESR)} = ESR * \left(\frac{IOUT(MAX)}{1-D} + \frac{\Delta\mathrm{IL}}{2}\right) \tag{2.18}$$

2.3 Buck Boost Converter

Buck Boost converter is a converter type that converts the input voltage into a larger or smaller output voltage by switching and produces a non-isolated output voltage.

Figure 2.3 shows the circuit structure of the buck boost converter.

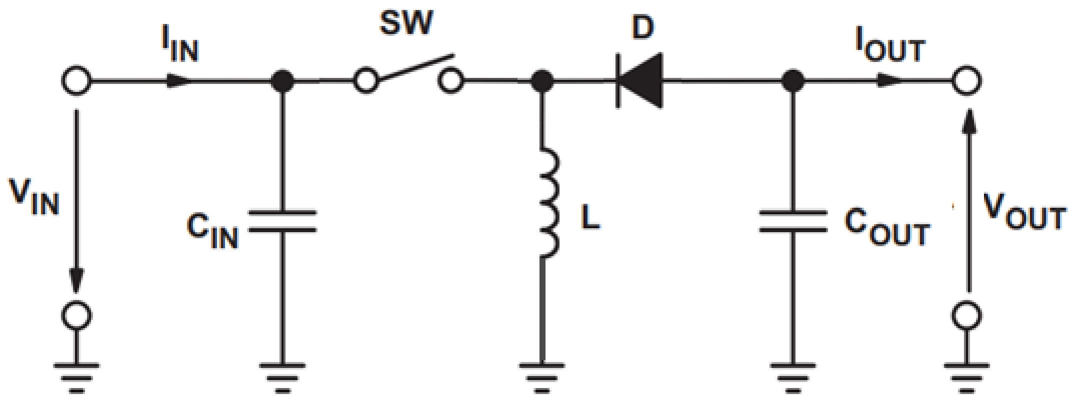

Figure 2.3 : Power stage of buck boost converter.

Nowadays, the use of this circuit structure has decreased considerably. Because, as can be seen from **Figure 2.3**, VIN and VOUT are in reverse polarity. That's why it is called inverting buck boost converter.

When designing a buck boost converter, the duty cycle value must be calculated. Duty cycle value is calculated with equation 2.19 [21].

$$D = \frac{-\mathrm{VOUT} + \mathrm{VF}}{-\mathrm{VOUT} + \mathrm{VF} + \mathrm{VIN}} \tag{2.19}$$

The maximum duty cycle value of the buck boost converter is calculated with equation 2.20 [21].

$$D = \frac{-\mathrm{VOUT} + \mathrm{VF}}{-\mathrm{VOUT} + \mathrm{VF} + \mathrm{VINMIN}} \tag{2.20}$$

The maximum switching current of the buck boost converter is calculated with equation 2.21 [21].

$$\mathrm{ISW(MAX)} = \mathrm{IOUT(MAX)} \times \frac{\mathrm{VIN(MIN)} + \mathrm{VF} - \mathrm{VOUT}}{\mathrm{VINMIN}} + \frac{\mathrm{IL(PP)}}{2} \tag{2.21}$$

2.4 Bi-directional Buck Boost Converter

Bi-directional Buck Boost Converter has a synchronous four switch buck boost converter structure. The circuit topology of the four-switch buck boost converter is as shown in **Figure 2.4** [16].

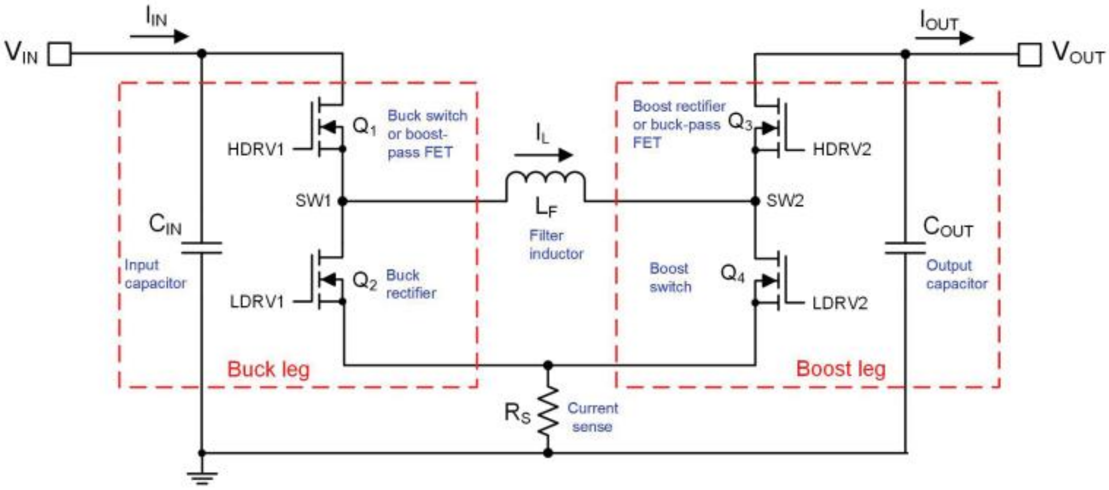

Figure 2.4 : Power stage of four switch buck boost converter.

Four switch buck boost converter structure consists of Buck leg, Boost leg, inductor, current sense, input and output capacitors. This structure operates in two directions: Forward Direction Mode and Reverse Direction Mode.

Depending on the input and output voltages, switching operations occur in 3 different modes: buck mode, buck boost mode and boost mode [16].

Forward direction operation mode has two 3 conversion mode.

- Buck mode when VIN > VOUT,
- Buck boost mode when VIN ≤ VOUT and VIN ≥ VOUT,
- Boost Mode when VIN < VOUT.

Reverse direction operation mode has two 3 conversion mode:

- Buck mode when VOUT > VIN,
- Buck boost mode when VIN ≤ VOUT and VIN ≥ VOUT,
- Boost mode when VOUT < VIN.

2.4.1 Forward direction buck mode

In forward direction buck mode operation, Q1 and Q2 MOSFETs in the Buck leg are switched, Q3 MOSFET is in conduction and Q4 MOSFET is in cut-off. The visual of buck mode switching is shown in **Figure 2.5** [16]. In this structure, there is a Q2 MOSFET instead of the free-pass diode in the buck structure. More power loss is observed on this diode than on MOSFET.

The reason for this is due to the forward voltage values of the free-pass diode. This situation is not seen in MOSFET. Because the MOSFET shows a very low resistance and voltage drop when switched for conduction. Q3 and Q4 MOSFETs are not included in the standard buck converter structure. In this structure, the buck converter structure is provided by driving the Q3 MOSFET with 100% duty cycle and the Q4 MOSFET with 0% duty cycle.

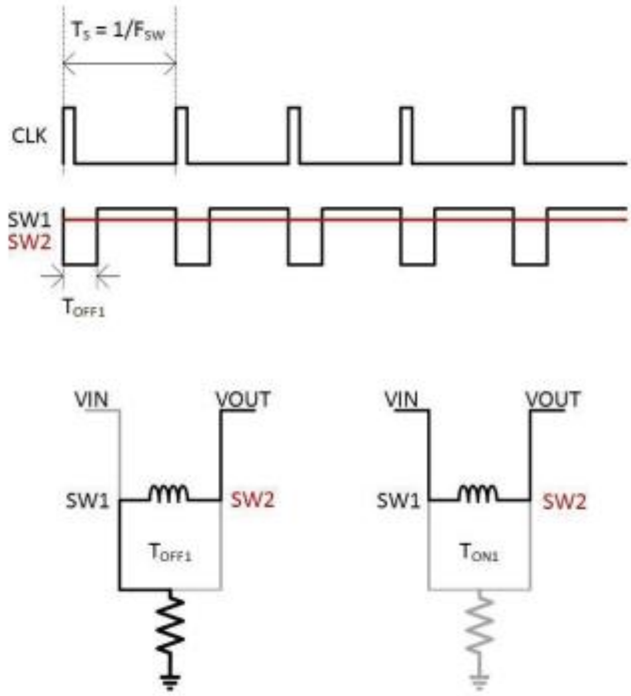

Figure 2.5 : Forward mode buck mode switching.

2.4.2 Reverse direction buck mode

In reverse direction buck mode operation, Q3 and Q4 MOSFETs in the Boost leg are switched, Q1 MOSFET is in conduction and Q2 MOSFET is in cut-off. The visual of buck mode switching is shown in **Figure 2.6** [16].

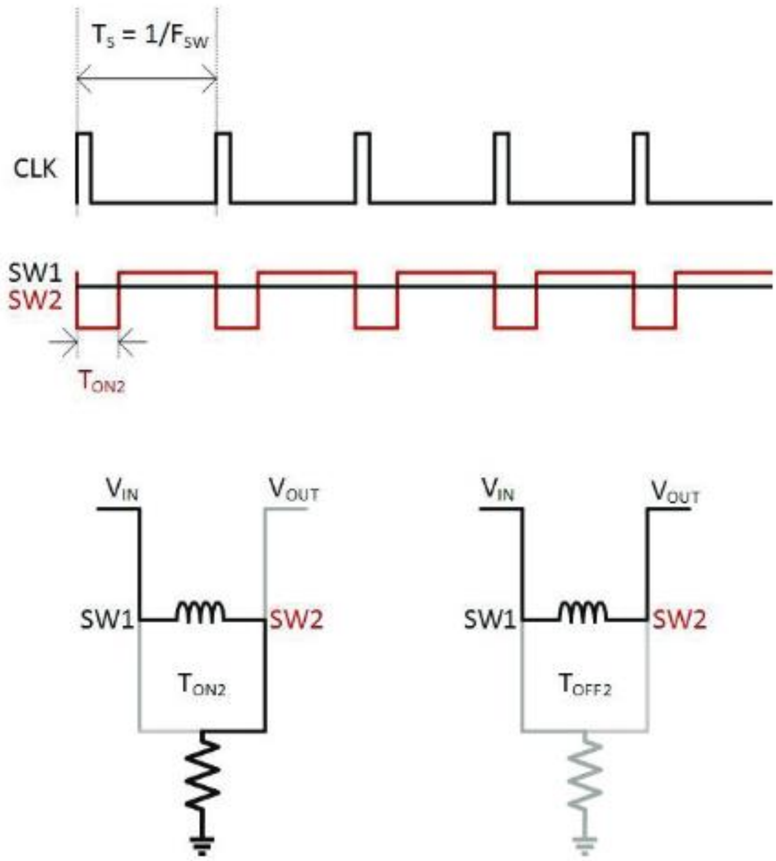

Figure 2.6 : Reverse mode buck mode switching.

2.4.3 Forward direction boost mode

In forward direction boost mode operation, Q3 and Q4 MOSFETs in the Boost leg are switched, Q1 MOSFET is in conduction and Q2 MOSFET is in cut-off. The visual of boost mode switching is shown in **Figure 2.7**[16]. The same boost mode switching topology is seen here. In this structure, there is a Q4 MOSFET instead of the free-pass diode in the boost structure. More power loss is observed on this diode than on MOSFET. The reason for this is due to the forward voltage values of the free-pass diode. This situation is not seen in MOSFET. Because the MOSFET shows a very low resistance and voltage drop when switched for conduction. Q1 and Q2 MOSFETs are not included in the standard boost converter structure. In this structure, the boost converter structure is provided by driving the Q1 MOSFET with 100% duty cycle and the Q2 MOSFET with 0% duty cycle.

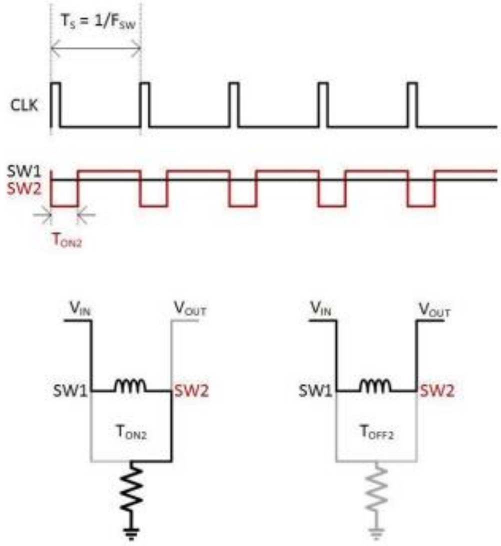

Figure 2.7 : Forward mode boost mode switching.

2.4.4 Reverse direction boost mode

In reverse direction boost mode operation, Q1 and Q2 MOSFETs in the Buck leg are switched, Q3 MOSFET is in conduction and Q4 MOSFET is in cut-off. The visual of boost mode switching is shown in **Figure 2.8** [16].

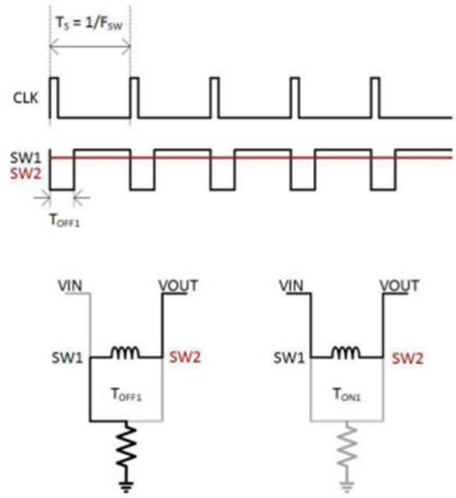

Figure 2.8 : Reverse mode boost mode switching.

2.4.5 Forward direction buck boost mode

In Buck Boost Mode operation, all MOSFETs Q1, Q2, Q3 and Q4 in the Buck leg and Boost leg are switched. In the Buck leg, Q1 and Q2 MOSFETs are switched fully reverse to each other, and in the Boost Leg, Q3 and Q4 MOSFETs are switched fully reverse to each other. As seen in **Figure 2.9** and **Figure 2.10** [16], switching occurs at SW1 and SW2 points every two cycles.

In one of these two cycles, the Buck leg is switched, and in the other cycle, the Boost leg is switched. If the input voltage is more than the output voltage, a switching occurs as in **Figure 2.9**, and if the input voltage is less than the output voltage, a switching occurs as in **Figure 2.10**.

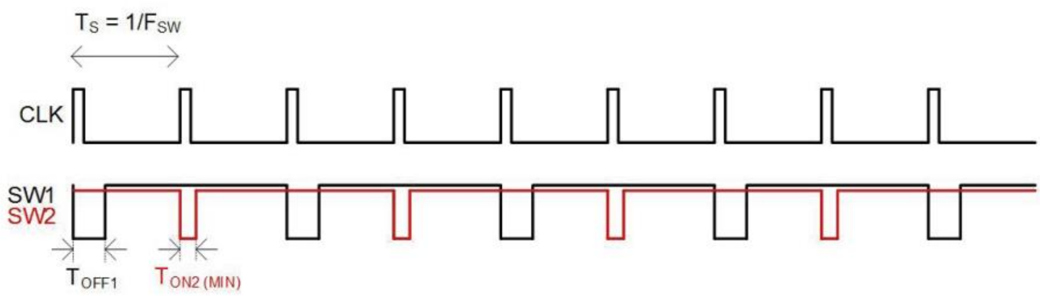

Figure 2.9 : Forward mode buck-boost switching waveforms (VIN > VOUT).

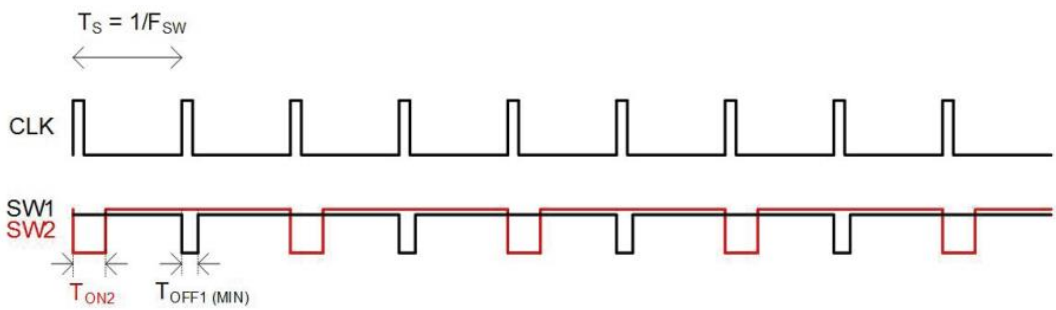

Figure 2.10 : Forward mode buck-boost switching waveforms (VOUT > VIN).

2.4.6 Reverse direction buck boost mode

The switching structure is almost the same as Forward Buck Mode operation. Only the operations VIN > VOUT and VOUT > VIN are reversed. Visuals of Reverse Buck Boost Mode switching can be found in **Figure 2.11** and **Figure 2.12**.

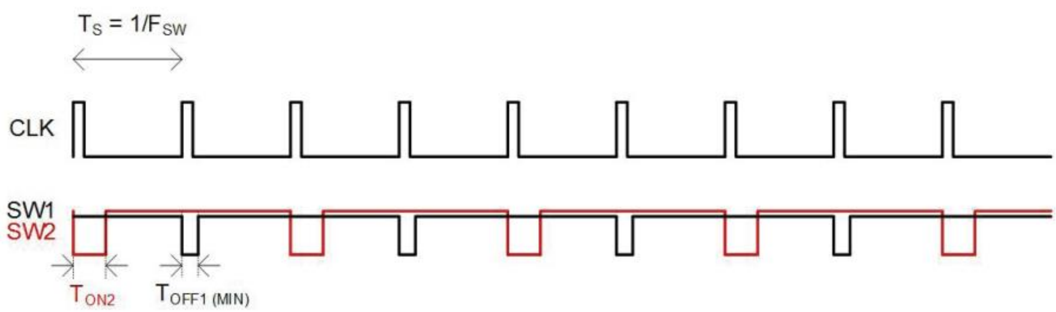

Figure 2.11 : Reverse mode buck-boost switching waveforms (VIN > VOUT).

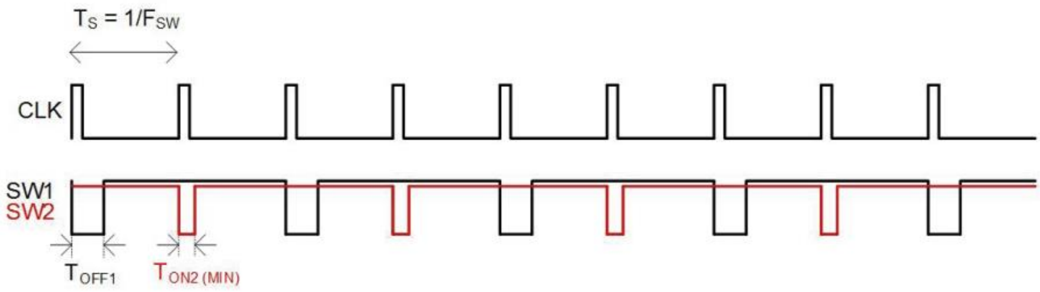

Figure 2.12 : Reverse mode buck-boost switching waveforms (VOUT > VIN).

2.5 Valley Current and Peak Current Limit

DC to DC converters have a limit on their output current. After the output current exceeds a certain current value, the converter can turn off its output or limit this current. The situation when it turns off its output is called hiccup mode. If the current level rises above the threshold current, the output is turned off. It tries to open the output again after a certain period of time after the output is closed. If the output current is below the threshold level, the output output is driven normally. However, if a current above the limit is still drawn from the output, the output turns off again. Figure 2.13 [22] shows an image of the Hiccup mode working. The output is turned off due to exceeding the threshold level at time T1. There is a waiting period at time T2. This waiting time is generally used to cool the heated switching element. From moment T3, the output is turned on in soft start mode, that is, by softening the output voltage. In the T3 time period, the output is turned off again because the current limit exceeds the threshold level.

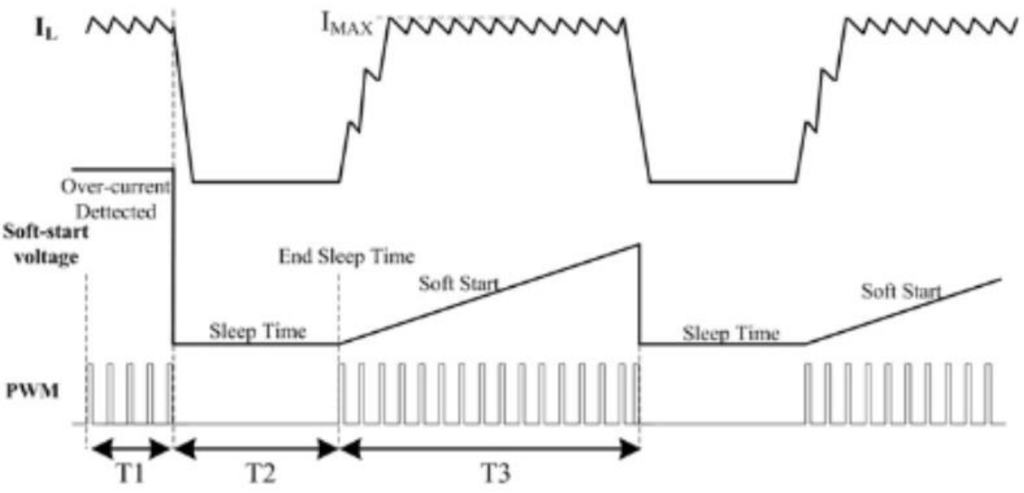

Figure 2.13 : Principal diagram of hiccup mode over current protection.

At Time A of Figure 2.14 [23], the DC to DC converter produces the set fixed output voltage. In Time B, there is an increase in the load current over time. At the end of the Time B period, the load current reaches the current limit level. In this case, an attempt is made to prevent the increase of the load current by extending the switching off time. The load current decreases during the time the MOSFET remains OFF. During the time when the MOSFET is ON, the load current increases. In other words, while the current limit is made in the OFF-time period of the MOSFET, there is no limitation in the ON time period. This limiting event is called Valley Current Limit.

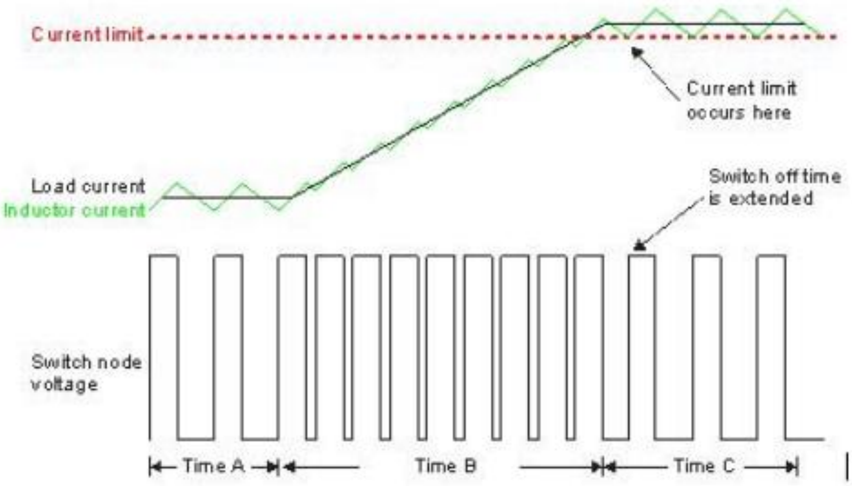

Figure 2.14 : Valley current limit.

At Time A of Figure 2.15 [23], the DC to DC converter produces the set fixed output voltage. In my Time B time period, there is an increase in the load current over time. At the end of the Time B period, the load current reaches the current limit level. In this case, an attempt is made to prevent the increase of the load current by narrowing the ON time of the switching. The load current decreases while the MOSFET remains ON. During the time when the MOSFET is OFF, the load current increases. In other words, while the current limit is made in the ON time period of the MOSFET, there is no limitation in the OFF time period. This limiting event is called Peak Current Limit.

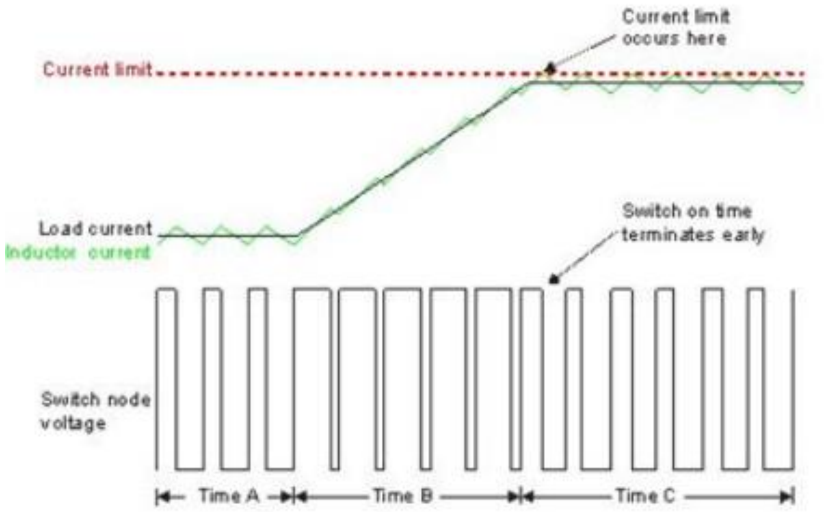

Figure 2.15 : Peak current limit.

2.6 Bootstrap and Charge Pump Circuitry

N-channel MOSFETs are widely used in switching power supplies. Voltages higher than 5V – 6V are applied to the Gate and Source pins of MOSFETs to conduct transmission. This is not a problem for the MOSFETs located on the low side of the Four Switch Buck Boost Converter structure. Because the gate driver can provide voltage up to approximately 20V. Since the source pin of the MOSFET on the low side is ground referenced, this voltage level is sufficient for the gate driver. However, for MOSFETs on the high side, this is a problem that must be overcome. For this purpose, bootstrap and charge pump structures are used for high side MOSFETs. Bootstrap structure is used where there is switching. Charge pump is used where there is no switching and the MOSFET is in continuous conduction. A visual of a standard bootstrap circuit is shown in Figure 2.16 [24]. The gate driver includes high side and low side drivers. The bootstrap circuit includes diode, resistor, and capacitor. The bootstrap circuit is connected to the high side driver.

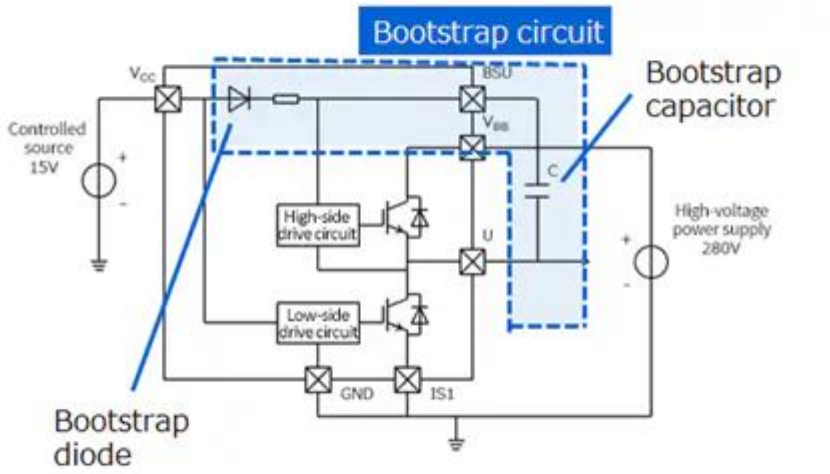

Figure 2.16 : Bootstrap circuitry.

The operation of the Bootstrap circuit occurs in two phases. In the first phase, the bootstrap capacitor (C) is charged. In the second phase, the capacitor is discharged. While the high side driver output is driven LOW, the capacitor (bootstrap) is charged through the diode, resistor, and gate driver low side driver. The visual of charging is shown in Figure 2.17[24].

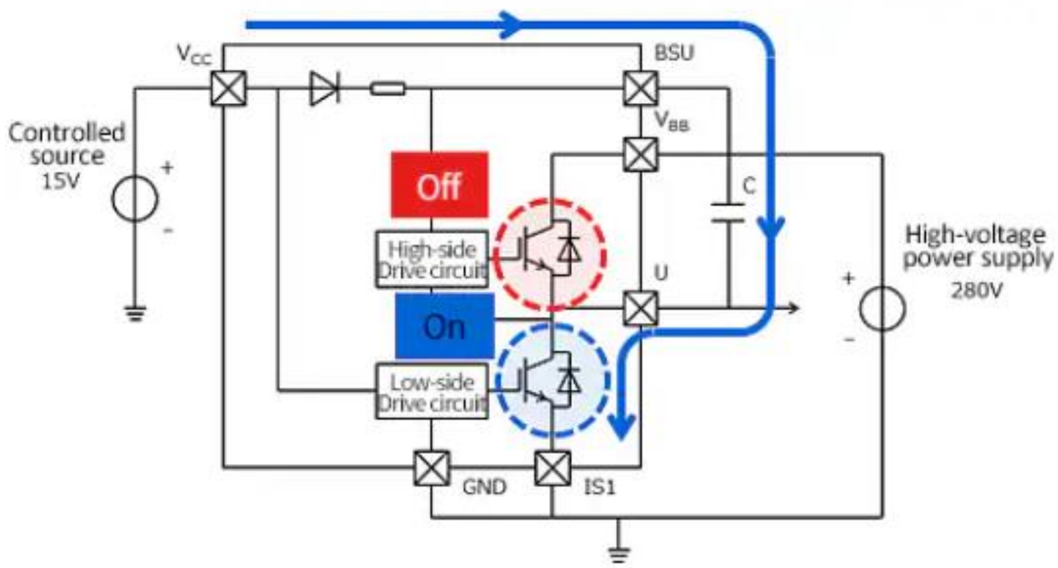

Figure 2.17 : Bootstrap charge operation.

While the high side driver output is driven high, the capacitor (bootstrap) feeds the high side driver as a discharge. It can drive the N-channel MOSFET in this way by high side driver bootstrap capacitor. The visual of charging the Bootstrap capacitor is shown in Figure 2.18 [24].

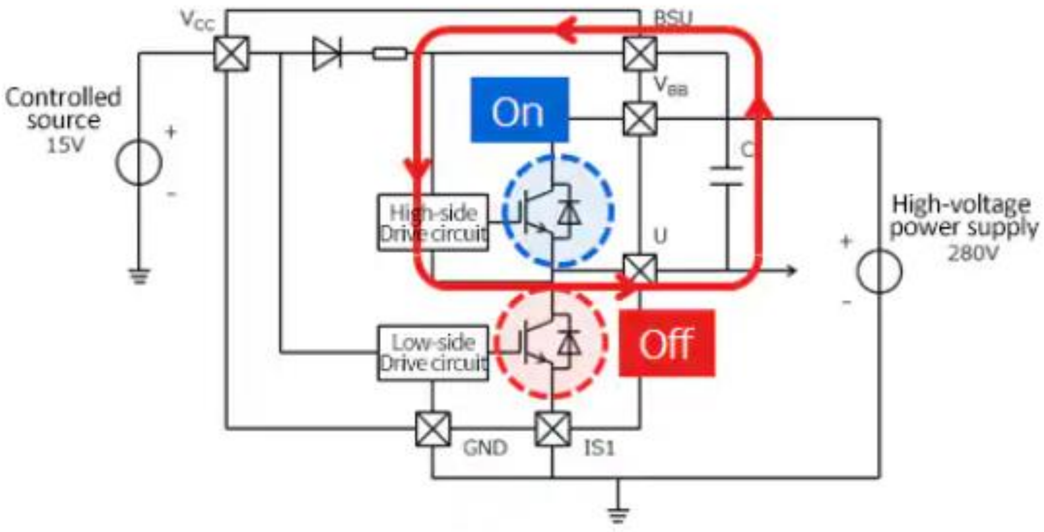

Figure 2.18 : Bootstrap discharge operation.

The minimum amount of capacitance to be used in the bootstrap circuit design depends on the input capacitance of the N-Channel MOSFET to be driven. Calculation of the bootstrap capacitance minimum value is included in equation 2.22 [25].

$$Cboot \geq Cgate * 10 \tag{2.22}$$

The charge pump structure is used with the bootstrap structure. The charge pump structure simply consists of 2 diodes, 1 capacitor and 2 resistors. As seen in Figure 2.19, the negative pin of the C1 capacitor is switched with a certain frequency. Meanwhile, D1 and D2 enter transmission and cut-off. Meanwhile, the C2 capacitor is charged to a higher voltage due to switching. This voltage can be used continuously by the gate driver after it is charged.

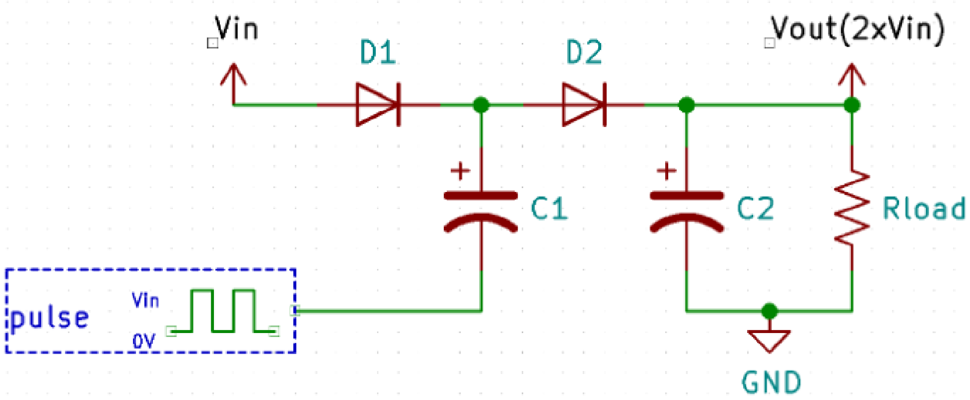

Figure 2.19 : Basic schematic for charge pump circuitry.

2.7 MOSFET Considerations and Power Dissipation Values

When choosing the optimum MOSFET for buck boost converter, it is necessary to pay attention to many values: Input voltage range, output voltage range, Rdson value, maximum drain source current, SOA, thermal resistance, package, and operating frequency. It is important to select the appropriate MOSFET based on the requirements of the design.

Since MOSFET is used as a switching element in the circuit, there are losses on it. Switching can only be achieved within the current and voltage limits that the selected MOSFET can withstand. If the maximum limits of the MOSFET are exceeded, the MOSFET will be damaged. Therefore, many problems arise in the operation of the circuit and the converter cannot function properly. Losses on MOSFET are divided into two: conduction loss and switching loss.

2.7.1 Forward buck mode power loss values

If the converter operates as a forward buck, the switching loss on Q1 is calculated as in equation 2.23.

$$Q1 = \frac{IOUT^2 * Rdson * VOUT}{VIN} + \frac{\mathrm{IOUT} * VIN * tsw * Fsw}{2} \tag{2.23}$$

Switching loss on Q2 is calculated as in equation 2.24.

$$Q2 = \frac{IOUT^2 * Rdson * (VIN - VOUT)}{VIN} \tag{2.24}$$

During forward buck mode operation, the power dissipation value is 0W because Q4 is not transmitting. Since Q3 is in continuous transmission, the switching loss value is equal to zero. However, there is a conduction loss value. The conduction loss value on Q3 is calculated as in equation 2.25.

$$Q3 = IOUT^2 * Rdson \tag{2.25}$$

2.7.2 Reverse buck mode power loss values

If the converter operates as a reverse buck, the switching loss on Q3 is calculated as in equation 2.26.

$$Q3 = \frac{IOUT^2 * Rdson * VIN}{VOUT} + \frac{\mathrm{IOUT} * VOUT * tsw * Fsw}{2} \tag{2.26}$$

Switching loss on Q4 is calculated as in equation 2.27.

$$Q4 = \frac{IOUT^2 * Rdson * (VOUT - VIN)}{VOUT} \tag{2.27}$$

During reverse buck mode operation, the power dissipation value is 0W because Q2 is not conducting. Since Q1 is in continuous transmission, the switching loss value is equal to zero. However, there is a conduction loss value. The conduction loss value on Q1 is calculated as in equation 2.28.

$$Q1 = IOUT^2 * Rdson \tag{2.28}$$

2.7.3 Forward boost mode power loss values

If the converter operates as a forward boost, the switching loss value on Q3 is calculated as in equation 2.29.

$$Q3 = \frac{IOUT^2 * Rdson * VOUT}{VIN} \tag{2.29}$$

Switching loss on Q4 is calculated as in equation 2.30.

$$Q4 = \frac{(IOUT^2 * VOUT^2)}{VIN^2} * \frac{(VOUT - VIN) * Rdson}{VOUT}$$
$$+ IOUT * VOUT^2 * tsw * \frac{Fsw}{2 * VIN} \tag{2.30}$$

During forward boost mode operation, the power dissipation value is 0W because Q2 is not conducting. Since Q1 is in continuous transmission, the switching loss value is equal to zero. However, there is a conduction loss value. The conduction loss value on Q1 is calculated as in equation 2.31.

$$Q1 = \frac{IOUT^2 * VOUT^2}{VIN^2} * Rdson \tag{2.31}$$

2.7.4 Reverse boost mode power loss values

If the converter operates as a reverse boost, the switching loss value on Q1 is calculated as in equation 29.

$$Q1 = \frac{IOUT^2 * Rdson * VIN}{VOUT} \tag{2.32}$$

Switching loss on Q4 is calculated as in equation 2.33.

$$Q4 = \frac{(IOUT^2 * VIN^2)}{VOUT^2} * \frac{(VIN - VOUT) * Rdson}{VIN} + IOUT * VIN^2 * tsw * \frac{Fsw}{2 * VOUT} \tag{2.33}$$

During reverse boost mode operation, the power dissipation value is 0W because Q4 is not conducting. Since Q3 is in continuous transmission, the switching loss value is equal to zero. However, there is a conduction loss value. The conduction loss value on Q3 is calculated as in equation 2.34.

$$Q3 = \frac{IOUT^2 * VIN^2}{VOUT^2} * Rdson \tag{2.34}$$

In addition to all these, switching should not occur simultaneously between the Q1 and Q2 MOSFETs and between the Q3 and Q4 MOSFETs. There must be a deadtime between the MOSFETs of Q1 and Q2 to prevent them from operating at the same time. Otherwise, these MOSFETs will go into a short state and Figure 2.20the source will become ground or even short. The same situation applies to the Q3 and Q4 MOSFETs. If there is no deadtime, electromagnetic noise increases, losses increase and efficiency decreases. There are two separate dead times between the Q1 and Q2 MOSFETs during the rise time of the Q1 MOSFET and the rise time of the Q2 MOSFETs. Total dead time is the sum of these two dead times. Figure 2.20 contains a visual indicating this situation.

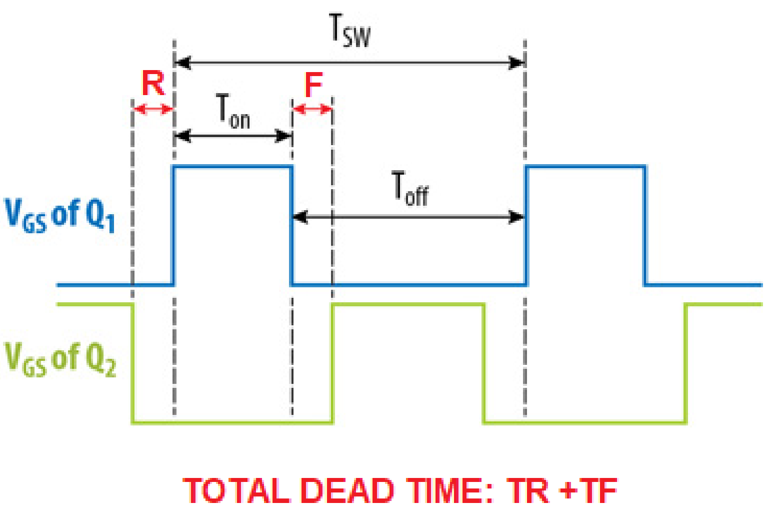

Figure 2.20: Switching Dead Time.

2.8 TM4C123GH6PM Microcontroller

TM4C123GH6PM microcontroller is used as the basis of the four-switch buck boost converter. The processor performs many operations such as reading input and output voltages, reading input and output current, and producing PWM output. The entire algorithmic structure is built on this processor. TM4C123GH6PM is a 32-bit Arm Cortex-M4F based processor. Some features of this processor:

- 80MHz maximum operation frequency,
- Two PWM modules,
- Two 12-bit ADC modules,
- 1 RTC.

The high-level block diagram of the TM4C123GH6PM processor is shown in Figure 2.21 [26].

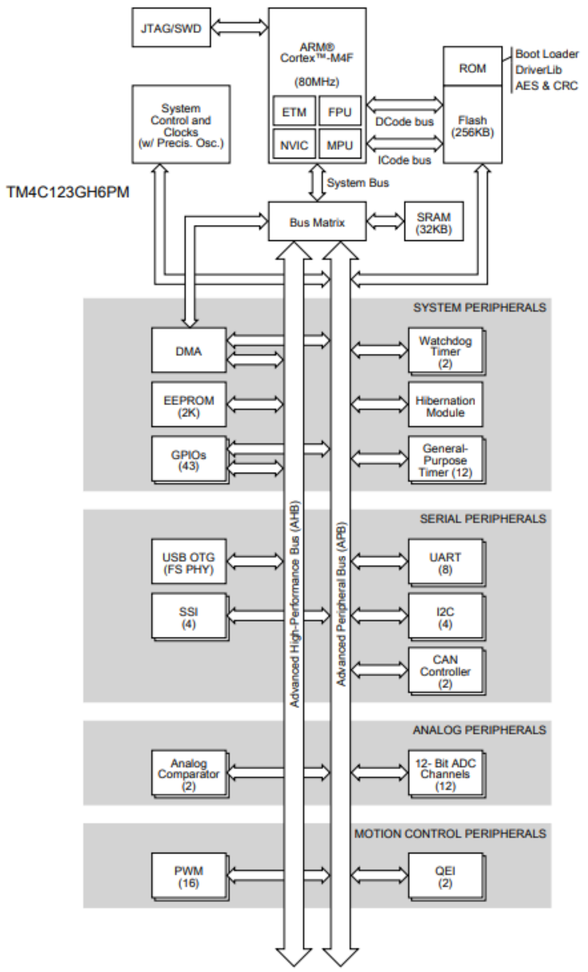

Figure 2.21 : TM4C123GH6PM microcontroller high-level block diagram.

2.8.1 TM4C123GH6PM GPIO module

TM4C123GH6PM consists of 6 physical GPIO blocks [26]. These blocks are called ports: Port A, Port B, Port C, Port D, Port E, Port F. There are 43 programmable input or output pins in total. TM4C123GH6PM Digital I/O Pads are shown in Figure 2.22. [26].

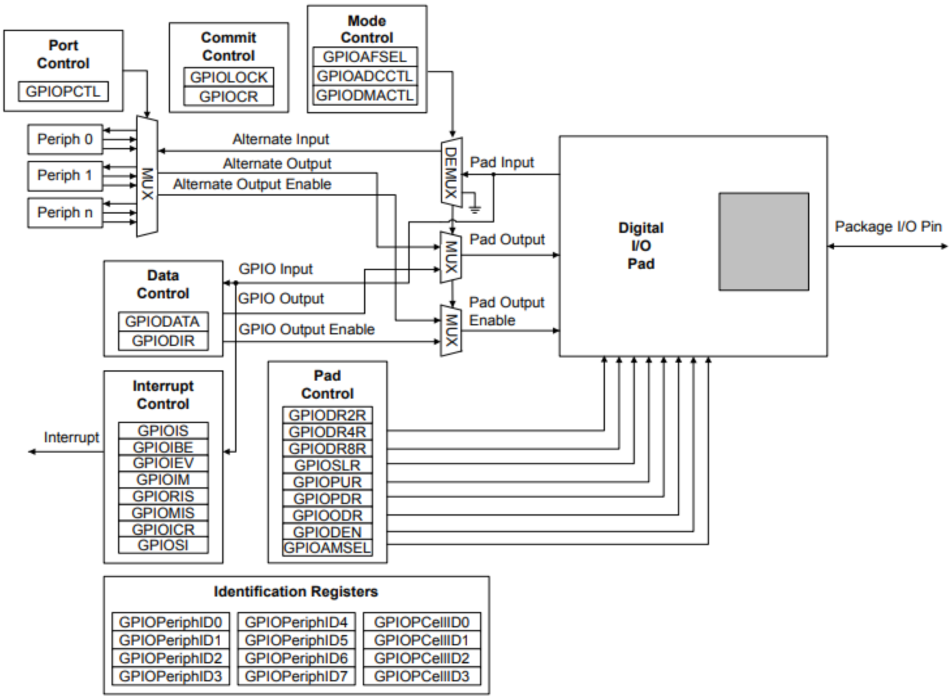

Figure 2.22 : TM4C123GH6PM digital I/O pads.

2.8.2 TM4C123GH6PM ADC module

TM4C123GH6PM microcontroller has 2 ADC modules [26] as shown in Figure 2.23. Each ADC module has 12-bit conversion resolution and 12 input channels. In addition, there is an internal temperature sensor. Channel inputs can be configured as single-ended or differential-input. The ADC module also has hardware sampling capability. It can sample up to 64 samples.

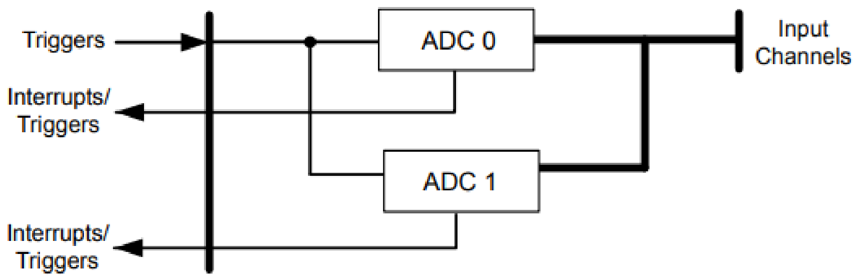

Figure 2.23 : TM4C123GH6PM implementation of two ADC blocks.

2.8.3 TM4C123GH6PM PWM module

TM4C123GH6PM contains 2 PWM modules and each PWM module contains 4 PWM generators. There are 16 PWM outputs in total. Each PWM generator works simultaneously with the same timer and frequency. The block diagram of the processor's PWM module is shown in Figure 2.24.

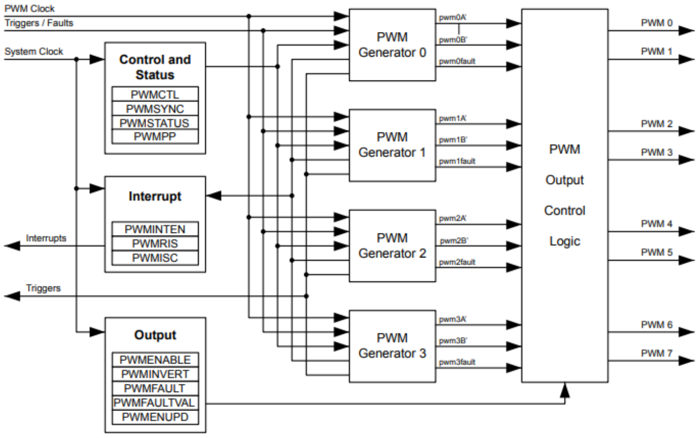

Figure 2.24 : TM4C123GH6PM PWM module diagram.

PWM Module can operate in both down and up/down mode with a 16-bit counter. One of the most distinctive features of the PWM module is that it can produce PWM dead time. It can create dead time for the set amount of time between 2 signals coming from the same PWM generator output. The process of driving the gate driver of the DC to DC converter will be easier with this feature. In this way, zero voltage switching (ZVS) can be performed without the need for an extra dead time generator.

Each PWM Generator block within the PWM modules is shown in Figure 2.25.

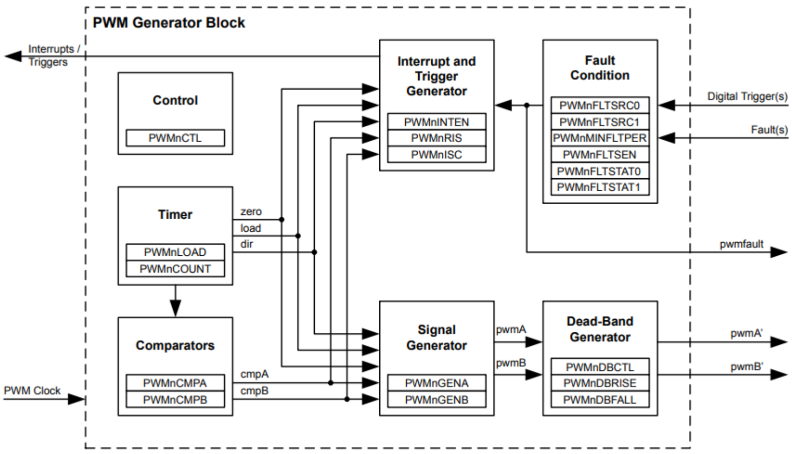

Figure 2.25 : PWM Generator block diagram

3 SYSTEM DESIGN

The bi-directional buck boost converter circuit includes voltage divider circuitries, sense resistors, bi-directional current sense amplifiers, buck leg, boost leg, temperature sensors, indicator leds, microcontroller and low dropout regulator. Since the input and output voltages are high for the processor, these voltages must be reduced at certain rates. Therefore, it is converted into voltages in the appropriate range for the processor with the voltage divider circuit. The voltages on the sense resistors at the inputs and outputs are measured by the bi-directional current sense amplifier circuit and transferred to the mirocontroller. The amplifier can measure current in both forward and reverse directions. Buck leg and boost leg contain MOSFET and Gate Driver circuit. The switching signals applied to the gate driver increase the voltage levels required to drive the MOSFET. It contains buck leg and boost leg, bootstrap, and charge pump circuits together. Both 100% duty cycle and variable duty cycle signals can be produced. Temperature measurements of the electronic card and switching MOSFETs are carried out with temperature sensors. It can physically seen whether it is in working condition, whether there is an error part, and whether power is applied the Indicator LEDs on the board. The voltage level required by the microcontroller is produced with the low drop regulator. The microcontroller is powered from both input and output. The microcontroller constitutes the brain of the circuit. Thanks to analog inputs, temperature, current and voltage information is transferred to these inputs by making various transformations. Based on this information, the microcontroller, gate driver and indicator LEDs are driven.

General operating information of the converter is as follows:

Input/Output voltage range: 9V-50V,

Input/Output maximum current: up to 5A,

Operating Frequency: 50kHz –300kHz, default(100kHz)

Operating temperature range: -40°C to +105°C,

The block diagram of the architecture is in **Figure 3.1**.

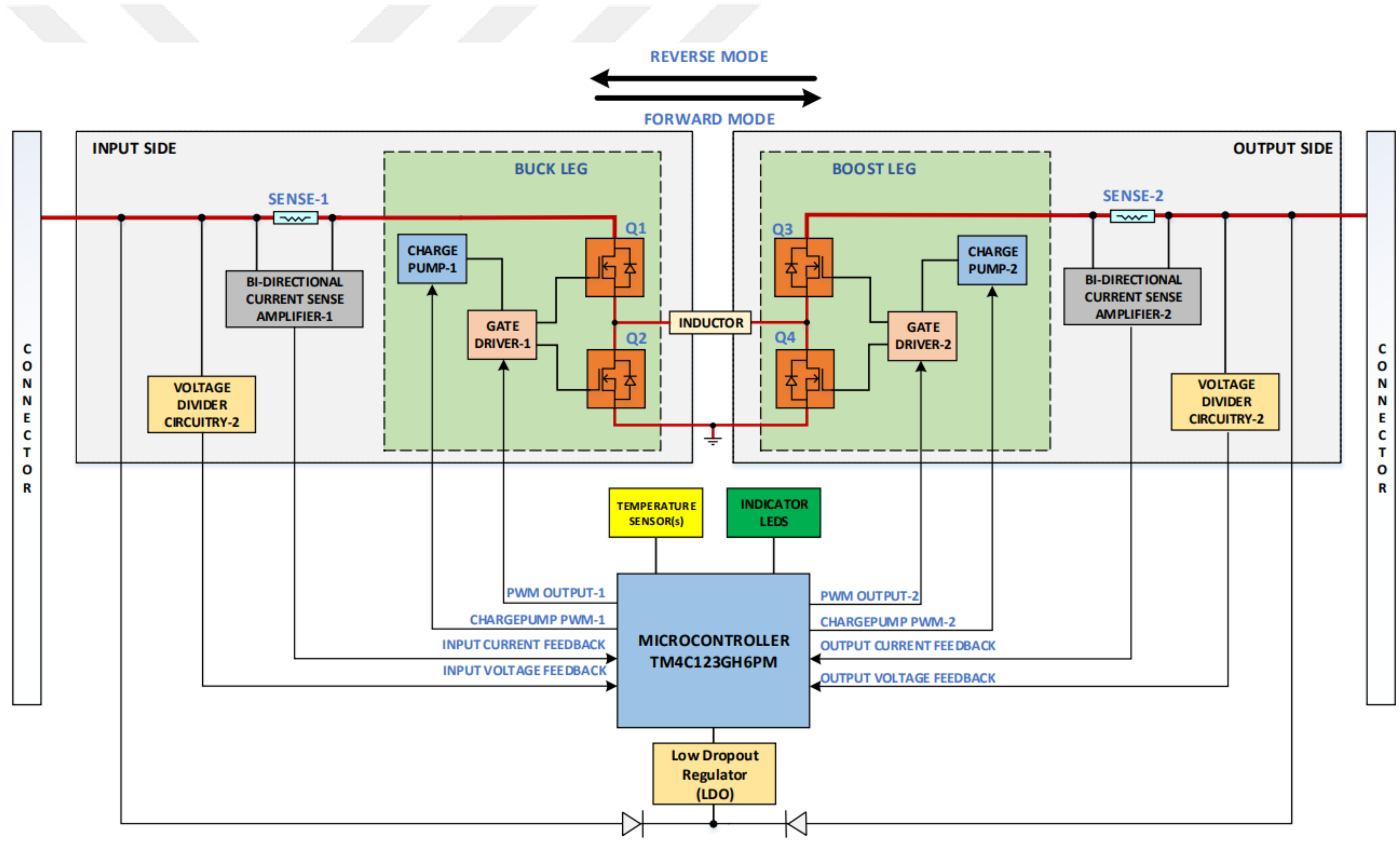

Figure 3.1 : Main block diagram of bi-directional buck boost converter.

4 SOFTWARE DESIGN OF THE CONVERTER

4.1 Main System Algorithm

The central processing unit of the DC to DC converter is TM4C123GH6PM microcontroller. The microcontroller takes measurements from the input units and drives the necessary peripheral units accordingly. The system level flowchart of the software written in the C programming language within the microcontroller is shown in Figure 4.1.

If voltage is applied to the input or output of the DC to DC converter, the voltage proper for the processor is produced by the LDO and power input is provided to the microcontroller. Before the software starts, the registers are reset by powering on the microcontroller.

There are basically 8 steps in the software.

In the first step, the peripheral units to be used are configured. The configured units are basically as follows:

- General Purpose Input Output (GPIO),
- Pulse Width Modulation (PWM),
- Analog to Digital Converter (ADC),
- Nested Vectored Interrupt Controller (NVIC),
- Universal asynchronous receiver-transmitter (UART).

In the second step, it is verified that all these configuration parameters are set correctly.

The second step is the variable definition. In this step, many status variables that are required for the converter to work are defined. Main variables of the software are shown in Table 4.1.

Table 4.1 : Main variables of the software.

Variable	Definition
MODE_BUCK_FW	States Forward Mode Buck Conversion
MODE_BOOST_FW	States Forward Mode Boost Conversion
MODE_BUCKBOOST_FW	States Forward Mode Buck Boost Conversion
MODE_BUCK_RVS	States Reverse Mode Buck Conversion
MODE_BOOST_RVS	States Reverse Mode Boost Conversion
MODE_BUCKBOOST_RVS	States Reverse Mode Buck Boost Conversion
MODE_VIN_UVLO	Input Under voltage Detection
MODE_VIN_VOUT_UVLO	Input and Output Under voltage Detection
MODE_VINOVLO	Input Overvoltage Detection
MODE_VOUTOVLO	Output Overvoltage Detection
MODE_NOSWITCH	No Switching
VIN_CONSTANT	Input Voltage Coefficient of The Hardware
VOUT_ CONSTANT	Output Voltage Coefficient of The Hardware
IIN_ CONSTANT	Input Current Coefficient of The Hardware
IOUT_ CONSTANT	Output Current Coefficient of The Hardware
PWM_OUTPUT-1	Duty cycle of GATE DRIVER-1
PWM_OUTPUT-2	Duty cycle of GATE DRIVER-2
PID_Coeff	PID Coefficients

In the third step, the following basic parameters are set. If these parameters are not set, default values are used. Main parameters of the software are shown in Table 4.2.

Table 4.2 : Main parameters of the software.

Variable	Definition
VIN	Input Voltage
VOUT	Output Voltage
VINUVLO	Input Threshold Voltage
VINOVP	Maximum Input Voltage
VOUTOVP	Maximum Output Voltage
VOUTUVLO	Minimum Output Voltage
IIN_FWD_LIM	Forward Input Current Limit
IOUT_FWD_LIM	Forward Output Current Limit
IIN_RVS_LIM	Reverse Input Current Limit
IOUT_RVS_LIM	Forward Output Current Limit
FWD_MODE_EN	Forward Mode Operation Enable
RVS_MODE_EN	Reverse Mode Operation Enable

Starting from the fourth step, a continuous working cycle is entered. In ADC channels, input voltage, output voltage, input current, output current and IC temperature data are read and interpreted.

In the 5th step, the suitability of the input or output voltage values is checked. These protections are generally Input Overvoltage Protection, Output Overvoltage Protection, Input and Output Under Voltage Protection.

If a voltage outside the input and output threshold values determined in the previous steps is detected, the switching process is terminated. If a value is within the threshold values, Forward or Reverse switching is performed according to the input and output voltage values.

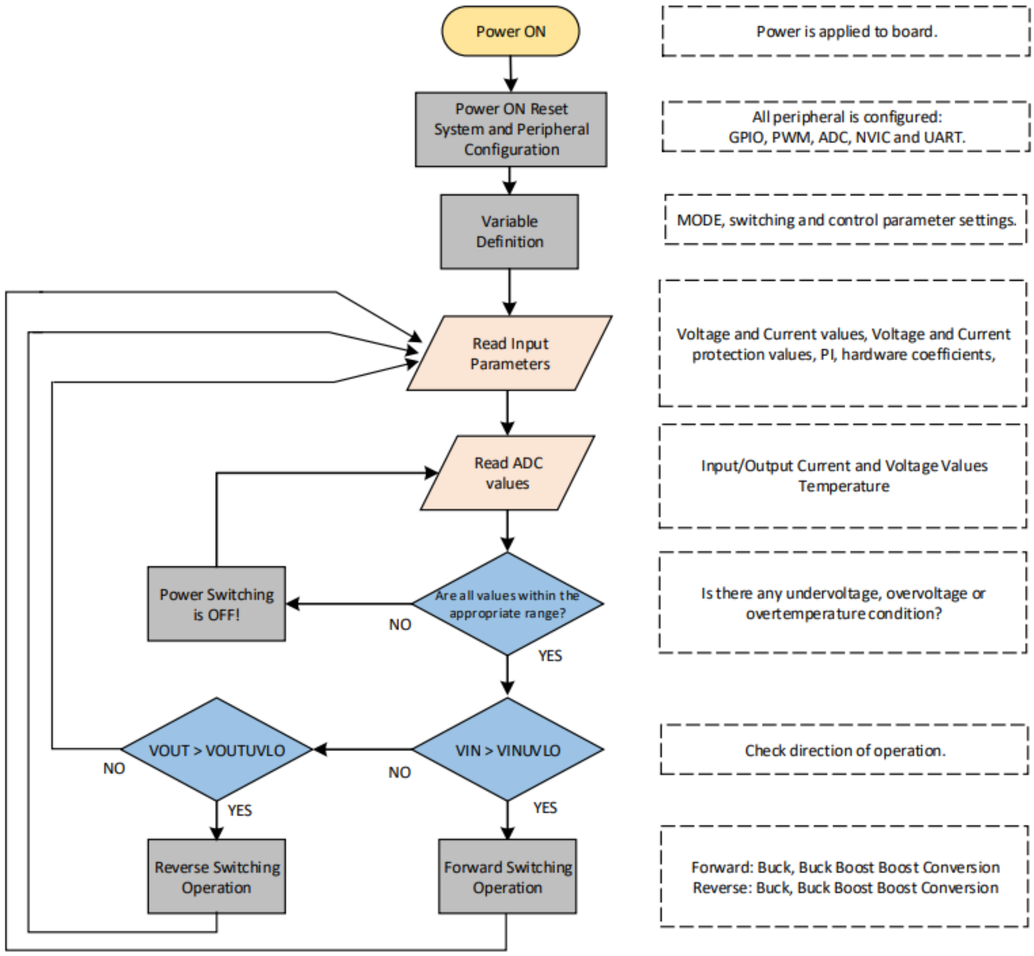

Figure 4.1 : Bi-directional buck boost converter system flowchart.

4.2 Peripheral Configuration Algorithm

The processor is configured before proceeding with the necessary conversion steps. The flowchart of peripheral configuration is shown in Figure 4.2. First, the clock on the processor is set. The processor clock line is activated, and the operating frequency is determined. GPIO, PWM, ADC, NVIC and UART peripherals are then configured.

The configuration of the GPIO peripheral unit determines which pins will be assigned as input/output, the types of input-outputs and the withstand current.

With the configuration of the PWM peripheral unit, which pins will be used as PWM, the selection of the PWM module, the frequency of the wave, the activation of the PWM generator and the dead time are determined.

With the configuration of the ADC peripheral unit, which pins will be used as ADC inputs, selecting the ADC module, determining the hardware sampling value, determining the sequencer, and resetting the interrupt register are performed.

With the configuration of the NVIC peripheral unit, the interrupt priority order under which conditions the interrupt will be provided and the activation of the interrupt registers are made.

With the configuration of the UART peripheral unit, which pins will be used for data flow, baud rate and parity information are determined.

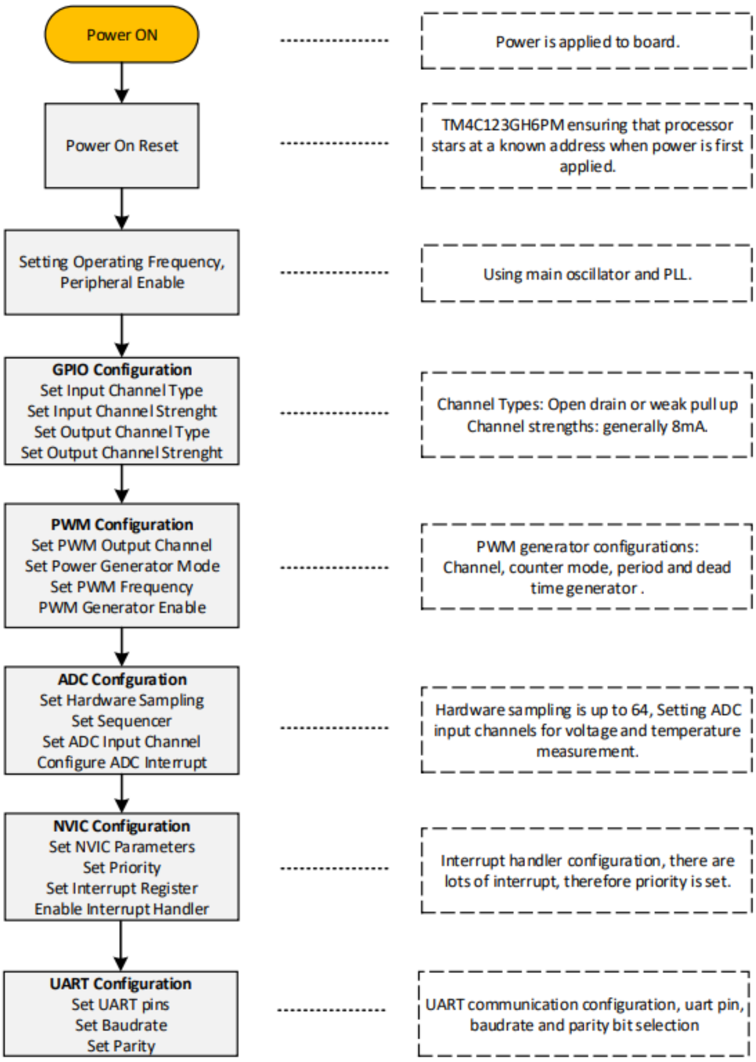

Figure 4.2 : Peripheral configuration flowchart.

4.3 Forward Operation Algorithm

If the input voltage is greater than the minimum input threshold voltage (VINUVLO), the converter operates in the forward direction. The flowchart of forward operation is shown in Figure 4.3. First, the input and output currents read raw from the ADC are calculated and converted into real values. Three different operating states occur depending on the input voltage value; buck mode, buck boost mode and boost mode. If the input voltage is greater than the output voltage, it is in buck mode, if the input voltage is close to the output voltage, it is in buck boost mode, if the output voltage is greater than the input voltage, it is in boost mode, and if a voltage other than these is read, the switching is stopped.

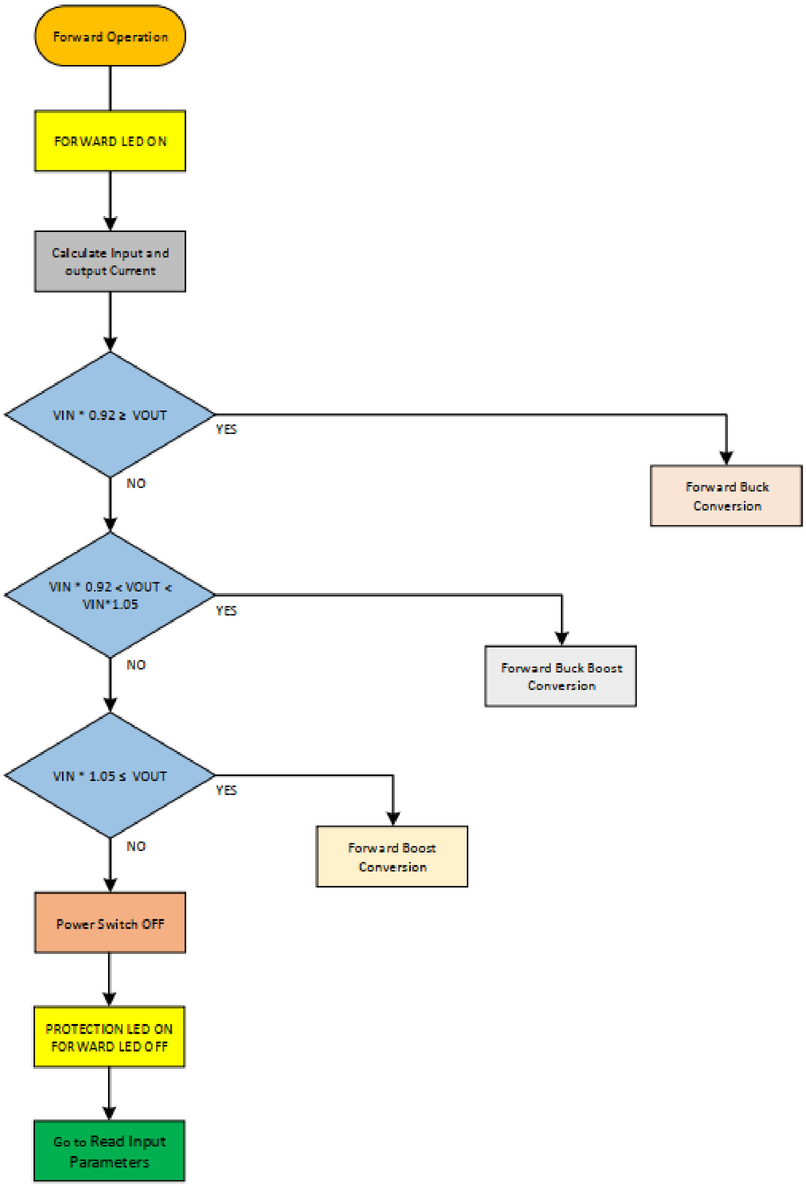

Figure 4.3 : Forward mode operation flowchart.

4.3.1 Forward buck mode conversion algorithm

In buck mode operation, Set Mode is equal to FORWARD BUCK CONVERTER. The flowchart of forward buck mode is shown in Figure 4.4. It is checked whether the current exceeds the limit current value. If the current is above the current limit, the Current Error value is calculated and the PWM OUTPUT-1 value is found according to this value. If the current is below the limit value, the Voltage Error value is calculated and the PWM OUTPUT-1 value is found according to this value. It is checked whether the PWM OUTPUT-1 value is between its minimum and maximum limits. If this value is greater than 96%, PWM OUTPUT-1 = 96, if less than 4%, PWM OUTPUT-1 = 4. The PulseWidthBuck value is given to the GATE DRIVER-1. The GATE DRIVER-2 is driven by 100% PWM.

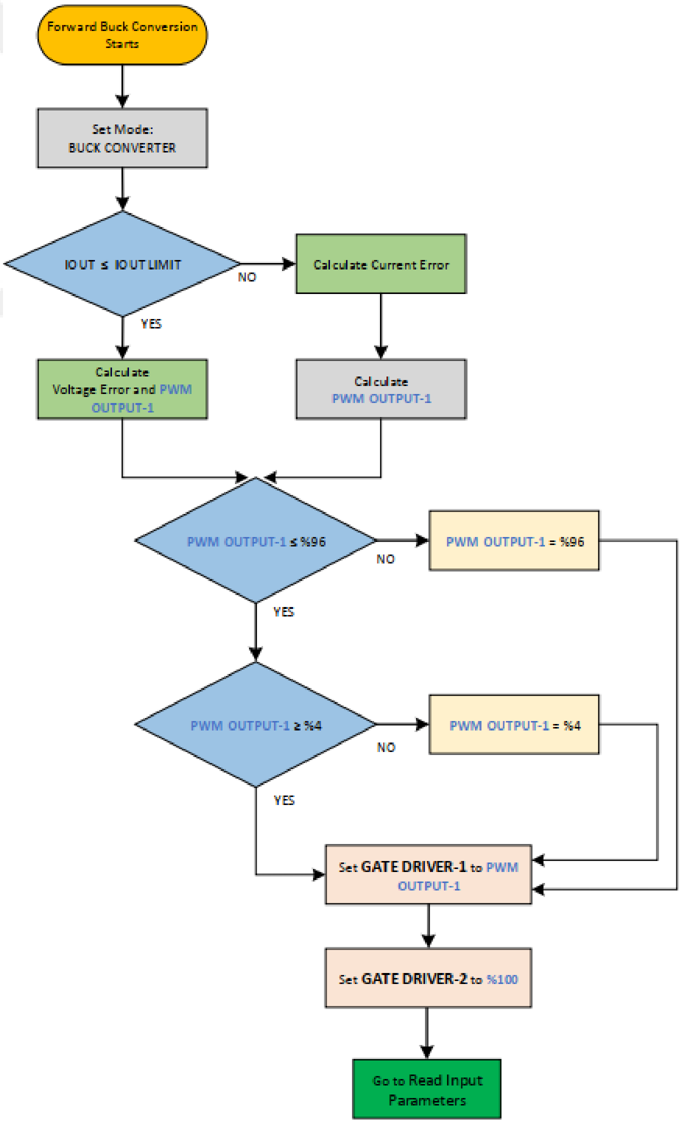

Figure 4.4 : Forward buck conversion flowchart.

4.3.2 Forward buck boost mode conversion algorithm

In buck boost mode operation, Set Mode is equal to FORWARD BUCK BOOST CONVERTER. The flowchart of forward buck boost mode is shown in Figure 4.5. It is checked whether the current exceeds the limit current value. If the current is above the current limit, the Current Error value is calculated and the PWM OUTPUT-2 value is found according to this value. If the current is below the limit value, the Voltage Error value is calculated and the PWM OUTPUT-2 value is found according to this value. It is checked whether the PWM OUTPUT-2 value is between its minimum and maximum limits. If this value is greater than 96%, PWM OUTPUT-2= 96, if less than 4%, PWM OUTPUT-2= 4. The PWM OUTPUT-2 value is given to the GATE DRIVER-2. The GATE DRIVER-1 is driven with 90% PWM.

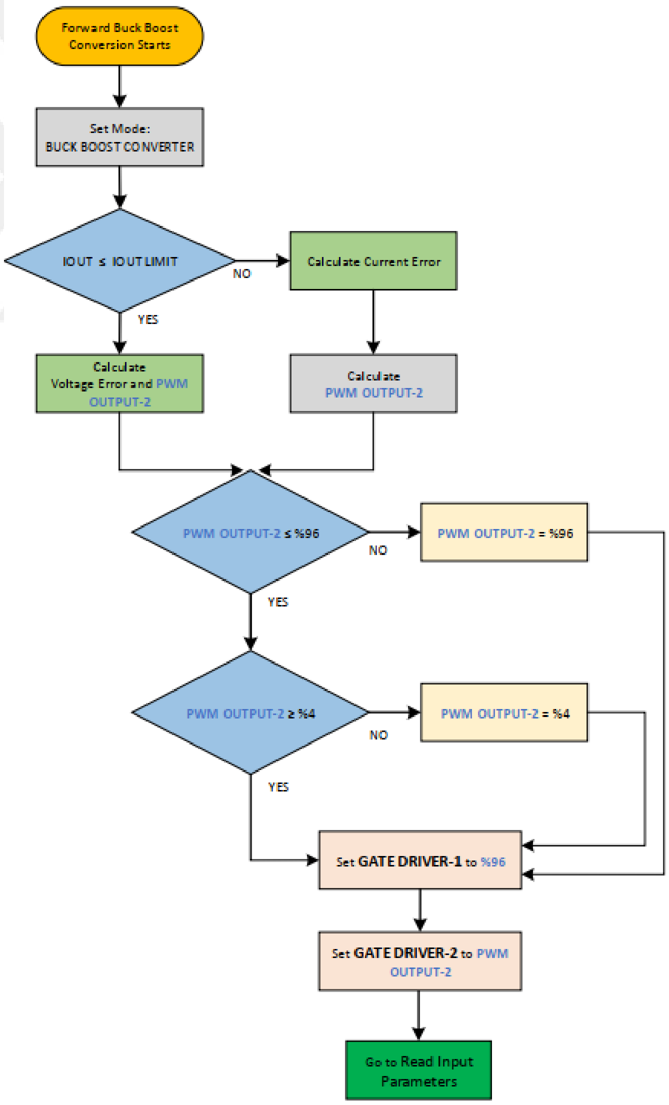

Figure 4.5 : Forward buck boost conversion flowchart.

4.3.3 Forward boost mode conversion algorithm

In boost mode operation, Set Mode is equal to FORWARD BOOST CONVERTER. The flowchart of forward boost mode is shown in Figure 4.6. It is checked whether the current exceeds the limit current value. If the current is above the current limit, the Current Error value is calculated and the PWM OUTPUT-2 value is found according to this value. If the current is below the limit value, the Voltage Error value is calculated and the PWM OUTPUT-2 value is found according to this value. It is checked whether the PWM OUTPUT-2 value is between its minimum and maximum limits. If this value is greater than 96%, PWM OUTPUT-2 = 96, if less than 4%, PWM OUTPUT-2 = 4. The PWM OUTPUT-2 value is given to the GATE DRIVER-2. The GATE DRIVER-1 is driven with 100% PWM.

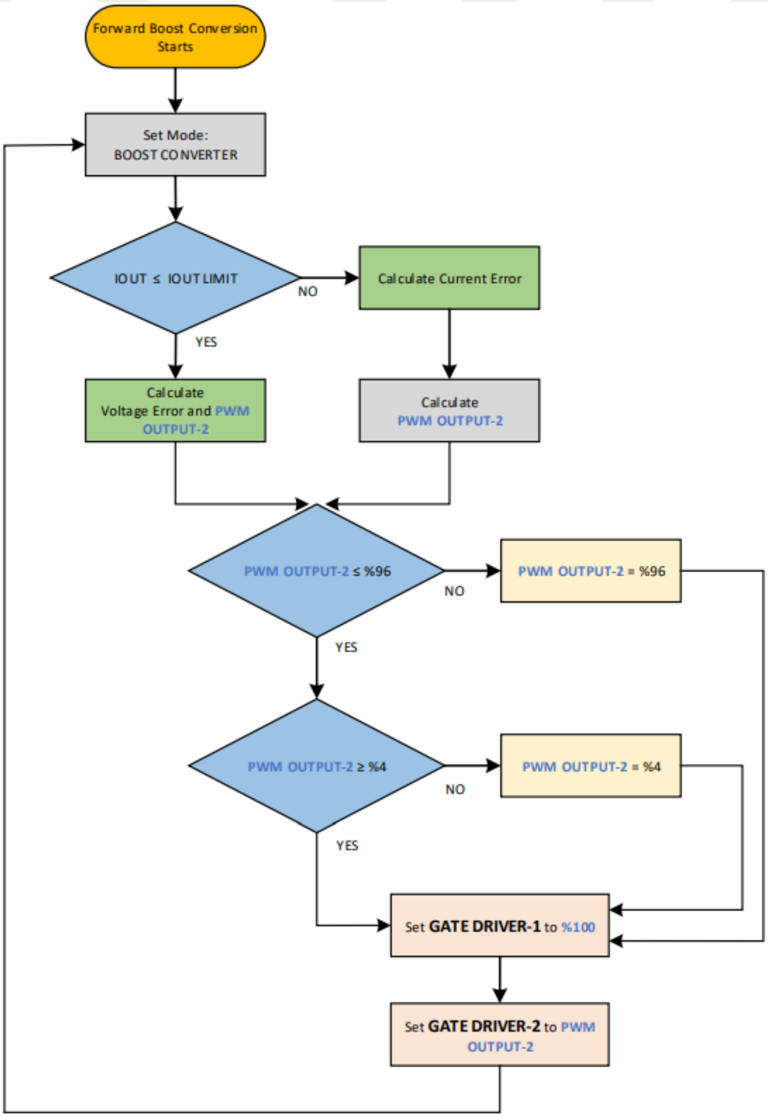

Figure 4.6 : Forward boost conversion flowchart.

4.4 Reverse Operation Algorithm

If the input voltage is below the minimum set input voltage and the output voltage is greater than the minimum output voltage, the converter operates in the reverse direction. The flowchart of reverse operation is shown in Figure 4.7. First, the input and output currents read raw from the ADC are calculated and converted into real values.

Three different operating states occur depending on the input voltage value; buck mode, buck boost mode and boost mode. If the input voltage is greater than the output voltage, it is in boost mode, if the input voltage is close to the output voltage, it is in buck boost mode, if the output voltage is greater than the input voltage, it is in buck mode, and if a voltage other than these is read, the switching is stopped.

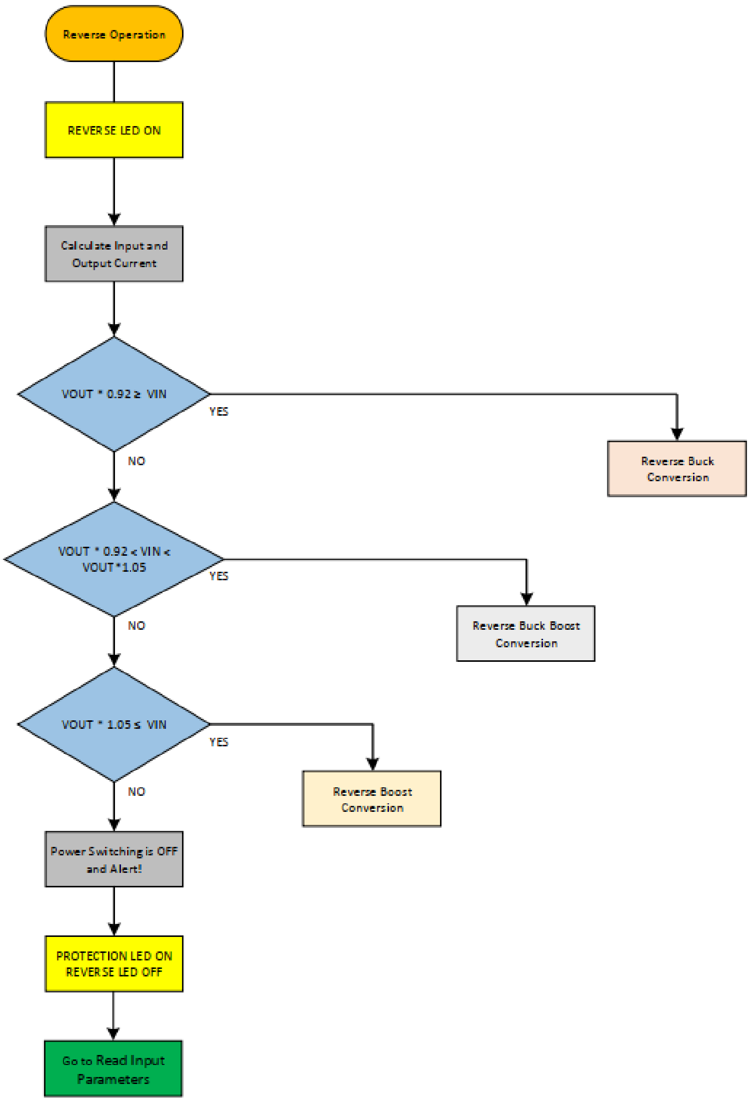

Figure 4.7 : Reverse mode operation flowchart.

4.4.1 Reverse buck mode conversion algorithm

In Reverse Buck mode operation, Set Mode is equal to REVERSE BUCK CONVERTER. The flowchart of reverse buck mode is shown in Figure 4.8. It is checked whether the current exceeds the limit current value. If the current is above the current limit, the Current Error value is calculated and the PWM OUTPUT-2 value is found according to this value. If the current is below the limit value, the Voltage Error value is calculated and the PWM OUTPUT-2 value is found according to this value. It is checked whether the PWM OUTPUT-2 value is between its minimum and maximum limits. If this value is greater than 96%, PWM OUTPUT-2 = 96, if less than 4%, PWM OUTPUT-2 = 4. The PWM OUTPUT-2 value is given to the GATE DRIVER-2. The GATE DRIVER-1 is driven with 100% PWM.

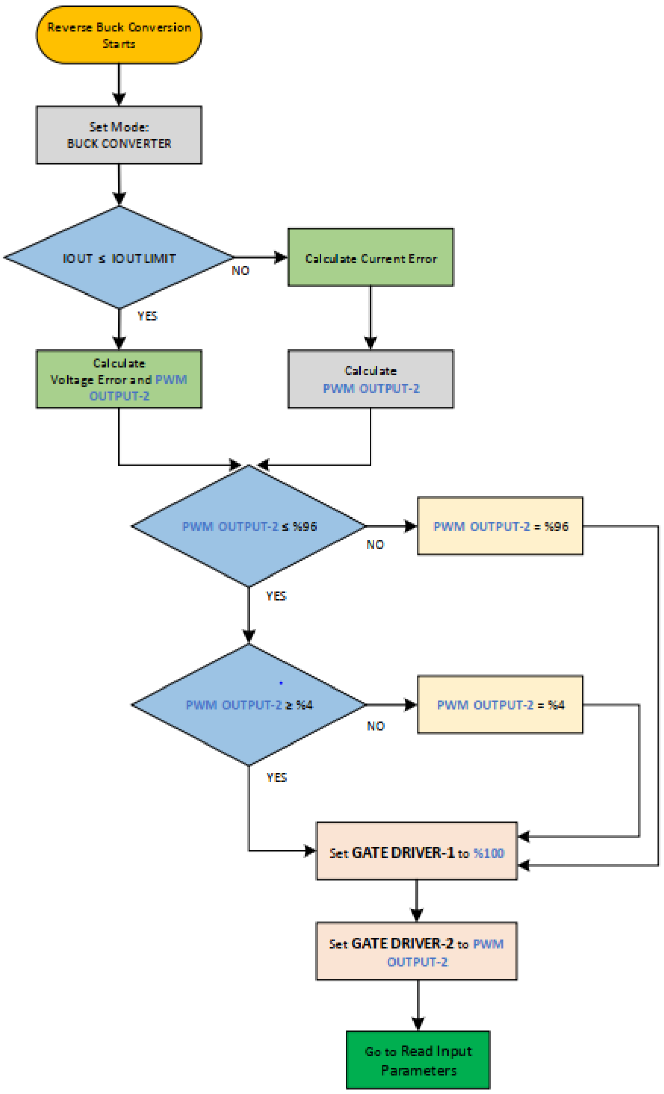

Figure 4.8 : Reverse buck conversion flowchart.

4.4.2 Reverse buck boost mode conversion algorithm

In reverse buck boost mode operation, Set Mode is equal to REVERSE BUCK BOOST CONVERTER. The flowchart of reverse buck boost mode is shown in Figure 4.9. It is checked whether the current exceeds the limit current value. If the current is above the current limit, the Current Error value is calculated and the PWM OUTPUT-1 value is found according to this value. If the current is below the limit value, the Voltage Error value is calculated and the PWM OUTPUT-1 value is found according to this value. It is checked whether the PWM OUTPUT-1 value is between its minimum and maximum limits. If this value is greater than 96%, PWM OUTPUT-1 = 96, if less than 4%, PWM OUTPUT-1 = 4. The PWM OUTPUT-1 value is given to the GATE DRIVER-1. GATE DRIVER-2 is driven with 90% PWM.

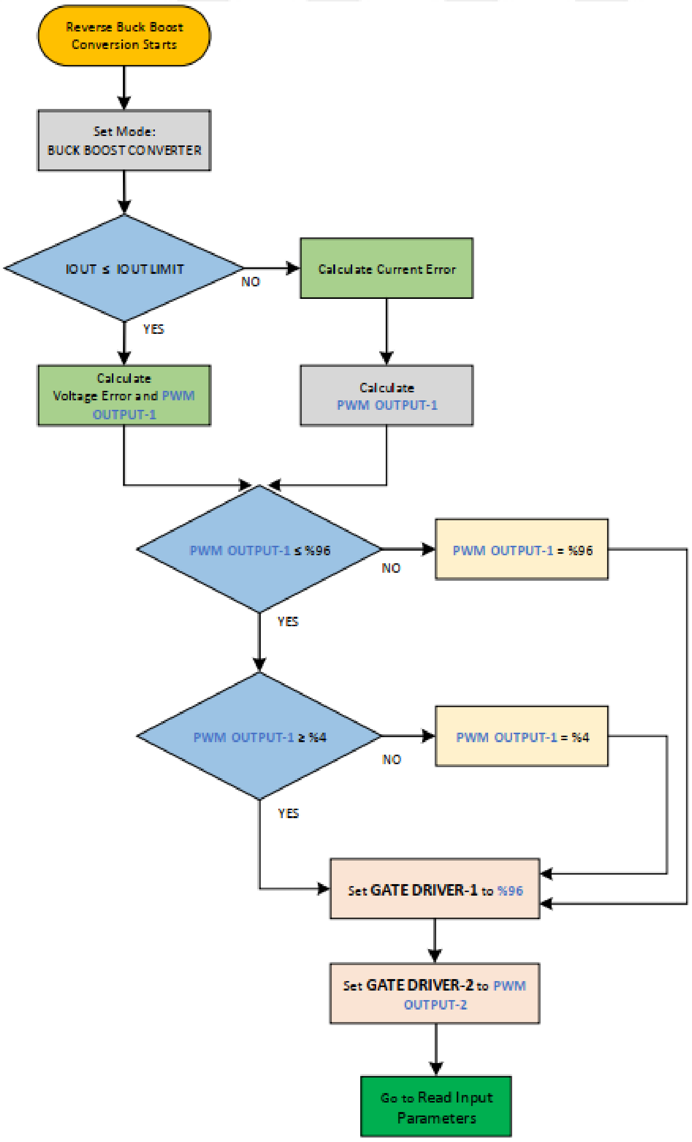

Figure 4.9: Reverse buck boost conversion flowchart.

4.4.3 Reverse boost mode conversion algorithm

In reverse boost mode operation, Set Mode is equal to REVERSE BOOST CONVERTER. The flowchart of reverse boost mode is shown in **Figure 4.10**. It is checked whether the current exceeds the limit current value. If the current is above the current limit, the Current Error value is calculated and the PWM OUTPUT-1 value is found according to this value. If the current is below the limit value, the Voltage Error value is calculated and the PWM OUTPUT-1 value is found according to this value. It is checked whether the PWM OUTPUT-1 value is between its minimum and maximum limits. If this value is greater than 96%, PWM OUTPUT-1 = 96, if less than 4%, PWM OUTPUT-1 = 4. The PWM OUTPUT-1 value is given to the GATE DRIVER-1. The GATE DRIVER-2 is driven by 100% PWM.

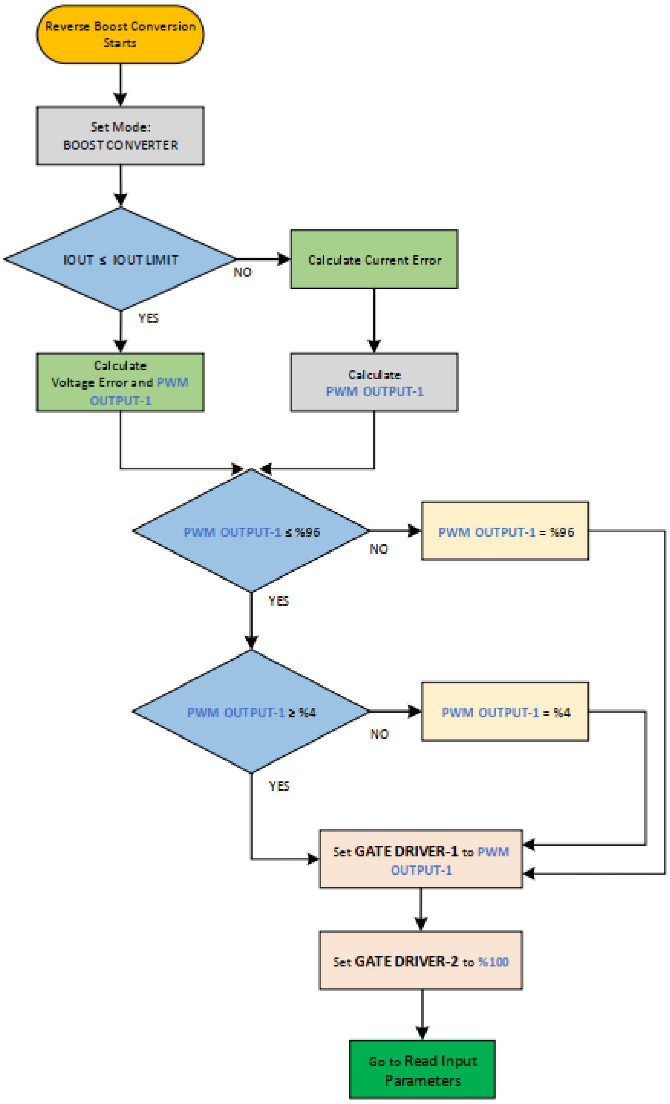

Figure 4.10: Reverse boost conversion flowchart.

5 HARDWARE DESIGN OF THE CONVERTER

Bidirictional buck boost converter design consists of two sections. These sections are hardware design and software design. Details about the software are explained in the "Bidiricitonal Buck Boost Converter Software Design" section. In this section, the hardware design is detailed. Hardware design of bi-directional buck boost converter consists of two stages: schematic and layout design. Altium Designer program is used for both schematic and layout design.

The schematic is a hierarchical design consisting of 7 pages, including “Top level”. These pages are named as follows.

- TOP_LEVEL
- TM4C123GH6PM_CONNECTION
- POWER_LEVEL
- SWITCHING
- LOW_SIDE_DRIVER
- CURRENT_SENSE
- STATUS_LEDs

The top-level connections of the schematic design are shown in “TOP_LEVEL”. TOP_LEVEL sheet is shown in **Figure 5.1**.

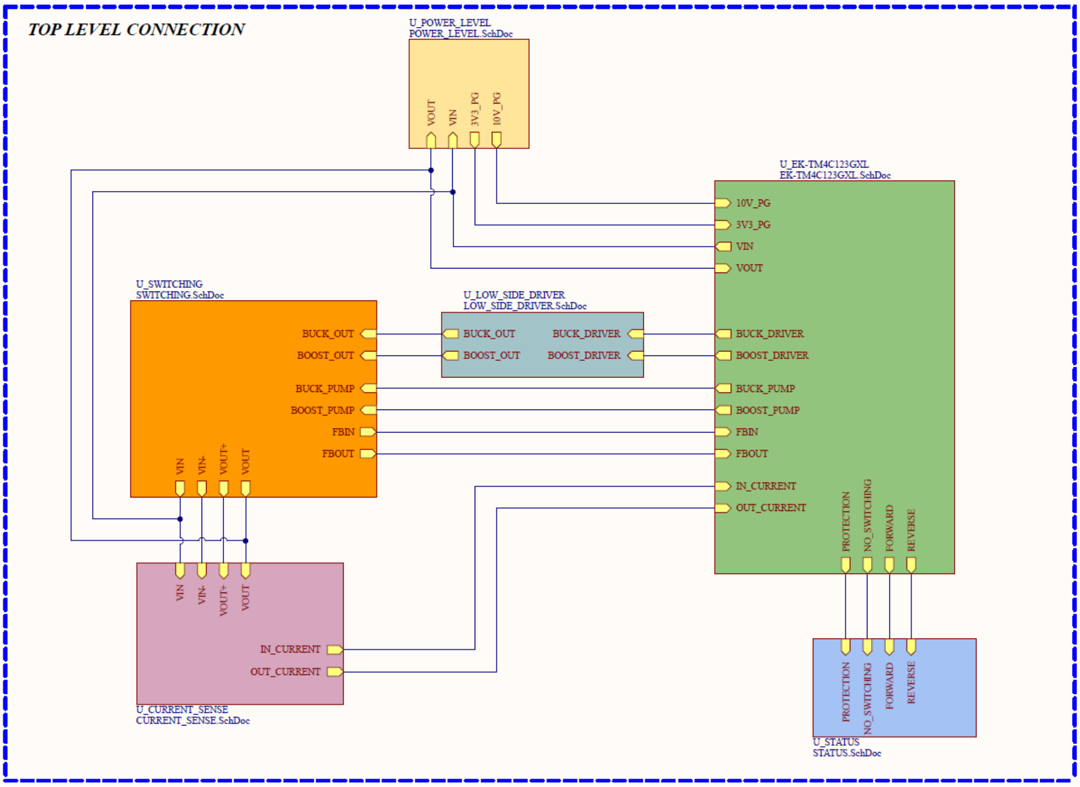

Figure 5.1 : TOP_LEVEL schematic of hardware.

The second page of the schematic is TM4C123GH6PM_CONNECTION. TM4C123GH6PM_CONNECTION schematic page is shown in Figure 5.2 . This page contains connections between the microprocessor and peripheral hardware. The signals that the processor receives as input and produces as output are located here. At the same time, the input and output connectors on the electronic card are also shown on this page.

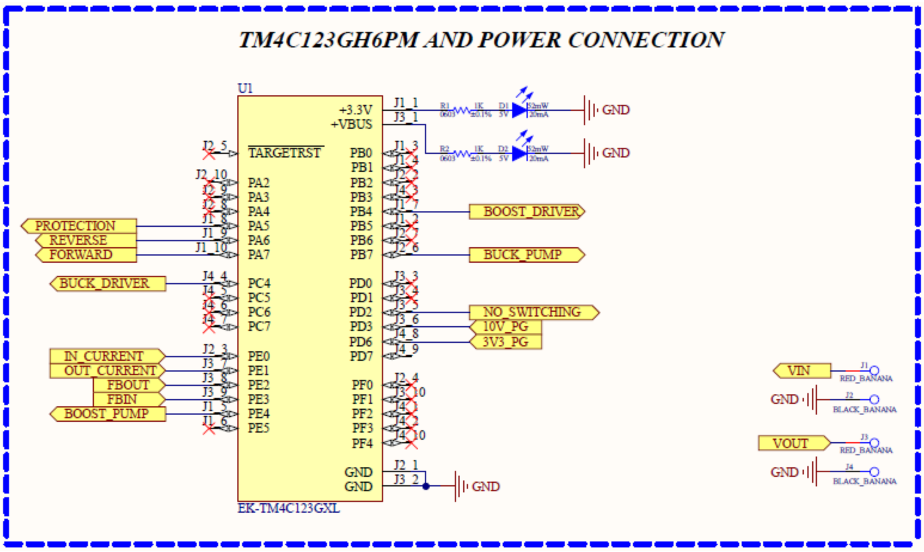

Figure 5.2 : TM4C123GH6PM_CONNECTION schematic of hardware.

The third page of the schematic is POWER_LEVEL. POWER_LEVEL schematic page is shown in Figure 5.3. On this page, the 10V and 3.3V voltages needed by the electronic circuit are produced.

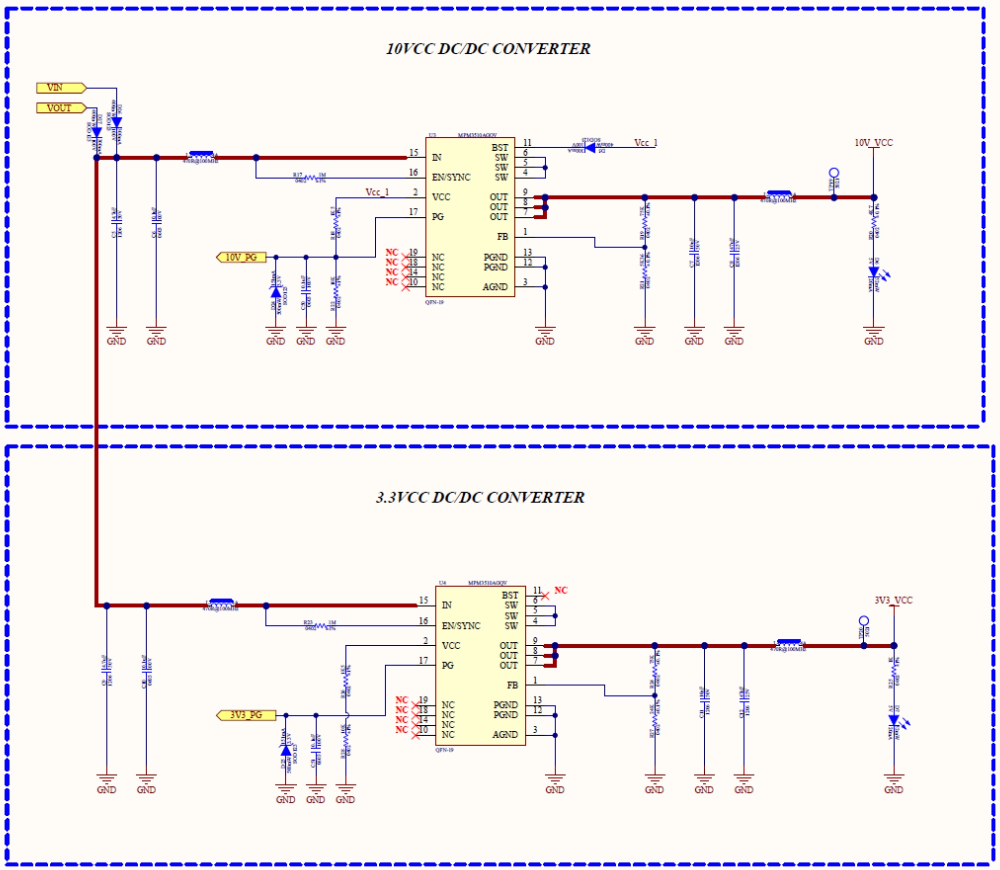

Figure 5.3 : POWER_LEVEL schematic of hardware.

The fourth page of the schematic is SWITCHING. SWITCHING schematic page is shown in Figure 5.4 and Figure 5.5. This page is the part where voltage conversion is performed by PWM switching. Switching MOSFETs, switching coil, voltage divider circuits, current measurement resistors, bootstrap circuits and charge pump circuits are included on this page.

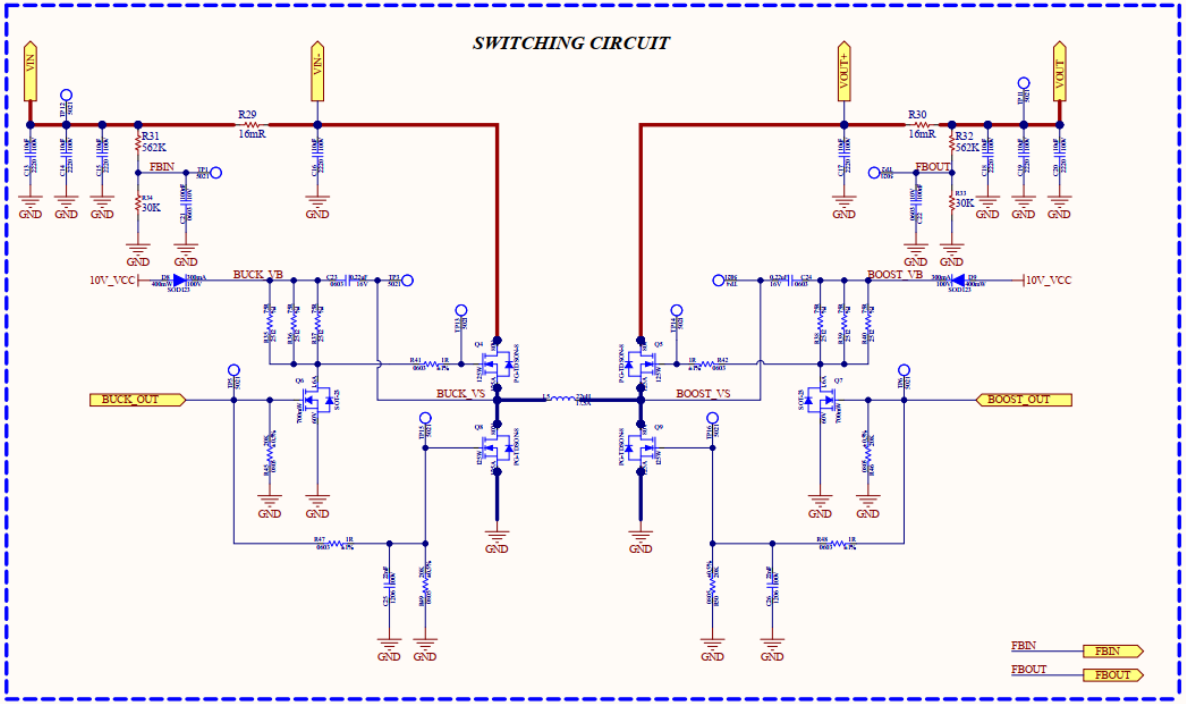

Figure 5.4 : SWITCHING schematic for SWITCHING CIRCUIT of hardware.

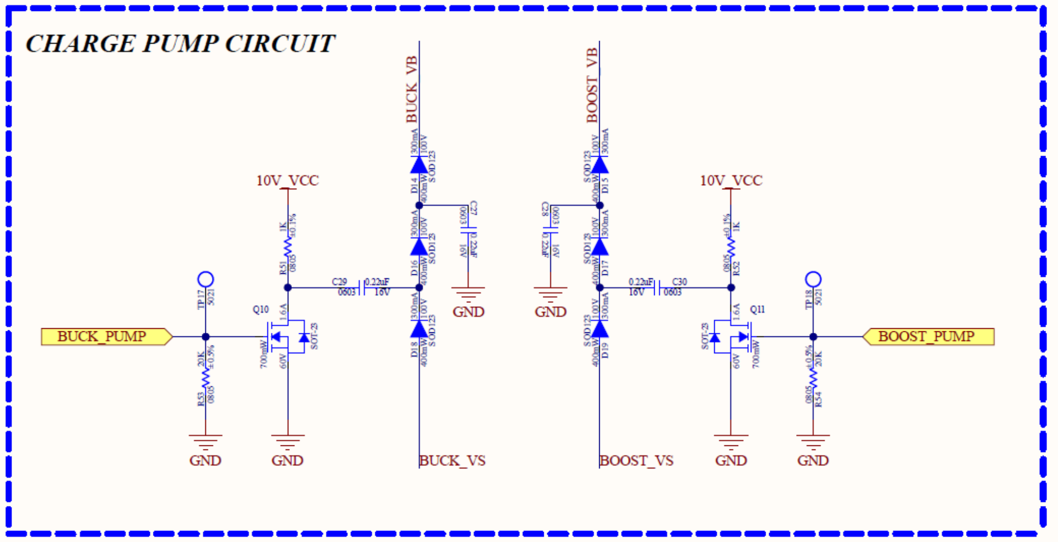

Figure 5.5 : SWITCHING schematic for CHARGE PUMP CIRCUIT of hardware.

LOW_SIDE_DRIVER schematic page is shown in Figure 5.6 and Figure 5.7. The fifth page of the schematic is LOW_SIDE_DRIVER. On this page, the PWM signals produced by the processor are increased from the logical level of 0V-3.3V to the level of 0V-10V.

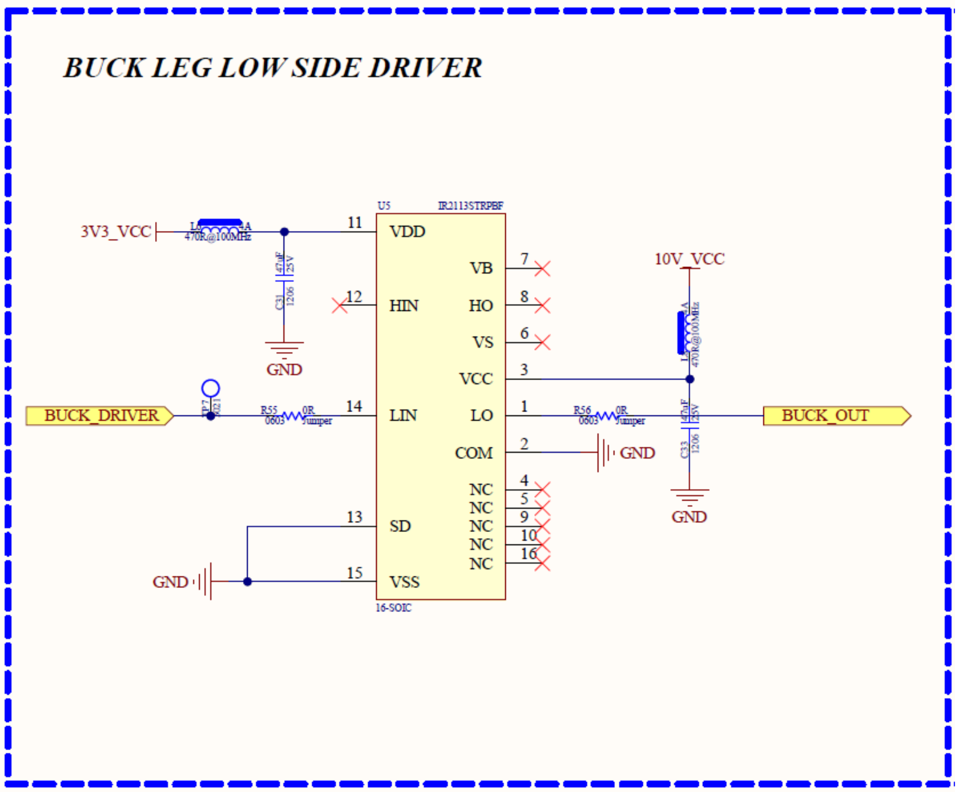

Figure 5.6 : LOW_SIDE_DRIVER schematic for buck leg of hardware.

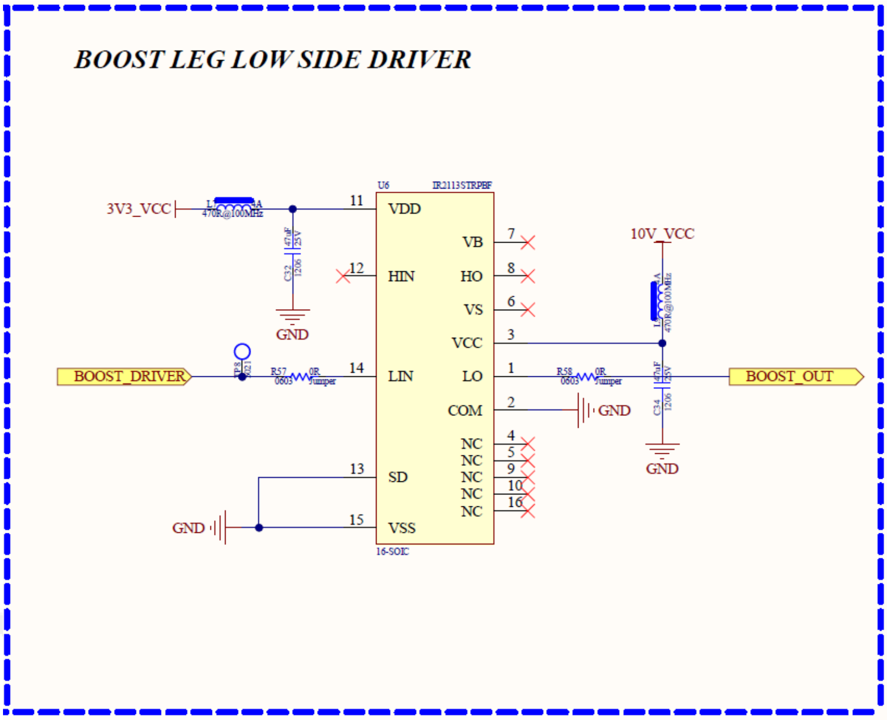

Figure 5.7 : LOW_SIDE_DRIVER schematic for boost leg of hardware.

The sixth page of the schematic is CURRENT_SENSE. CURRENT_SENSE schematic page is shown in Figure 5.8 and Figure 5.9. This page contains circuits that is used to bi-directional reading of input and output currents.

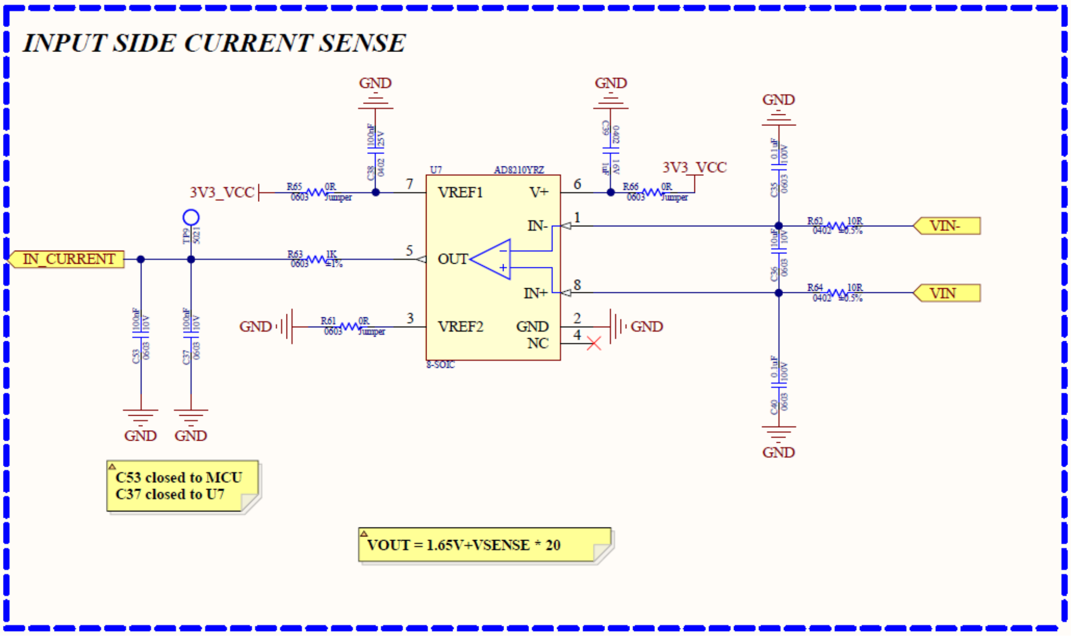

Figure 5.8 : CURRENT_SENSE schematic for input current of hardware.

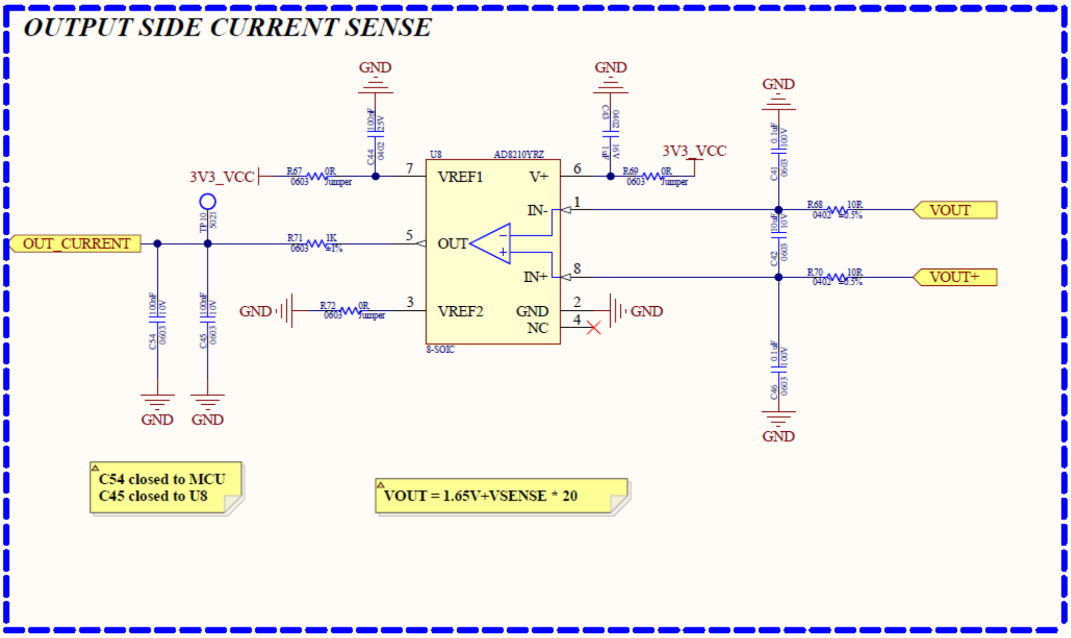

Figure 5.9 : CURRENT_SENSE schematic for output current of hardware.

The last page of the schematic design is STATUS_LEDs. There are 4 LED circuits on this page. This LED shows informative statuses at the basic level regarding switching. STATUS_LEDs schematic page is shown in Figure 5.10.

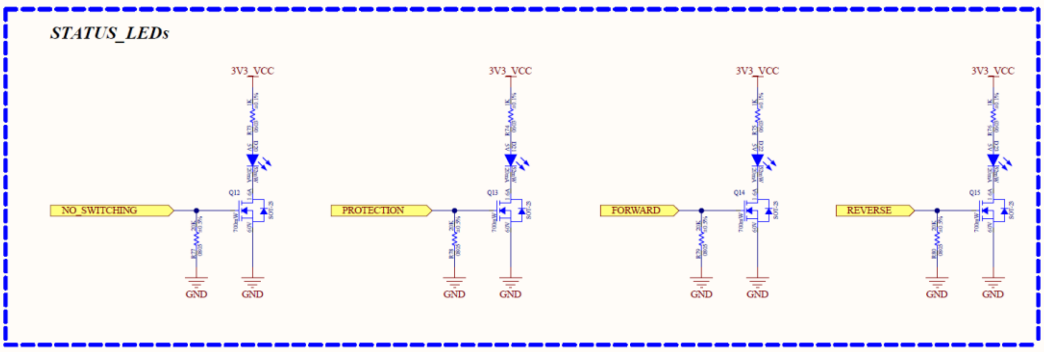

Figure 5.10 : STATUS_LEDs schematic hardware

6 TEST RESULTS

Within the scope of the bi-directional buck boost converter study, the converter was tested in many aspects. During these tests, the converter was operated in forward and reverse directions. During the tests, input voltage, output voltage, input current, output current, gate voltage of buck leg high side MOSFET and gate voltage of boost leg high side MOSFET were measured with an oscilloscope.

The test setup of the DC to DC converter is as shown in **Figure 6.1**.

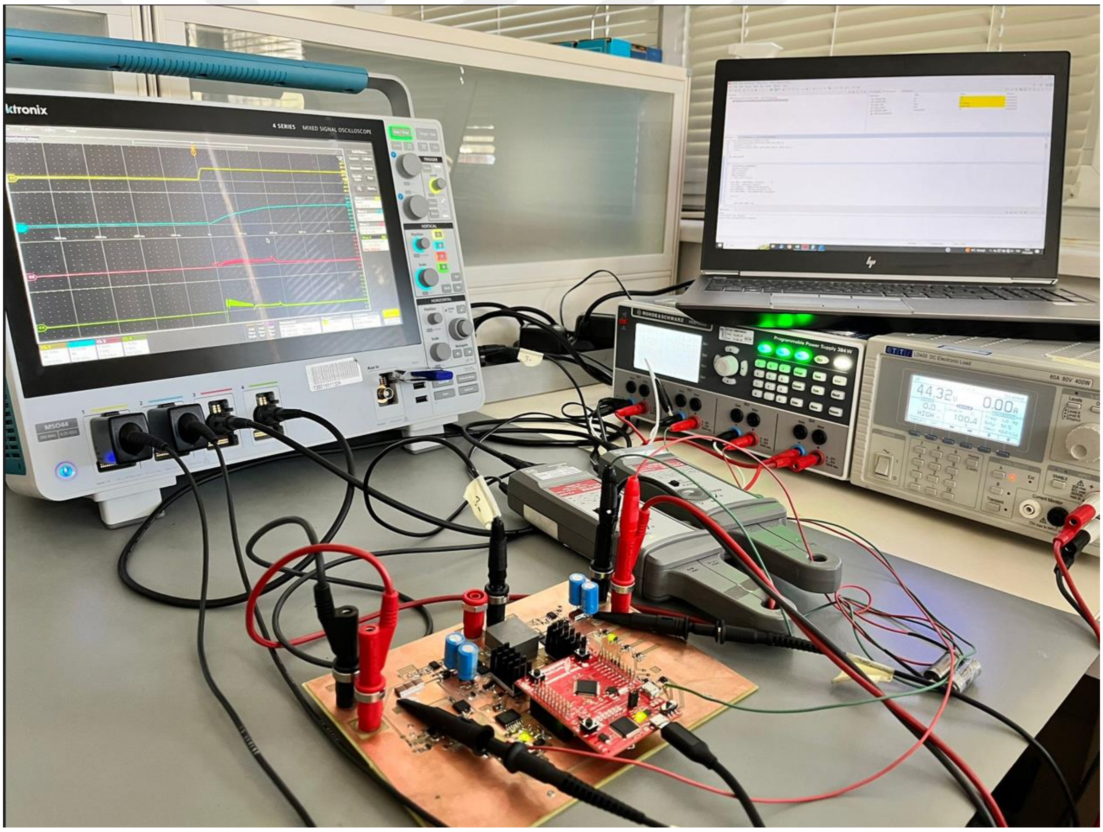

Figure 6.1 : Test setup of bi-directional buck boost converter.

Apart from these, some measurements were taken during the forward and reverse operation of the DC to DC converter. These measurements are values such as the efficiency of the DC to DC converter and the accuracy of input and output current readings.

6.1 Forward Mode Test

During the forward mode test, 3 different modes of the DC to DC converter, buck, buck boost and boost, were tested. The input voltage is set as variable voltage, and the output voltage is fixed as 28V. Voltage regulation and current limiting operations were observed during the test. The test setup for forward operation is shown in **Figure 6.2**.

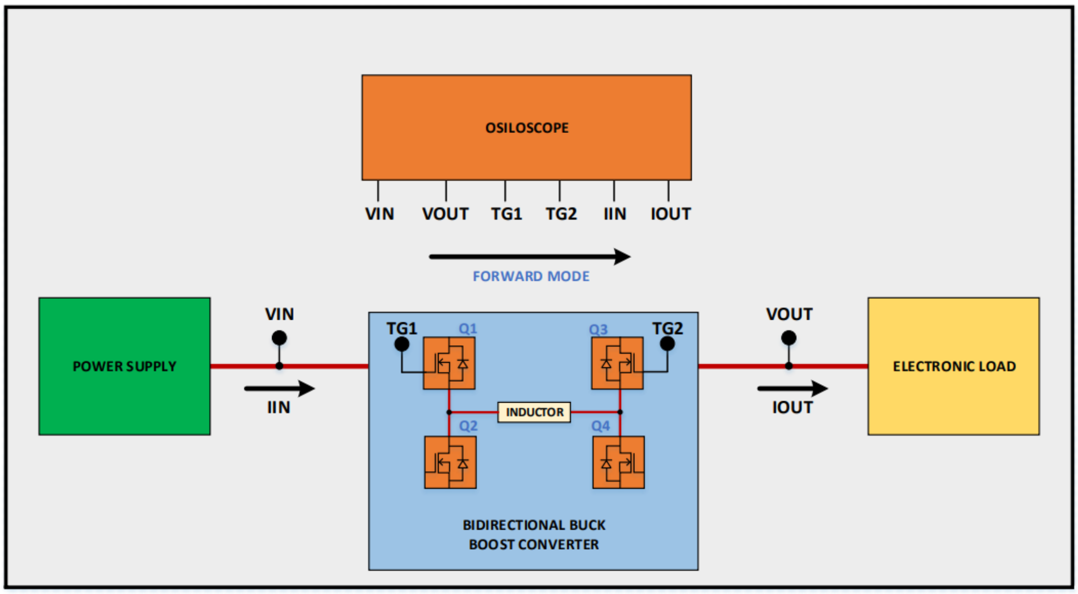

Figure 6.2 : Block diagram of the test setup of the forward direction.

The power supply voltage is 36V and the output voltage is set to 28V by software. The oscilloscope screenshot of this test is shown in **Figure 6.3**. If the input voltage is greater than the output voltage, switching occurs in buck mode. Therefore, switching occurs in the buck leg (MOSFETs Q1 and Q2). In the boost leg, the high side MOSFET (Q3) is in continuous conduction state and the low side MOSFET (Q4) is in cut-off state.

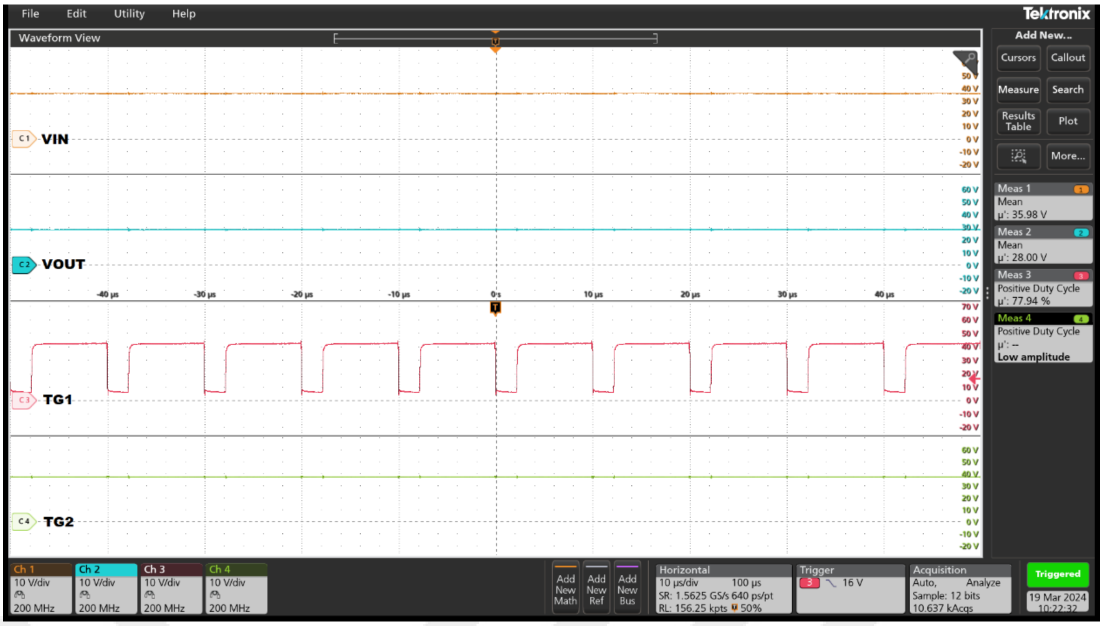

Figure 6.3 : Oscilloscope screenshot of forward buck converter.

Efficiency graph of forward direction at the buck mode is shown in **Figure 6.4**.

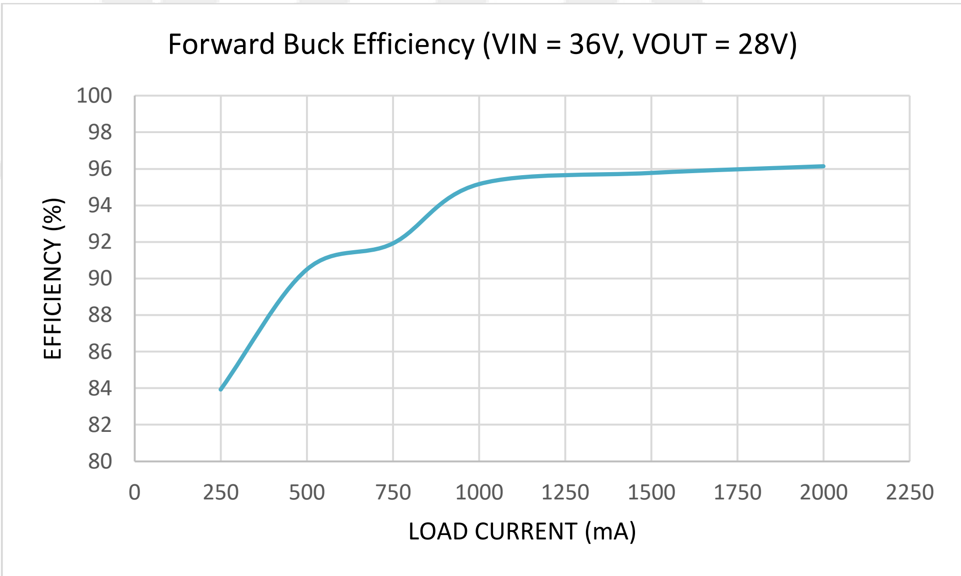

Figure 6.4 : Efficiency graph of forward direction at the buck mode.

The power supply voltage is 28V and the output voltage is set to 28V by software. The oscilloscope image of this test is shown in **Figure 6.5**. Since the input voltage is equal to the output voltage, switching occurs in buck boost mode. Therefore, switching occurs in the buck leg (MOSFETs Q1 and Q2) and Boost leg (MOSFETs Q3 and Q4).

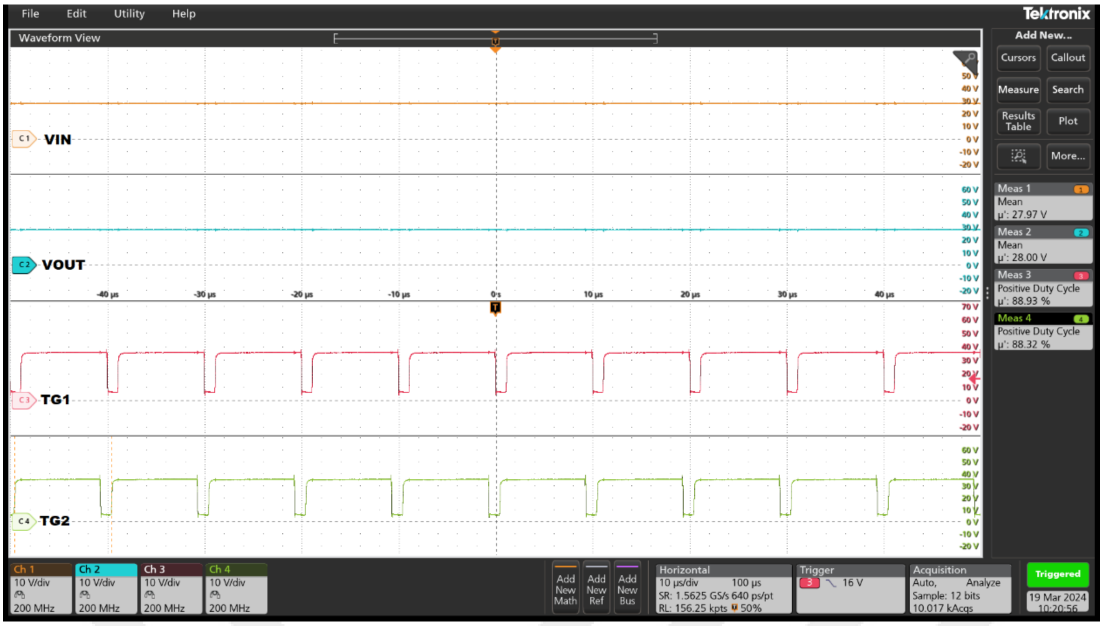

Figure 6.5 : Oscilloscope screenshot of forward buck boost converter.

Efficiency graph of forward direction at the buck boost mode is shown in **Figure 6.6**.

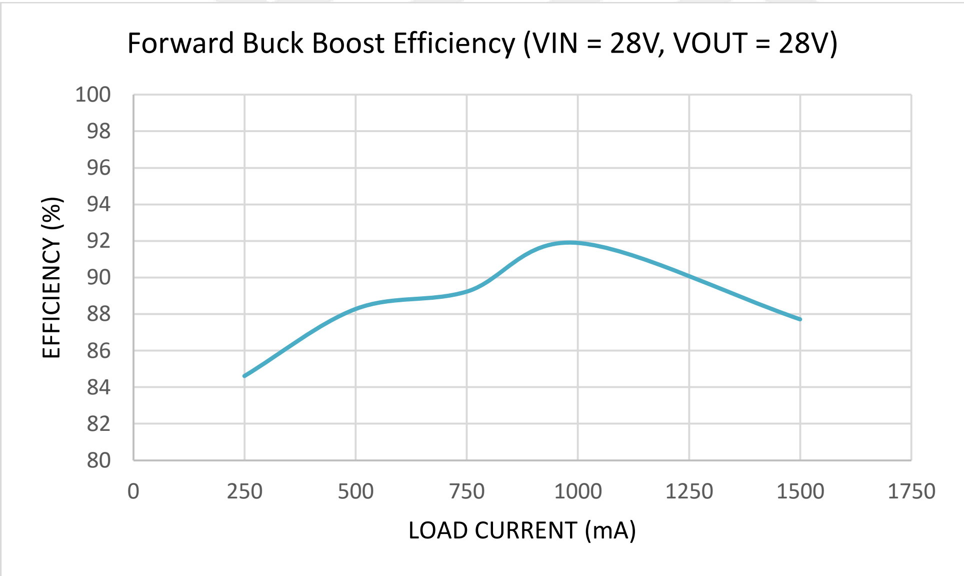

Figure 6.6 : Efficiency graph of forward direction at the buck boost mode.

The power supply voltage is 12V and the output voltage is set to 28V by software. The oscilloscope image of this test is shown in **Figure 6.7**. Since the input voltage is lower than the output voltage, switching occurs in boost mode. Therefore, switching occurs in the boost leg (MOSFETs Q3 and Q4). In the buck leg, the high side MOSFET (Q1) is in continuous conduction state and the low side MOSFET (Q2) is in cut-off state.

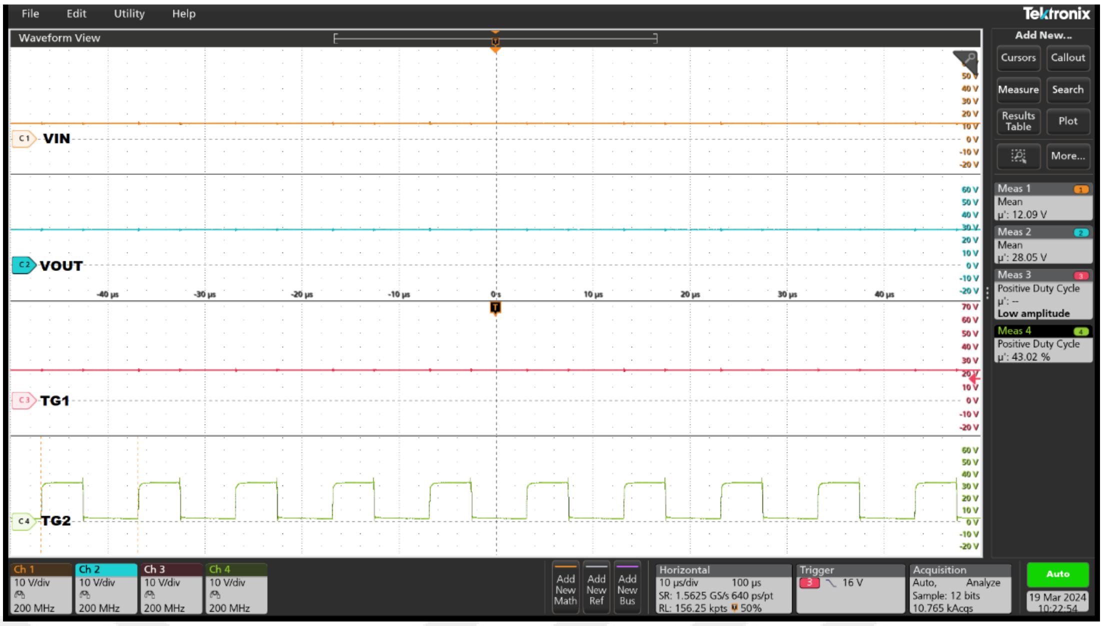

Figure 6.7 : Oscilloscope screenshot of forward boost converter.

Efficiency graph of forward direction at the boost mode is shown in **Figure 6.8**.

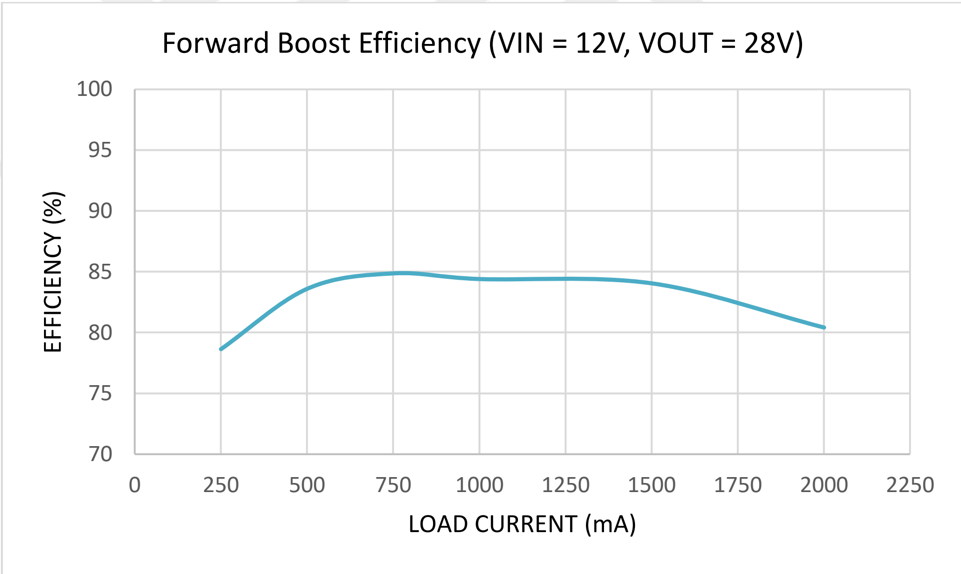

Figure 6.8 : Efficiency graph of forward direction at the boost mode.

The power supply voltage is 12V and output current is limited to 2.5A by the software. Output load is 10ohm. Expected output load is 2.8A but output current is software limited to 2.5A. This limiting process occurs by reducing the output voltage to approximately 24V. The oscilloscope image of this test is shown in **Figure 6.9**.

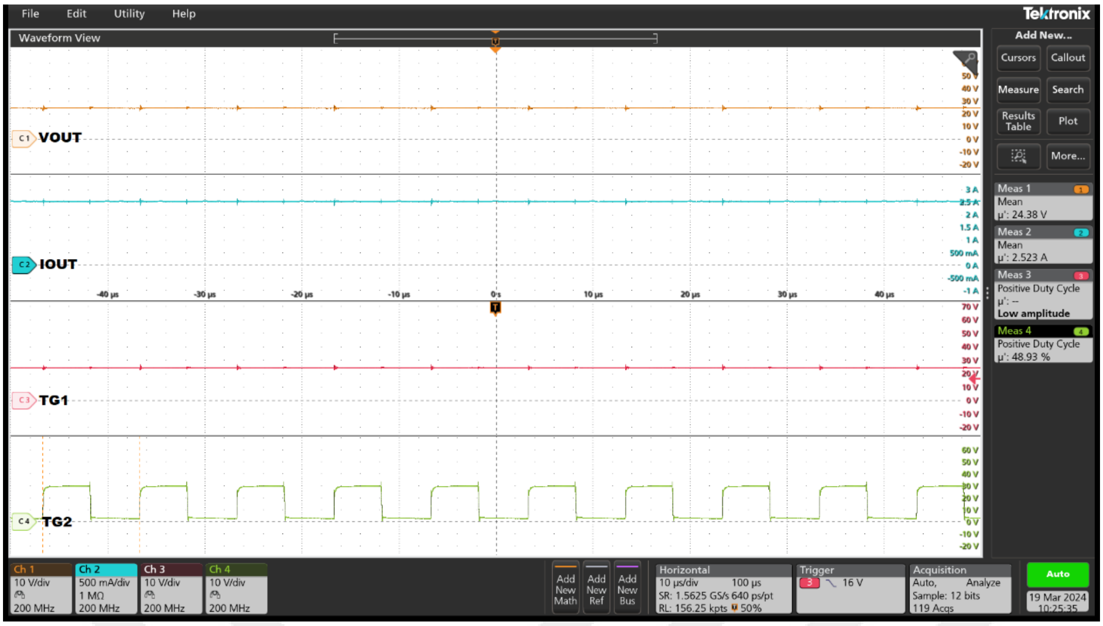

Figure 6.9 : Forward boost mode, 10ohm load at the output.

In this test, The power supply voltage is 12V and output load is 5ohm. Expected output load is 5.6A but output current is software limited to 2.5A. This limiting process occurs by reducing the output voltage to approximately 12V. The oscilloscope image of this test is shown in **Figure 6.10**.

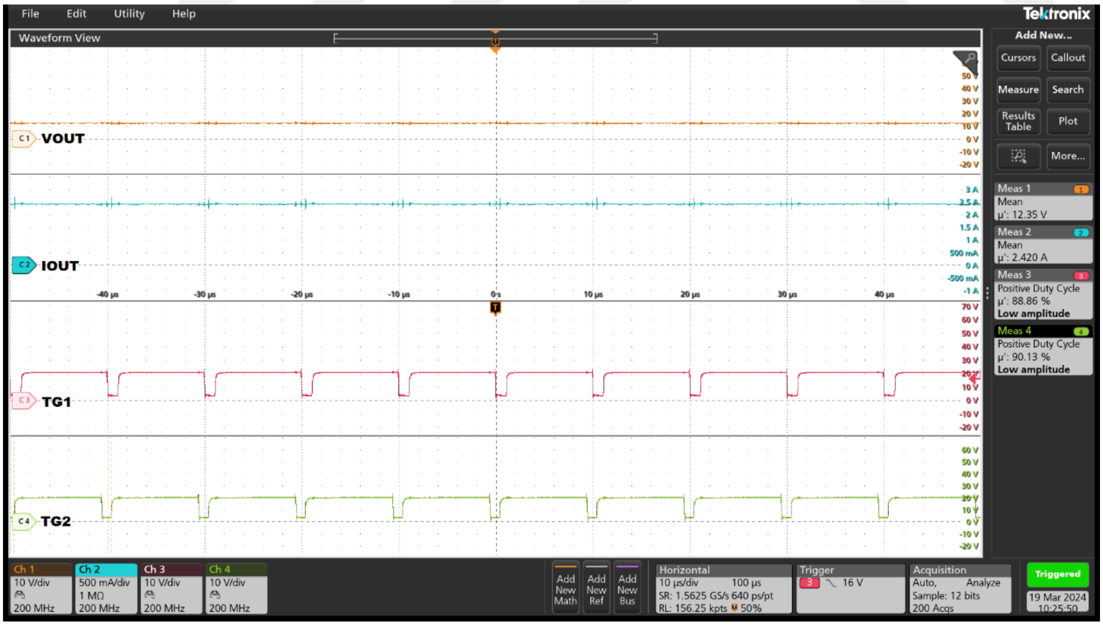

Figure 6.10 : Forward boost mode, 5ohm load at the output.

The power supply voltage is 28V and output current is limited to 2.5A by the software. Output load is 10ohm. Expected output load is 2.8A but output current is software limited to 2.5A. This limiting process occurs by reducing the output voltage to approximately 24V. The oscilloscope image of this test is shown in **Figure 6.11**.

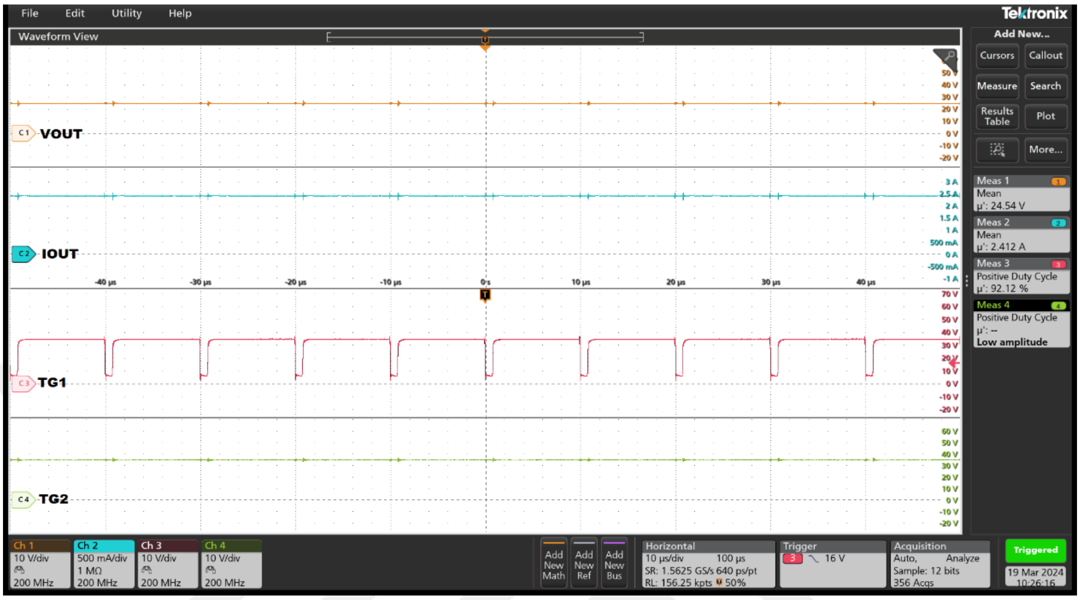

Figure 6.11 : Forward buck boost mode, 10ohm load at the output.

In this test, The power supply voltage is 28V and output load is 5ohm. Expected output load is 5.6A but output current is software limited to 2.5A. This limiting process occurs by reducing the output voltage to approximately 12V. The oscilloscope image of this test is shown in **Figure 6.12**.

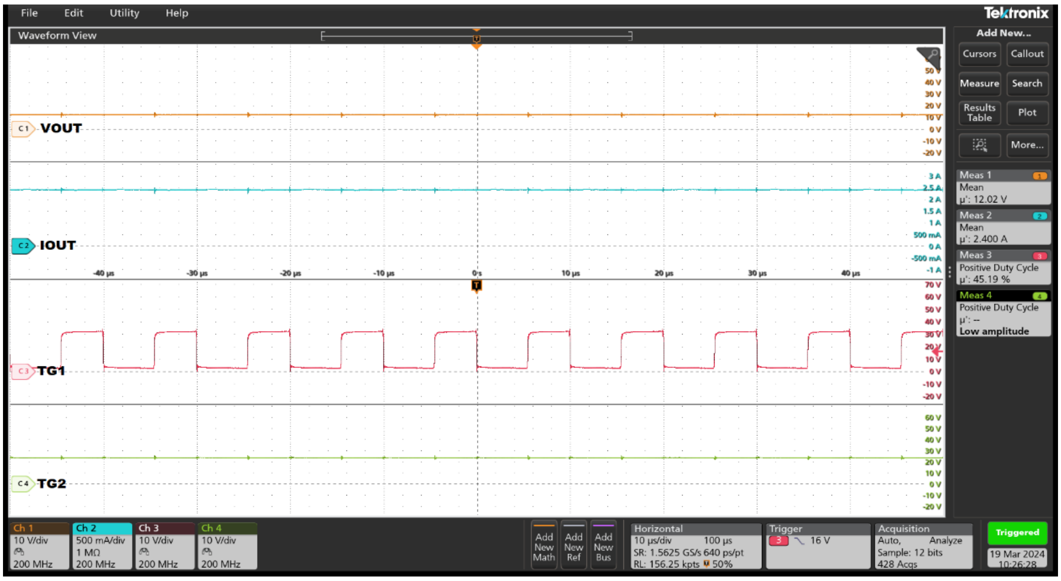

Figure 6.12 : Forward buck boost mode, 5ohm load at the output.

The power supply voltage is 36V and output current is limited to 2.5A by the software. Output load is 10ohm. Expected output load is 2.8A but output current is software limited to 2.5A. This limiting process occurs by reducing the output voltage to approximately 24V. The oscilloscope image of this test is shown in **Figure 6.13**.

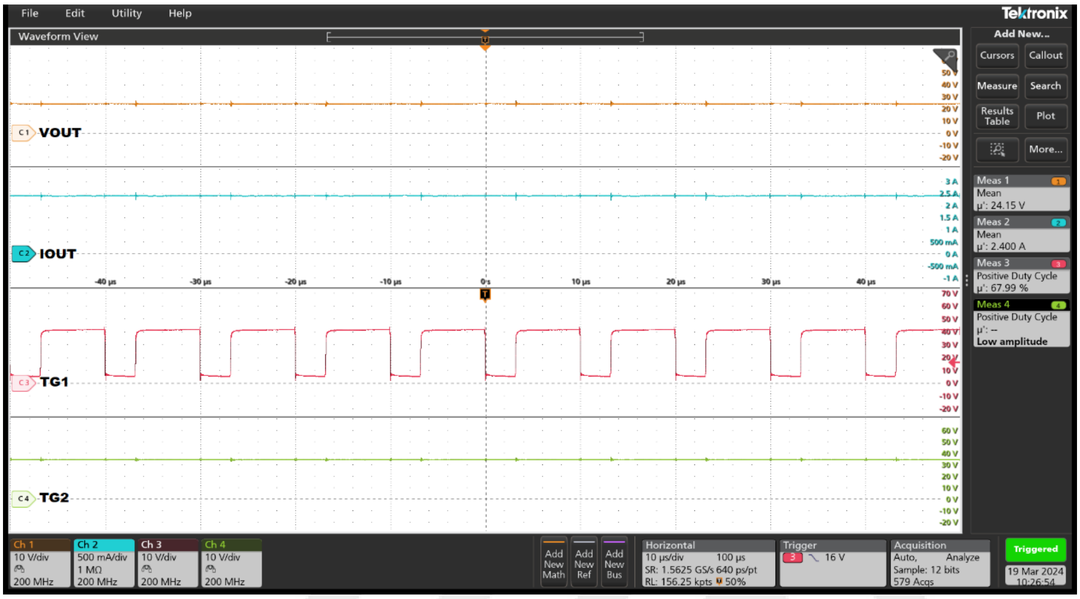

Figure 6.13 : Forward buck mode, 10ohm load at the output.

In this test, The power supply voltage is 36V and output load is 5ohm. Expected output load is 5.6A but output current is software limited to 2.5A. This limiting process occurs by reducing the output voltage to approximately 12V. The oscilloscope image of this test is shown in **Figure 6.14**.

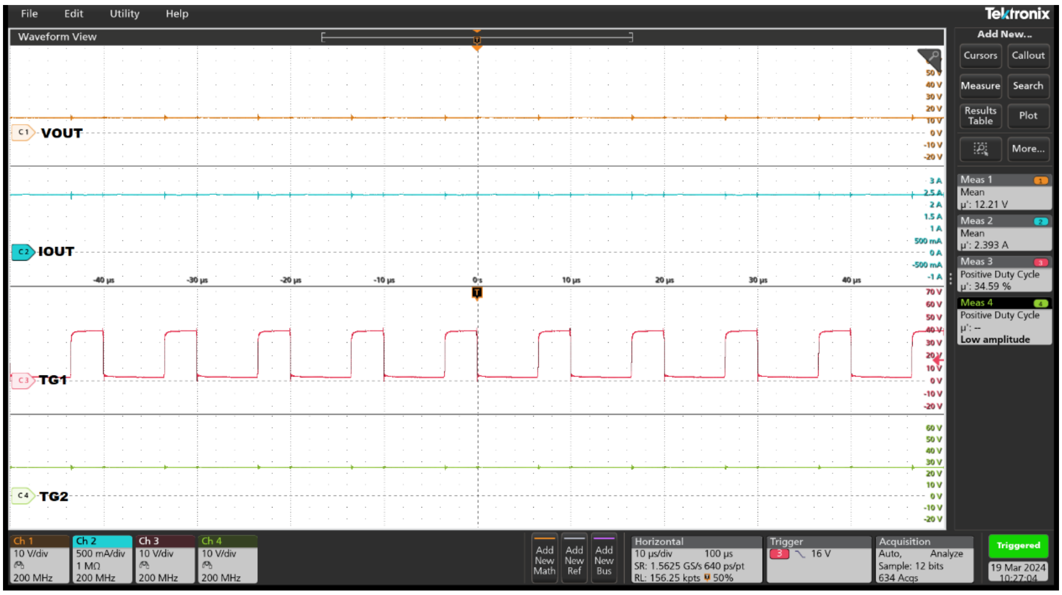

Figure 6.14 : Forward buck mode, 5ohm load at the output.

6.2 Reverse Mode Test

During the reverse mode test, 3 different modes of the DC to DC converter, buck, buck boost and boost, were tested. The input voltage is set as variable voltage, and the output voltage is fixed as 28V. Voltage regulation and current limiting operations were observed during the test. The test setup visual for reverse operation is shown in **Figure 6.15**.

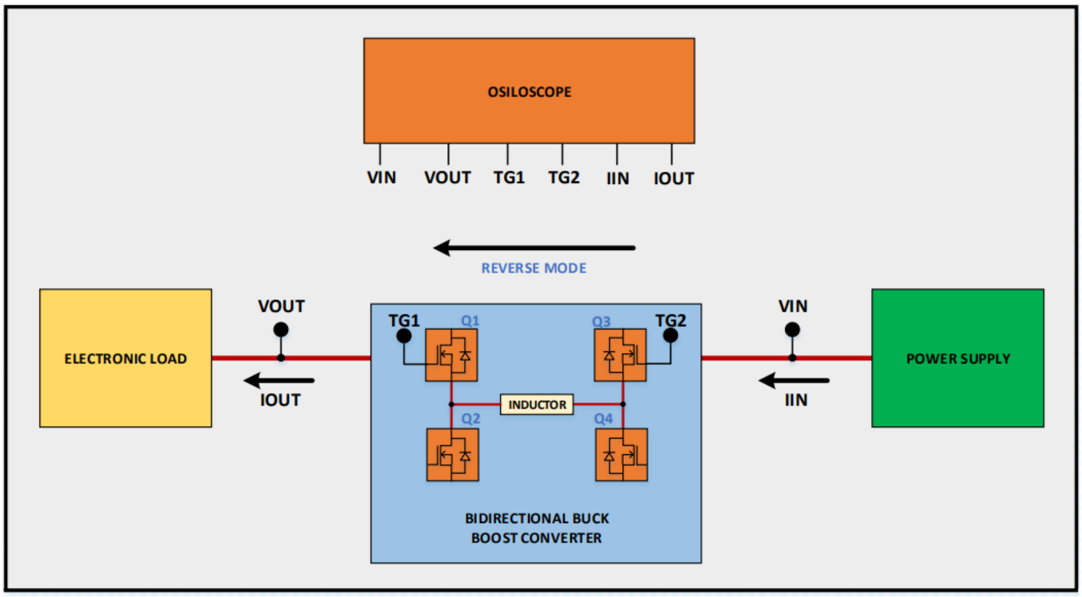

Figure 6.15 : Block diagram of the test setup of the reverse direction.

The the power supply voltage is 36V and the output voltage is set to 28V by software. The oscilloscope image of this test is shown in **Figure 6.16**. If the input voltage is greater than the output voltage, switching occurs in buck mode. Therefore, switching occurs in the boost leg (MOSFETs Q3 and Q4). In the buck leg, the high side MOSFET (Q1) is in continuous conduction state and the low side MOSFET (Q2) is in cut-off state.

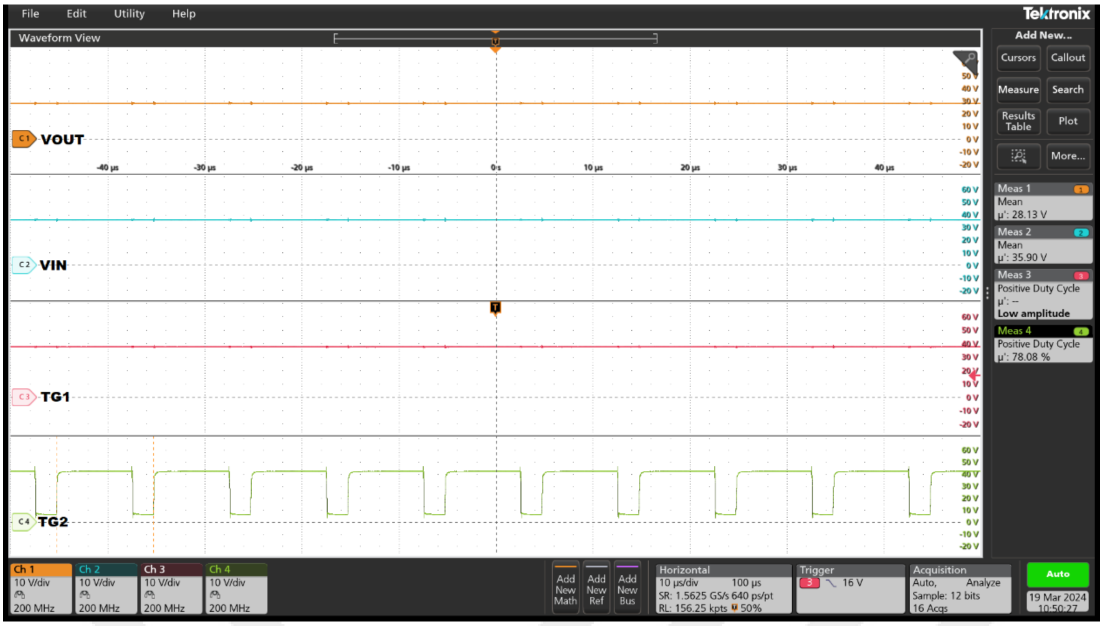

Figure 6.16 : Oscilloscope screenshot of reverse buck converter.

Efficiency graph of reverse direction at the buck mode is shown in **Figure 6.17**.

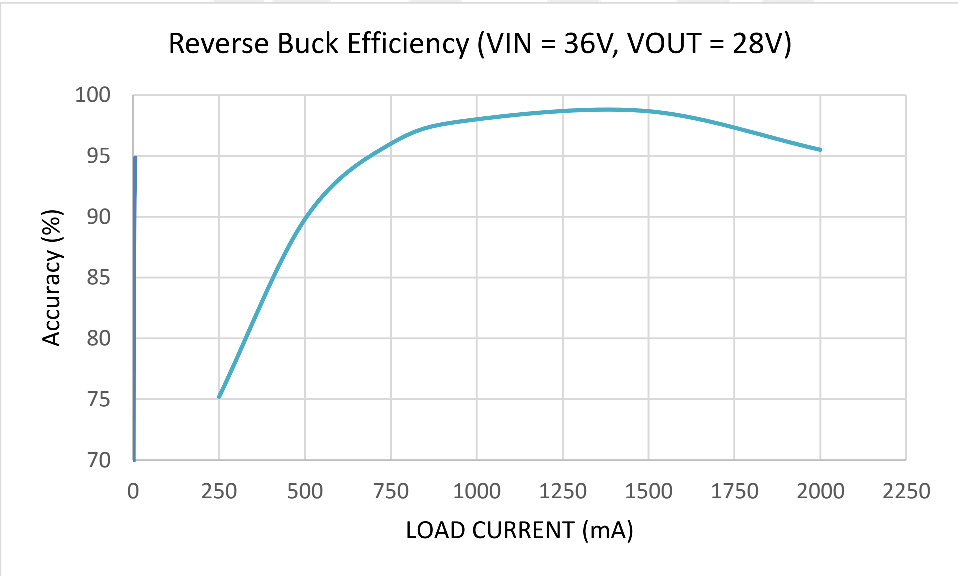

Figure 6.17 : Efficiency graph of reverse direction at the buck mode.

The input voltage of the power supply is 28V and the output voltage is set to 28V by software. The oscilloscope image of this test is shown in **Figure 6.18**. Since the input voltage is equal to the output voltage, switching occurs in buck boost mode. Therefore, switching occurs in the buck leg (MOSFETs Q1 and Q2) and Boost leg (MOSFETs Q3 and Q4).

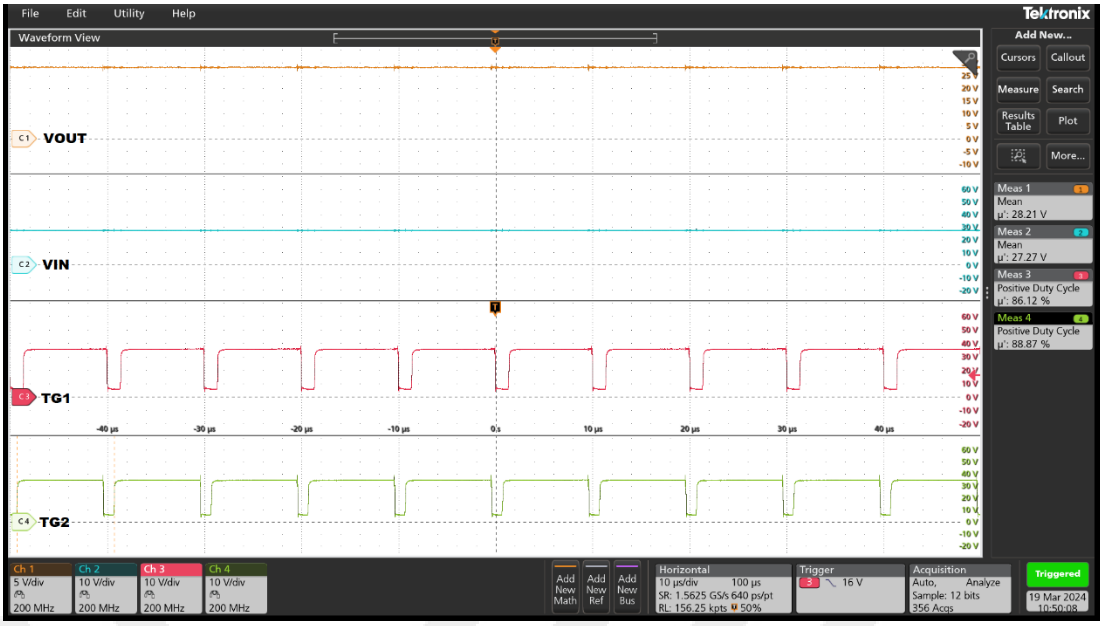

Figure 6.18 : Oscilloscope screenshot of reverse buck boost converter.

Efficiency graph of reverse direction at the buck boost mode is shown in **Figure 6.19**.

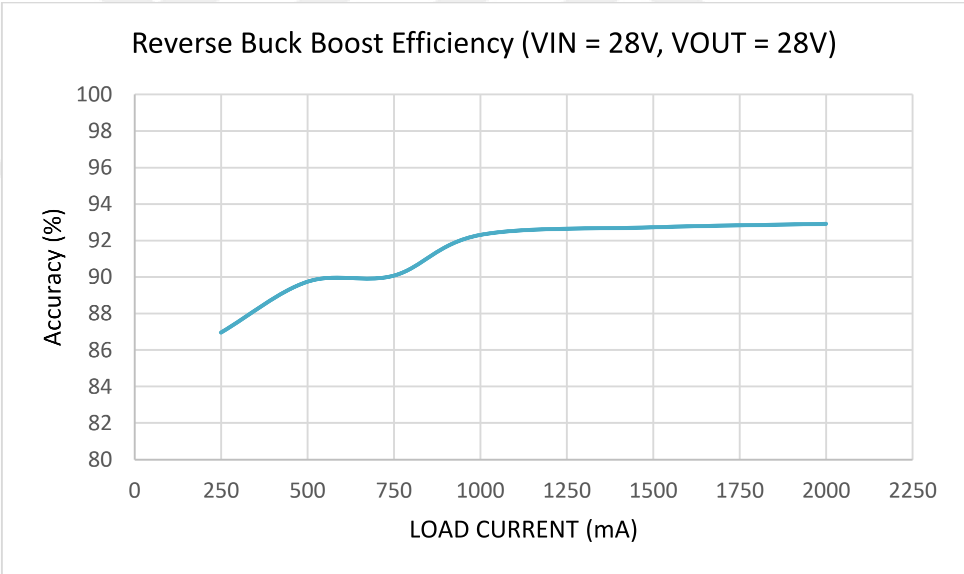

Figure 6.19 : Efficiency graph of reverse direction at the buck boost mode.

The input voltage of the power supply is 12V and the output voltage is set to 28V by software. The oscilloscope image of this test is shown in **Figure 6.20**. Since the input voltage is lower than the output voltage, switching occurs in boost mode. Therefore, switching occurs in the buck leg (MOSFETs Q1 and Q2). In the buck leg, the high side MOSFET (Q3) is in continuous conduction state and the low side MOSFET (Q4) is in cut-off state.

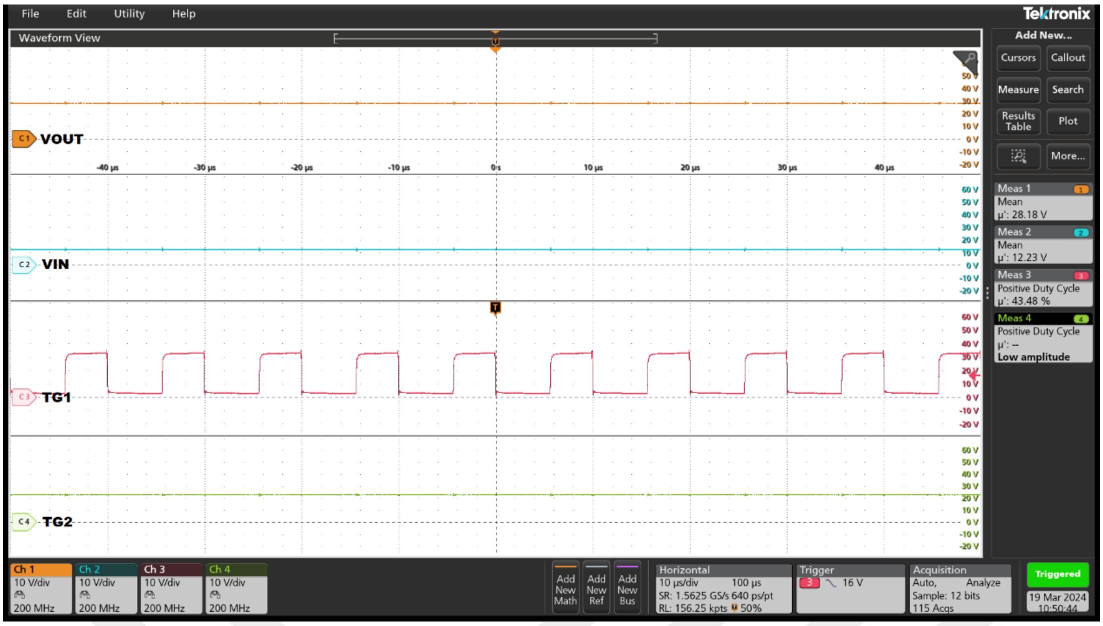

Figure 6.20 : Oscilloscope screenshot of reverse boost converter.

Efficiency graph of reverse direction at the boost mode is shown in **Figure 6.21**.

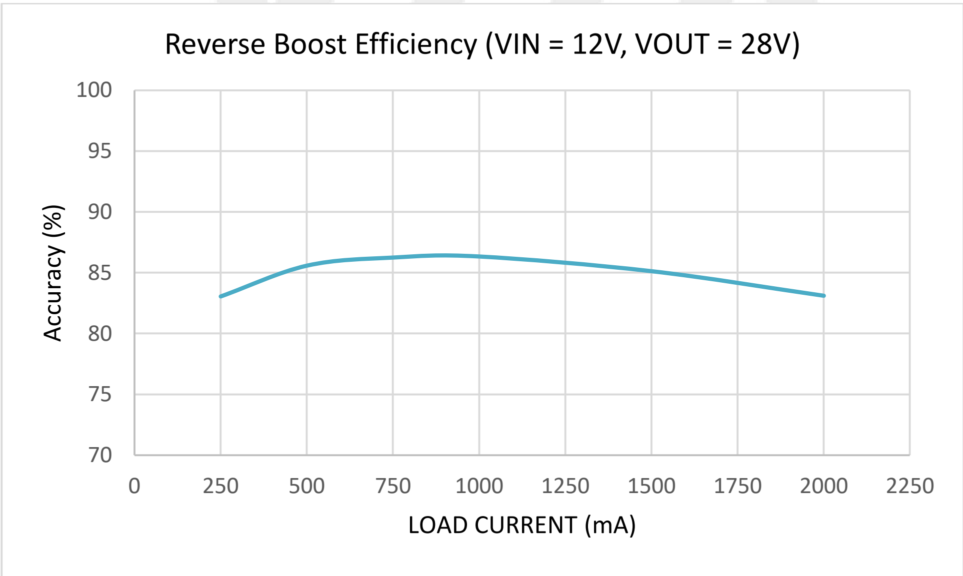

Figure 6.21 : Efficiency graph of reverse direction at the boost mode.

The input voltage of the power supply is 12V and output current is limited to 2.5A by the software. Output load is 10 ohm. Expected output load is 2.8A but output current is software limited to 2.5A. This limiting process occurs by reducing the output voltage to approximately 25V. The oscilloscope image of this test is shown in **Figure 6.22**.

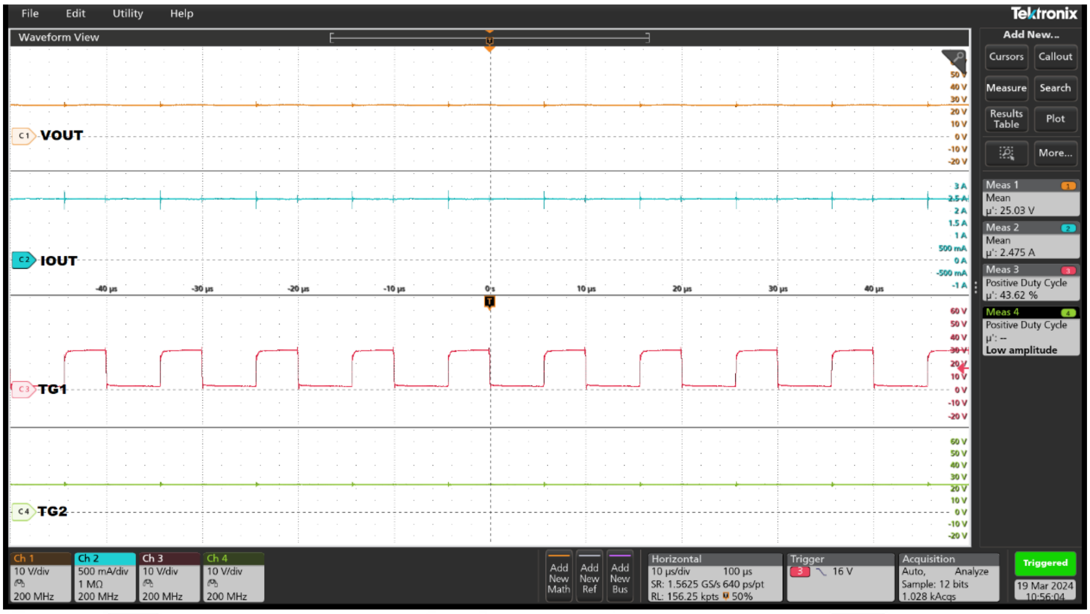

Figure 6.22 : Reverse boost mode, 10 ohm load at the output.

In this test, the input voltage of the power supply is 12V and output load is 5 ohm. Expected output load is 5.6A but output current is software limited to 2.5A. This limiting process occurs by reducing the output voltage to approximately 12V. The oscilloscope image of this test is shown in **Figure 6.23**.

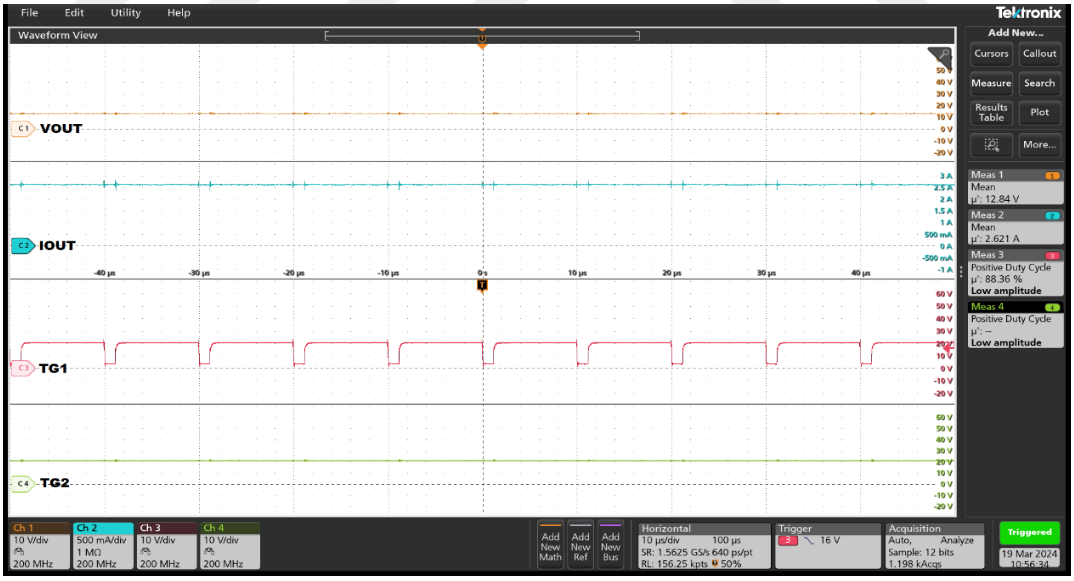

Figure 6.23 : Reverse boost mode, 10 ohm load at the output.

The input voltage of the power supply is 28V and output current is limited to 2.5A by the software. Output load is 10 ohm. Expected output load is 2.8A but output current is software limited to 2.5A. This limiting process occurs by reducing the output voltage to approximately 24V. The oscilloscope image of this test is shown in **Figure 6.24**.

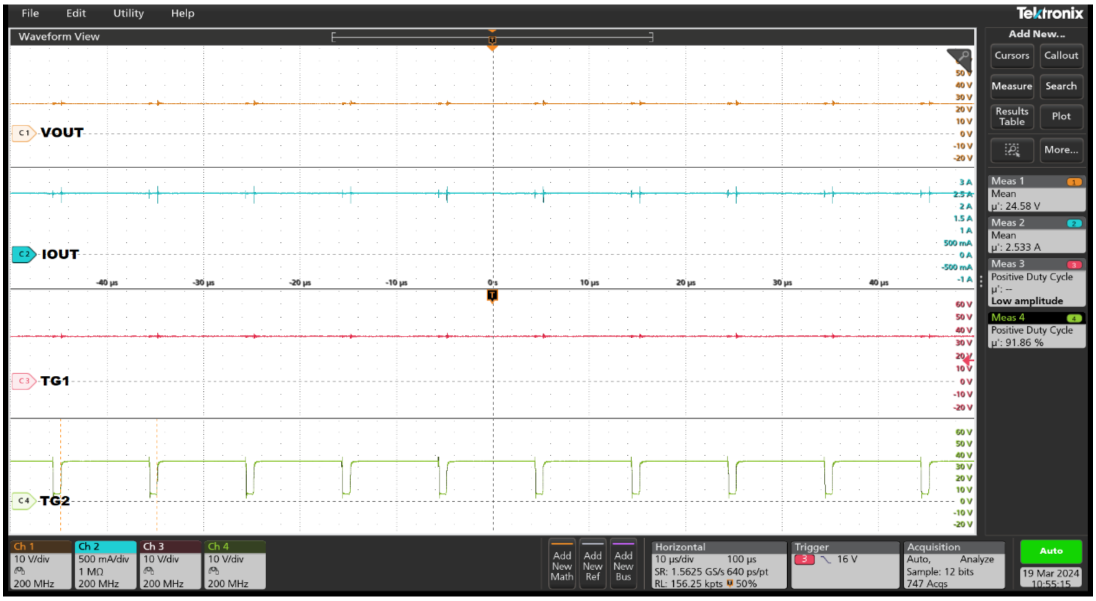

Figure 6.24 : Reverse buck boost mode, 10 ohm load at the output.

In this test, the input voltage of the power supply is 28V and output load is 5 ohm. Expected output load is 5.6A but output current is software limited to 2.5A. This limiting process occurs by reducing the output voltage to approximately 12V. The oscilloscope image of this test is shown in **Figure 6.25**.

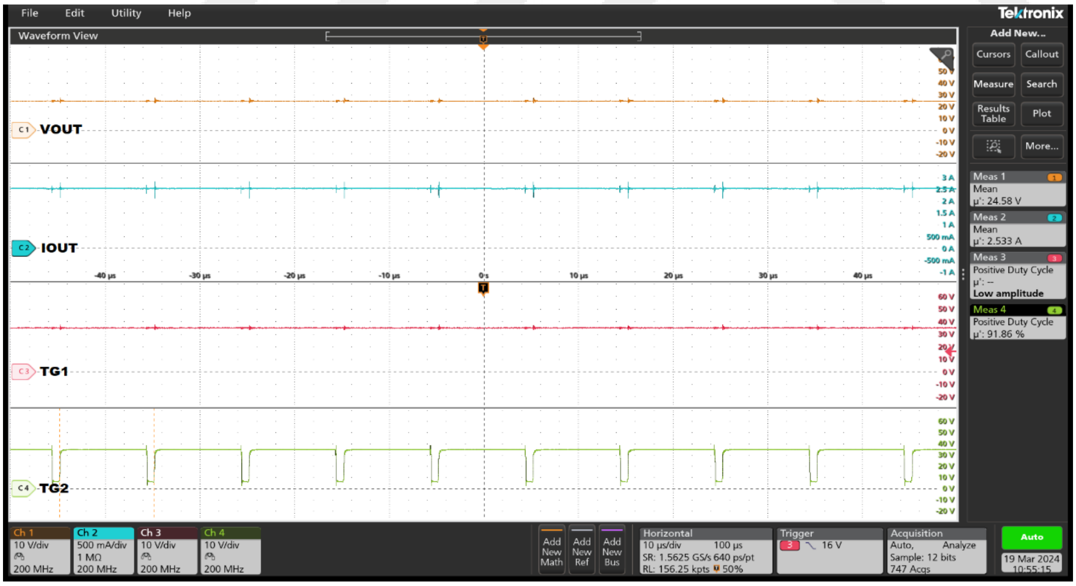

Figure 6.25 : Reverse buck boost mode, 5 ohm load at the output.

The input voltage of the power supply is 36V and output current is limited to 2.5A by the software. Output load is 10 ohm. Expected output load is 2.8A but output current is software limited to 2.5A. This limiting process occurs by reducing the output voltage to approximately 24V. The oscilloscope image of this test is shown in **Figure 6.26**.

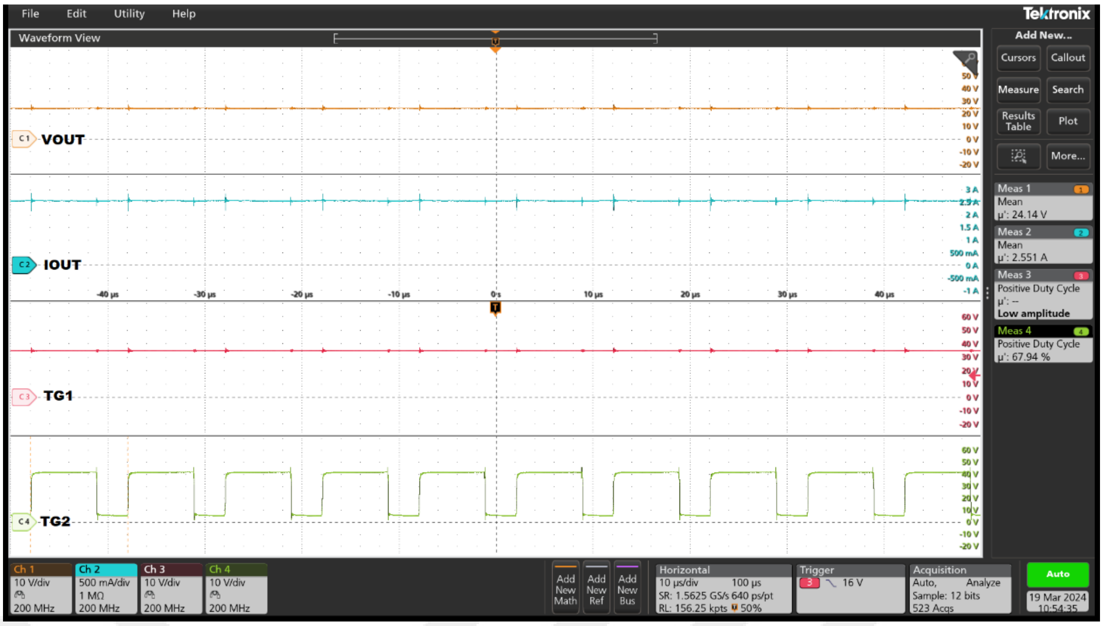

Figure 6.26 : Reverse buck mode, 10 ohm load at the output.

In this test, the input voltage of the power supply is 36V and output load is 5 ohm. Expected output load is 5.6A but output current is software limited to 2.5A. This limiting process occurs by reducing the output voltage to approximately 12V. The oscilloscope image of this test is shown in **Figure 6.27**.

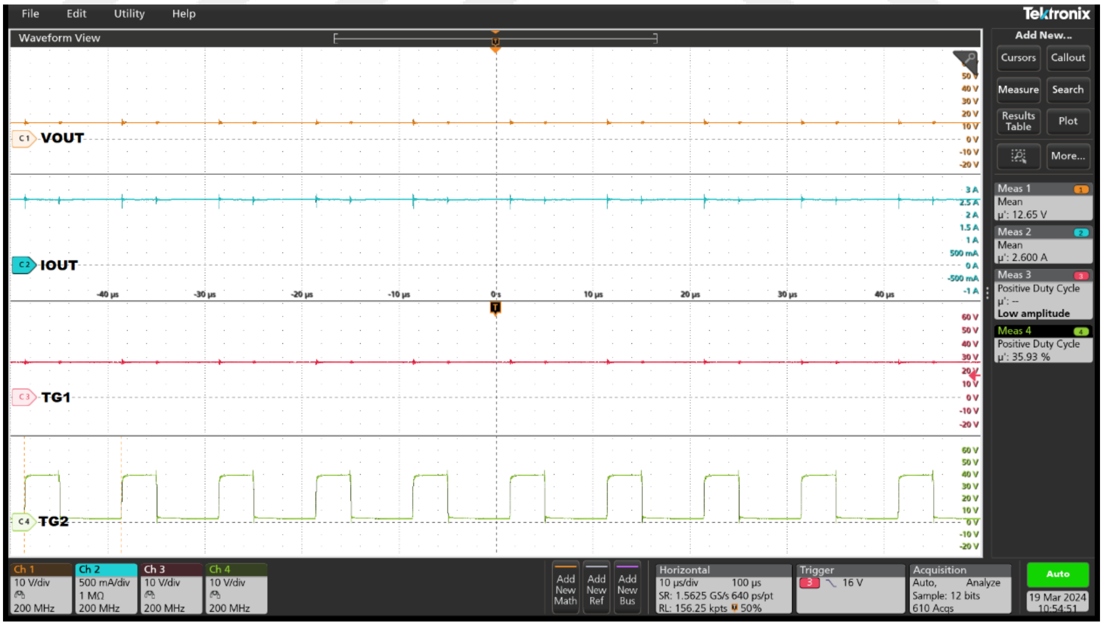

Figure 6.27 : Reverse buck mode, 5 ohm load at the output.

6.3 Input and Output Current Accuracy

Input and output currents are measured by the microprocessor with errors. These error values are different for each operating mode.

When operating in the forward direction at the buck mode, the input and output current reading accuracy from 250mA output current to 2000mA when the input voltage is 36V and the output voltage is 28V is given in **Figure 6.28**.

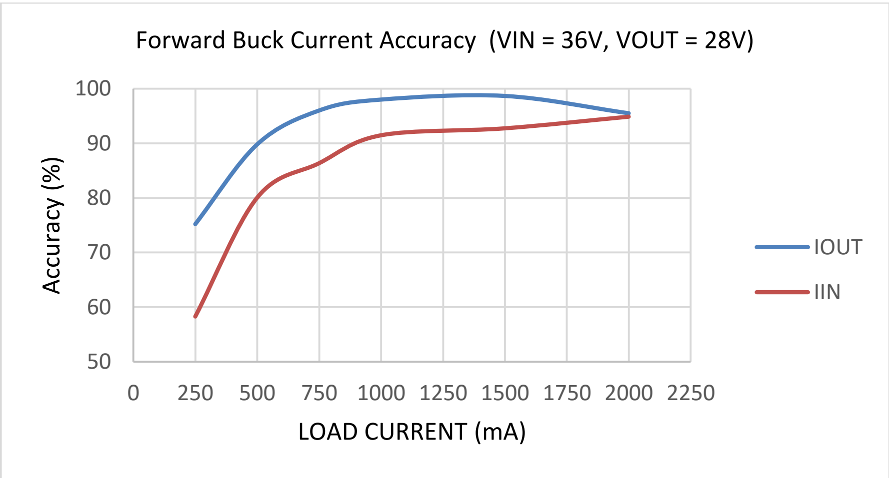

Figure 6.28 : Current reading accuracy of forward buck converter.

When operating in the forward direction at the buck boost mode, the input and output current reading accuracy from 250mA output current to 2000mA when the input voltage is 28V and the output voltage is 28V is given in **Figure 6.29**.

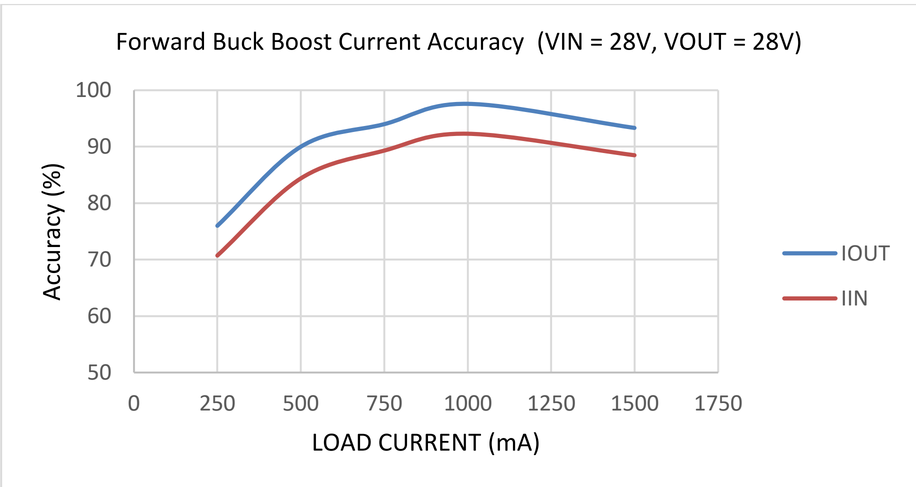

Figure 6.29 : Current reading accuracy of forward buck boost converter.

When operating in the forward direction at the boost mode, the input and output current reading accuracy from 250mA output current to 2000mA when the input voltage is 12V and the output voltage is 28V is given in **Figure 6.30**.

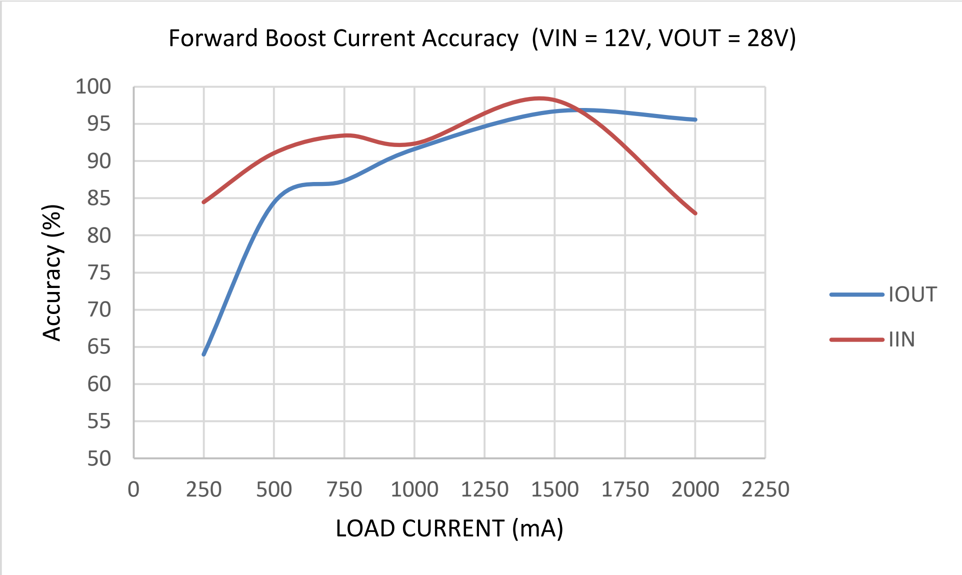

Figure 6.30 : Current reading accuracy of forward boost converter.

When operating in the reverse direction at the buck mode, the input and output current reading accuracy from 250mA output current to 2000mA when the input voltage is 36V and the output voltage is 28V is given in **Figure 6.31**.

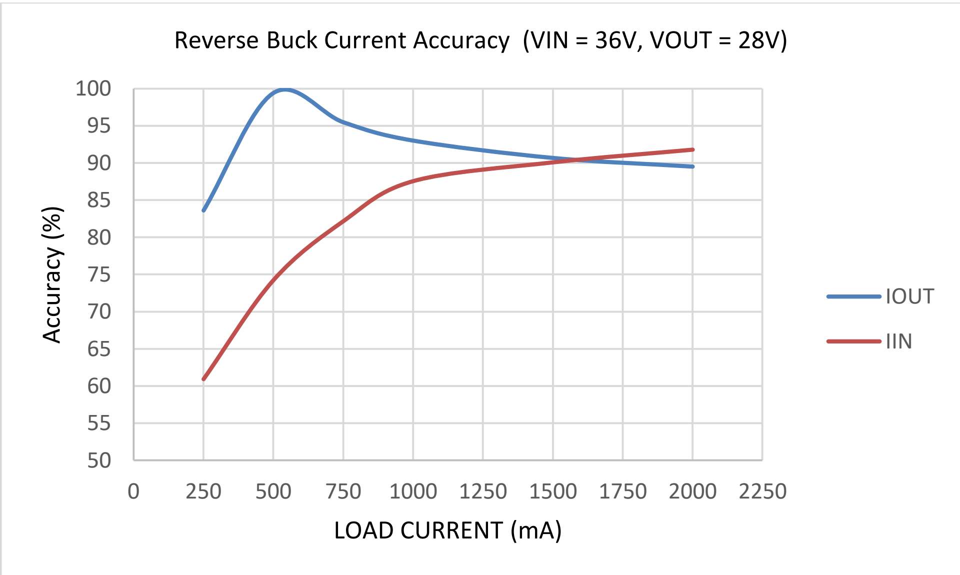

Figure 6.31 : Current reading accuracy of reverse buck converter.

When operating in the reverse direction at the buck boost mode, the input and output current reading accuracy from 250mA output current to 2000mA when the input voltage is 28V and the output voltage is 28V is given in **Figure 6.32**.

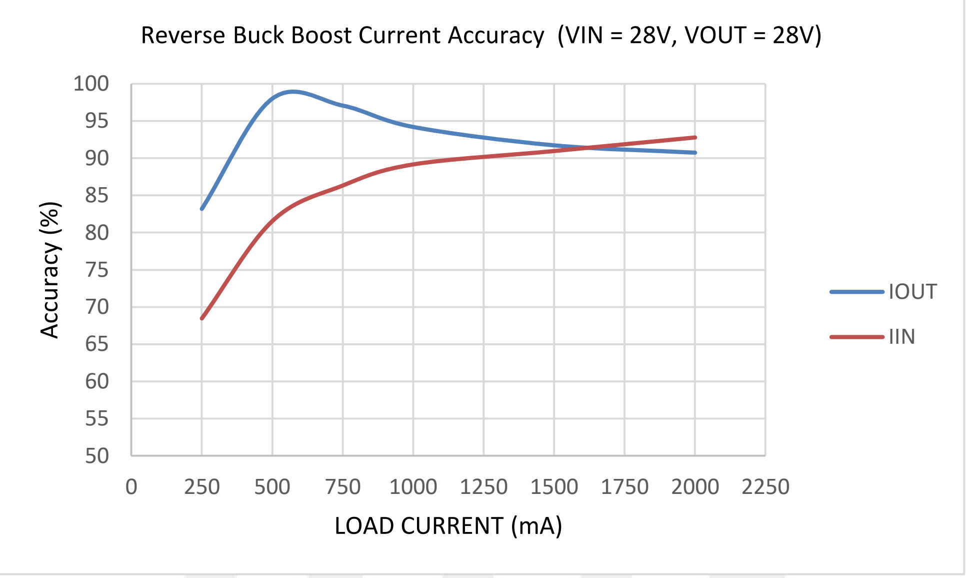

Figure 6.32 : Current reading accuracy of reverse buck boost converter.

When operating in the reverse direction at the boost mode, the input and output current reading accuracy from 250mA output current to 2000mA when the input voltage is 12V and the output voltage is 28V is given in **Figure 6.33**.

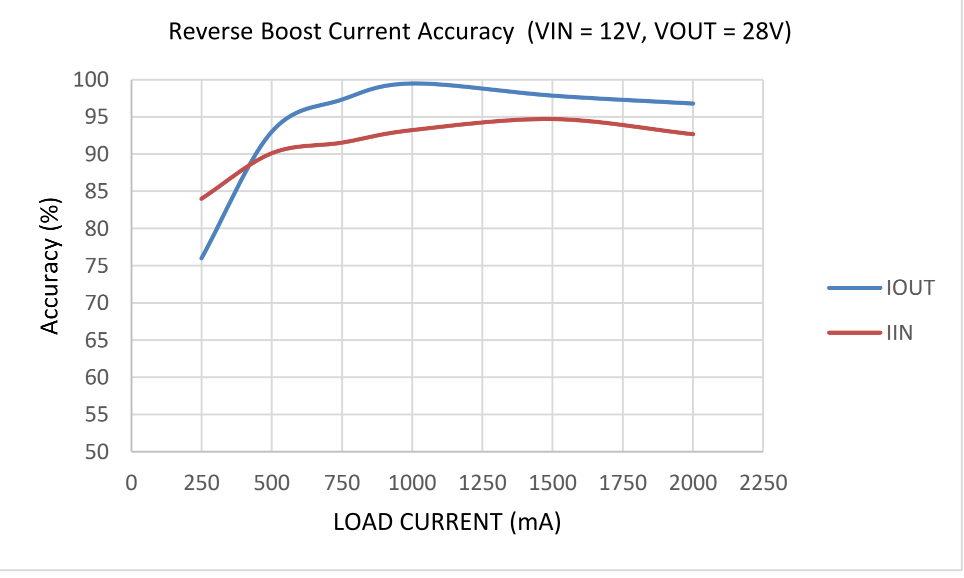

Figure 6.33 : Current reading accuracy of reverse boost converter.

6.4 Dead Time Test

The oscilloscope image of the gate voltages of Q1 and Q2 MOSFETs for input voltage 30V, output voltage 15V and forward operation is shown in Figure 6.34. There is an 30ns deadtime between Q1 MOSFET turning off and Q2 MOSFET turning on. In this way, Q1 and Q2 MOSFETs do not engage in conduction at the same time, preventing the source from being shorted to ground, thus reducing losses.

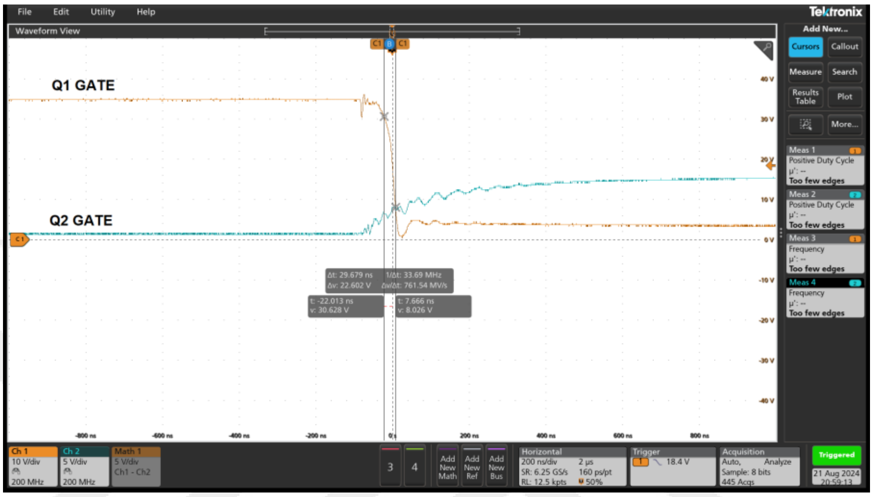

Figure 6.34: Dead Time of Q1 Falling Edge.

The oscilloscope image of the gate voltages of the Q1 and Q2 MOSFETs for the input voltage 30V, output voltage 15V and forward operation is shown in Figure 6.35. There is a deadtime of 85ns between Q1 MOSFET turning on and Q2 MOSFET turning off. In this way, Q1 and Q2 MOSFETs do not engage in conduction at the same time, preventing the source from being shorted to ground, thus reducing losses.

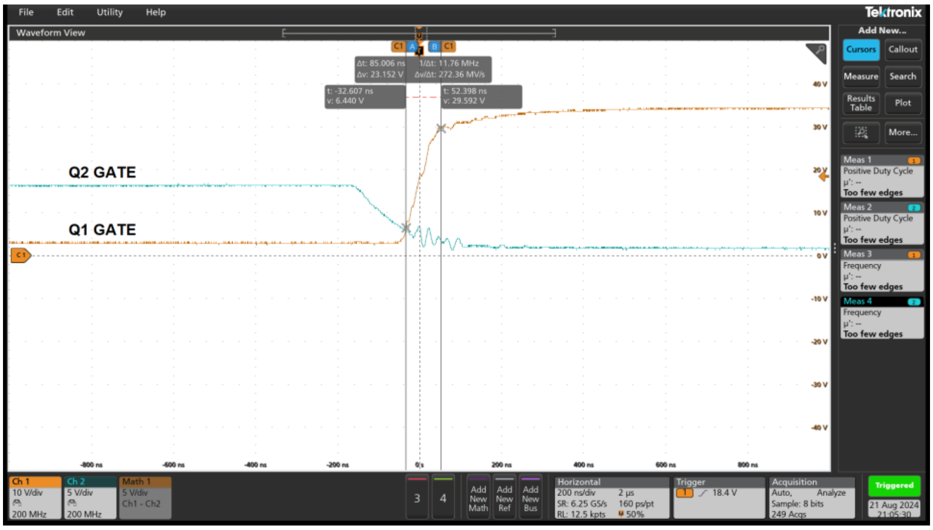

Figure 6.35: Dead Time of Q1 Rising Edge.

The oscilloscope image of the gate voltages of the Q1 and Q2 MOSFETs for the input voltage 30V, output voltage 15V and forward operation is shown in Figure 6.36.

MOSFETs Q1 and Q2 have a switching frequency of 100kHz. While the rise times of Q1 and Q2 MOSFETs are slow, their fall times are fast. In addition, the total duty cycle value cannot be 100% due to the dead time between the switching of Q1 and Q2 MOSFETs. Due to dead times of 30ns and 85ns, the total duty cycle value is 98.71%. The duty cycle value of 0.29% can be defined as dead duty.

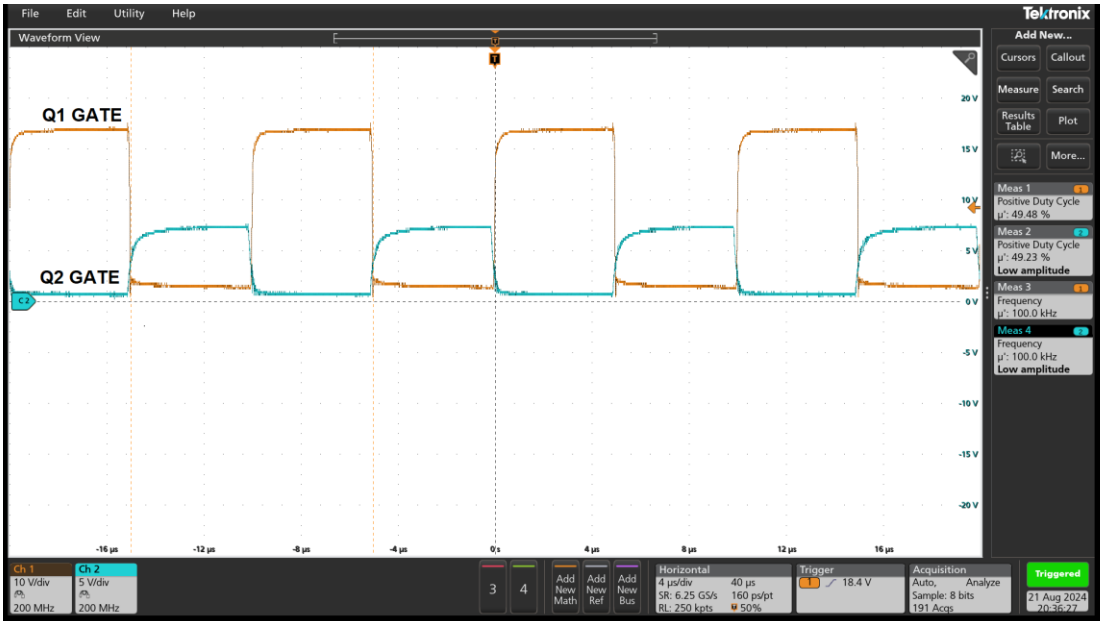

Figure 6.36: Q1 and Q2 Switching Dead Time.

7 CONCLUSIONS

In this thesis, starting from the basics, the working principle, calculations, system, hardware, and software design of the bi-directional buck boost converter are included. Consequently, test results of the design were produced.

At the beginning of the thesis, a literature review of bi-directional converter topologies was conducted. In this context, a topology that can work bi-directionally and is not isolated was chosen. Working principles, circuit structures, drive methods and calculations of buck, buck boost and boost converters in the topology are included. In addition to these calculations, losses on MOSFETs are included for each operating mode.

After giving main information about the bi-directional buck boost converter, software and hardware design stages were started.

Software developments were carried out on EK-TM4C123GXL, which contains the TM4C123GH6PM microprocessor. The environmental interfaces and software algorithm of the microprocessor, which is at the center of the system design, are explained with flowchart diagrams. In the hardware section, schematic diagrams that are the output of the Altium Designer program are included.

The visual figure of the bi-directional buck boost converter is shown in **Figure 7.1**.

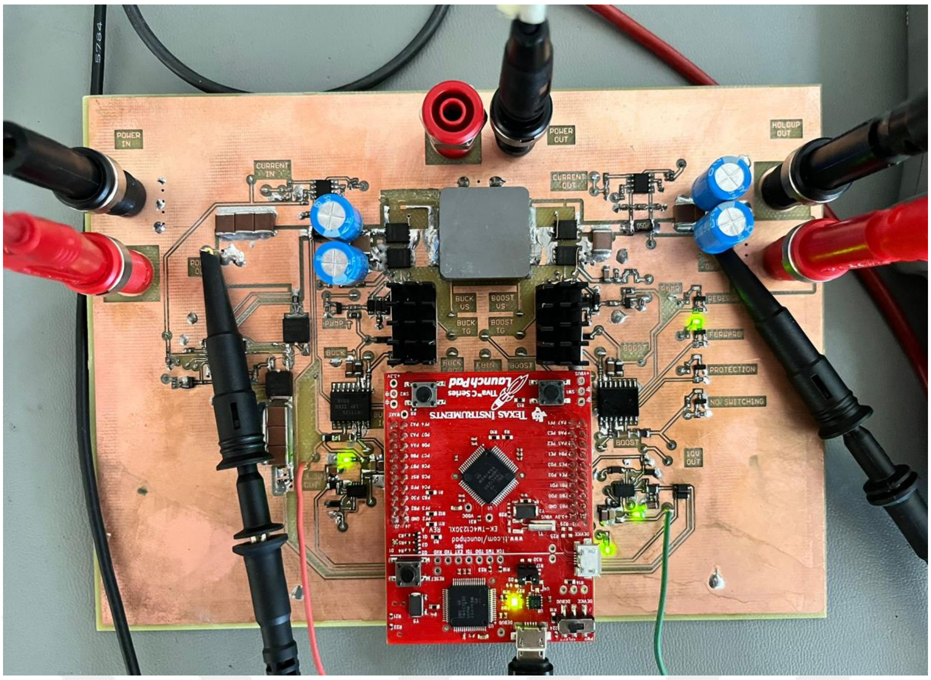

Figure 7.1 : Bidirectional buck boost converter.

Finally, the design resulting from the study has been tested and reported. Each operating mode of the design was tested one by one. Many errors and problems that emerged during testing have been corrected both in hardware and software. In particular, hardware and software measures have been taken to increase the acccuracy of voltage and current readings. In this way, high accuracy was achieved in the voltage regulation and current limiting values of the DC to DC converter.

REFERENCES

[1] **Camara M. B., Gualous H., Gustin F., Berthon A., and Dakyo B.** (2010). DC/DC converter design for supercapacitor and battery power management in hybrid vehicle applications—Polynomial control strategy, IEEE Trans. Ind. Electron., vol. 57, no. 2, pp. 587–597.

[2] **Bhattacharya T., Giri V. S., Mathew K., and Umanand L.** (2009). Multiphase bidirectional flyback converter topology for hybrid electric vehicles, IEEE Trans. Ind. Electron., vol. 56, no. 1, pp. 78–84.

[3] **Amjadi Z., and Williamson S. S. (**2010). A novel control technique for a switched-capacitor-converter-based hybrid electric vehicle energy storage system, IEEE Trans. Ind. Electron., vol. 57, no. 3, pp. 926–934.

[4] **Peng F. Z., Zhang F., and Qian Z.** (2003). A magnetic-less dc–dc converter for dual-voltage automotive systems, IEEE Trans. Ind. Appl., vol. 39, no. 2, pp. 511–518.

[5] **Nasiri A., Nie Z., Bekiarov S. B., and Emadi A.** (2008). An on-line UPS system with power factor correction and electric isolation using BIFRED converter, IEEE Trans. Ind. Electron., vol. 55, no. 2, pp. 722–730.

[6] **Schuch L., Rech C., Hey H. L., Grundling H. A., Pinheiro H., and Pinheiro J. R.** (2006). Analysis and design of a new high-efficiency bidirectional integrated ZVT PWM converter for DC-bus and battery-bank interface, IEEE Trans. Ind. Appl., vol. 42, no. 5, pp. 1321–1332.

[7] **Zhu X., Li X., Shen G., and Xu D.** (2010). Design of the dynamic power compensation for PEMFC distributed power system, IEEE Trans. Ind. Electron., vol. 57, no. 6, pp. 1935–1944.

[8] **Ma G., Qu W., Yu G., Liu Y., Liang N., and Li W.** (2009). A zero-voltageswitching bidirectional dc–dc converter with state analysis and softswitching-oriented design consideration, IEEE Trans. Ind. Electron., vol. 56, no. 6, pp. 2174–2184.

[9] **Peng F. Z., Li H., Su G. J., and Lawyer J. S.** (2004). A new ZVS bidirectional dc–dc converter for fuel cell and battery application, IEEE Trans. Power Electron., vol. 19, no. 1, pp. 54–65.

[10] Jin K., Yang M., Ruan X., and Xu M. (2010). Three-level bidirectional converter for fuel-cell/battery hybrid power system, IEEE Trans. Ind. Electron., vol. 57, no. 6, pp. 1976–1986.

[11] Gules R., Pacheco J. D. P., Hey H. L., and Imhoff J. (2008). A maximum power point tracking system with parallel connection for PV stand-alone applications, IEEE Trans. Ind. Electron., vol. 55, no. 7, pp. 2674–2683.

[12] Liao Z., and Ruan X. (2009). A novel power management control strategy for stand-alone photovoltaic power system, in Proc. IEEE IPEMC, pp. 445–449.

[13] Inoue S., and Akagi H. (2007). A bidirectional dc–dc converter for an energy storage system with galvanic isolation, IEEE Trans. Power Electron., vol. 22, no. 6, pp. 2299–2306.

[14] Chen L. R., Chu N. Y., Wang C. S., and Liang R. H. (2008). Design of a reflexbased bidirectional converter with the energy recovery function, IEEE Trans. Ind. Electron., vol. 55, no. 8, pp. 3022–3029.

[15] Lee S. Y., Pfaelzer G., and Wyk J. D. (2007). Comparison of different designs of a 42-V/14-V dc/dc converter regarding losses and thermal aspects, IEEE Trans. Ind. Appl., vol. 43, no. 2, pp. 520–530.

[16] Choudhary V., Hegarty T., Pace D. (2017). Under the hood of a noninverting buck-boost converter, Texas Instruments, [Power Supply Design Seminar 2016/17 SLUP346]. Retrieved from https://www.ti.com.

[17] Anbazhagan, L., Divya Navamani., and Krishnasamy V. (2019). A Comprehensive Review on Bidirectional Traxtion Converter for Electric Vehichles

[18] Texas Instruments (2018). 4-Switch Buck-Boost Bi-directional DC-DC Converter Reference Design [Test Report PMP21529]. Retrieved from https://www.ti.com.

[19] Hauke B. (2015). Basic Calculation of a Buck Converter's Power Stage [Application Report SLVA477B]. Retrieved from https://www.ti.com.

[20] Hauke B. (2022). Basic Calculation of a Boost Converter's Power Stage [Application Note SLVA372D]. Retrieved from https://www.ti.com.

[21] Weiss I. (2017). Basic Calculation of an Inverting Buck-Boost Power Stage [Application Report SLVA721A]. Retrieved from https://www.ti.com.

[22] Shi L., Mao X., and He H. (2012). Design of a hiccup mode over-current protection circuit for DC-DC switching converters

[23] Tucker J. (2022). Understanding Valley Current Limit [Technical Article SSZT694]. Retrieved from https://www.ti.com.

[24] URL-1. <https://toshiba.semicon-storage.com/> data retrieved: 04.02.2024

[25] Diallo M. (2023). Bootstrap Circuitry Selection for Half-Bridge Configurations [Application Note SLUA887A]. Retrieved from https://www.ti.com.

[26] Texas Instruments (2014). Tiva™ TM4C123GH6PM Microcontroller [Data Sheet TM4C123GH6PM]. Retrieved from https://www.ti.com.

CURRICULUM VITAE

Name Surname : **İLYAS SARIGÜL**

EDUCATION :

- **M.Sc.** **:** 2024, Istanbul Technical University, Faculty of Electrical and Electronics Engineering, Department of Electronics and Communication Engineering
- **B.Sc.** **:** 2020, Istanbul University, Faculty of Engineering, Department of Electrical and Electronics Engineering

PROFESSIONAL EXPERIENCE AND REWARDS:

- 2020-Current, Analog Design Engineer at TURKISH AEROSPACE INDUSTRY (TAI)
- 2019, Research and Development Engineer at BAYKAR

PUBLICATIONS, PRESENTATIONS AND PATENTS ON THE THESIS:

İ. SARIGÜL, Y. ÇAKIR. 2023 Reducing the Holdup Capacitor Value with the Converter Bidirectional Buck Boost Working at Avionic Standards, *First International Congress on Engineering and Sciences*, March 18/19, Istanbul, Turkey.